

INVESTIGATION OF PHYSICAL INTERACTION BETWEEN G $\alpha$ i AND G $\alpha$ s  
PROTEINS VIA FRET IN LIVE CELLS

A THESIS SUBMITTED TO  
THE GRADUATE SCHOOL OF NATURAL AND APPLIED SCIENCES  
OF  
MIDDLE EAST TECHNICAL UNIVERSITY

BY

SEYDA TUĞÇE BALKAN

IN PARTIAL FULFILLMENT OF THE REQUIREMENTS  
FOR  
THE DEGREE OF MASTER OF SCIENCE  
IN  
BIOCHEMISTRY

AUGUST 2021



Approval of the thesis:

**INVESTIGATION OF PHYSICAL INTERACTION BETWEEN *Gai* AND  
*Gas* PROTEINS VIA FRET IN LIVE CELLS**

submitted by **Seyda Tuğçe Balkan** in partial fulfillment of the requirements for the degree of **Master of Science in Biochemistry, Middle East Technical University** by,

Prof. Dr. Halil Kalıpçılar  
Dean, Graduate School of **Natural and Applied Sciences**

Assoc. Prof. Dr. Yeşim Soyer  
Head of the Department, **Biochemistry**

Assoc. Prof. Dr. Çağdaş Devrim Son  
Supervisor, **Biology, METU**

Dr. Fatma Küçük Baloğlu  
Co-Supervisor, **Biology, Giresun University**

**Examining Committee Members:**

Assoc. Prof. Dr. Tülin Yanık  
Biology , METU

Assoc. Prof. Dr. Çağdaş Devrim Son  
Biology, METU

Assist. Prof. Dr. Serkan Belkaya  
Molecular Biology and Genetics, Bilkent University

Assoc. Prof. Dr. Emrullah Görkem Günbaş  
Chemistry, METU

Assoc. Prof. Dr. Alpan Bek  
Physics, METU

Date: 11.08.2021

**I hereby declare that all information in this document has been obtained and presented in accordance with academic rules and ethical conduct. I also declare that, as required by these rules and conduct, I have fully cited and referenced all material and results that are not original to this work.**

Name Last name : Seyda Tuğçe Balkan

Signature :

## ABSTRACT

### INVESTIGATION OF PHYSICAL INTERACTION BETWEEN *Gai* AND *Gas* PROTEINS via FRET IN LIVE CELLS

Balkan, Seyda Tuğçe  
Master of Science, Biochemistry  
Supervisor : Assoc. Prof. Dr. Çağdaş Devrim Son  
Co-Supervisor: Dr. Fatma Küçük Baloğlu

August 2021, 111 pages

GPCR's are seven-transmembrane receptors that transmit external signals to the intracellular environment via secondary messenger systems through heterotrimeric G proteins. Heterotrimeric G proteins consist of  $\alpha$  and  $\beta$ - $\gamma$  subunits. Until recent years, scientists thought that GPCR signal transduction occurs between one GPCR and one heterotrimeric G protein; however, recently, it has been shown that GPCR's can make oligomers. Oligomerization of GPCR allows cells to tune the intensity of the signal and respond appropriately. Studies with A1 and A2A heterotetramer and A2A – D2R heterotetramer showed that these interactions theoretically allow G protein  $\alpha$  subunit dimer formation according to Navarro *et al.* and Ferré *et al.* This theoretical interaction has never been validated via an advanced fluorescent microscopy technique like FRET. This technique allows the detection of physical protein-protein interaction of fluorescently labeled proteins via resonance energy transfer between donor and acceptor fluorophores. In this study, *Gai* and *Gas* interaction was investigated by FRET technique. In addition, the effect of agonist treatment, CGS (CGS-21680), and quinpirole for A2A and D2R heterotetramer, respectively, was investigated. Furthermore, based on the G protein family member

K-Ras studies, which has high structural homology with G protein  $\alpha$  subunits, that forms a homodimer independent from its receptor (Dempke & Heinemann, 2009), we tested the effect of receptor binding on the physical interaction of G protein  $\alpha$  subunit using G protein  $\alpha$  subunit-specific minigenes.

Keywords: G $\alpha$  Proteins, Protein Interactions, FRET, Dimerization, Receptor Dependency

## ÖZ

### **G $\alpha$ i VE G $\alpha$ s PROTEİNLERİNİN FİZİKSEL ETKİLEŞİMLERİNİN CANLI HÜCRELERDE FRET METODU İLE ARAŞTIRILMASI**

Balkan, Seyda Tuğçe  
Yüksek Lisans, Biyokimya  
Tez Yöneticisi: Assoc. Prof. Dr. Çağdaş Devrim Son  
Ortak Tez Yöneticisi: Dr. Fatma Küçük Baloğlu

Ağustos 2021, 111 sayfa

Hücre zarını yedi defa geçen hücre zarı protein ailesi GPKR'ler, hücre dışı sinyalleri hücre içindeki ikincil haberci yoluna heterotrimerik G proteinleri ile iletirler. Heterotrimerik G proteinleri  $\alpha$  ve  $\beta$ - $\gamma$  altbirimlerinden oluşur. Geleneksel olarak bir GPKR'nin bir heterotrimerik G protein ile etkileştiği düşünülüyordu, ancak son yıllardaki çalışmalar GPKR oligomerizasyonunu göstermektedir. GPKR oligomerizasyonu, hücrelerin sinyal iletimi dengesini ve gereken cevabı vermesini sağlamaktadır. Navarro ve arkadaşlarının ve Ferré ve arkadaşlarının A1 ve A2A reseptör heterotetramerleri ve A2A ve D2 reseptör heterotetramerleri ile yaptıkları çalışmalar bu yapılarda teorik olarak G protein  $\alpha$  altbirimlerinin etkileşim yakınlığında bulunduğunu göstermektedir. Bu teorik etkileşim, daha önce, FRET gibi ileri floresan mikroskopi teknikleri kullanılarak valide edilmemiştir. FRET tekniği donör florofor ve akseptör florofor ile işaretlenen proteinlerin, donör ve akseptör proteinler arasında gerçekleşen enerji transferi vasıtası ile fiziksel protein-protein etkileşimlerinin incelenmesine izin vermektedir. Bu tez çalışmasında, G $\alpha$ i ve G $\alpha$ s etkileşimleri FRET tekniği ile araştırılmıştır. Ek olarak agonist varlığında, CGS (CGS-21680) ve Quinpirole kullanılarak A2A ve D2 reseptör heterotetramer etkisi araştırılmıştır. G protein ailesi üyesi ve G protein  $\alpha$  altbirimi ile yüksek yapısal

homolojisi olan K-Ras proteininin reseptör bağımsız homodimerizasyon çalışmalarına dayanılarak (Dempke & Heinemann, 2009), G $\alpha$  proteinlerinin reseptör etkileşimlerinin fiziksel etkileşimlerine olan etkisi, G $\alpha$  spesifik minigenler kullanılarak araştırılmıştır.

Anahtar Kelimeler: G $\alpha$  Proteini, Protein Etkileşimleri, FRET, Dimerizasyon, Receptor Bağımlılığı



To my family.

## ACKNOWLEDGMENTS

First of all, I wish to express my deepest gratitude to my advisor Assoc. Prof. Dr. Çağdaş Devrim Son for his guidance, advice, criticism, encouragements and insight throughout the research. It was a wonderful opportunity and such an amazing field of study. I am grateful to him for his fairness and helpfulness for his students. Without him this study would not be started or completed. I am grateful and I owe him a lot for for endless moral support, guidance and tolerance. I will always be grateful to him in my entire academic life.

Secondly, I would like to thank my co-advisor Dr. Fatma Küçük Baloğlu for her endless guidance, moral support, discipline and tolerance. I am grateful to her to give me a chance to work in her guidance and making the FES team. Without her, I would continue my academic career without an idol, I owe her a lot for being my idol not only for my scientific career, but also for my life. I will always be grateful to her in my entire life in many ways.

I would like to thank to my thesis examining committee; Assoc. Prof. Tülin Yanık, Assoc. Prof. Emrullah Görkem Günbaş, Assoc. Prof. Alpan Bek and Assist. Prof. Serkan Belkaya for their invaluable suggestions to complete my thesis study.

Also special thanks to Enise Nalli Sezer to be such an amazing lab mate and friend. I hope we can find a chance in our future career to work together besides our friendship for life. I will always remember our brainstorming and trouble-shooting times with our priceless friendship.

I would like to thank Orkun Cevheroğlu and Son-Lab Kök Hücre Team for their guidance and support.

I am grateful Hüseyin Evcı, Özge Atay, Murat Erdem and Ayça Hatıl for their guidance and endless mental and scientific support. I will always be grateful to them for my entire academic life.

I would like to thank all old and new SON Lab members to believe in me to complete this study and give me support. Especially special thanks to Öykü Deniz Demiralay, Damla Temel, Aiturgan Zhenbekova, Tolgahan Suat Sezen and İrem Aydın for their special support.

I would like to thank my best friends Ebrar Sinmez, Etkin Tarlan, Peri Beşarat, Fatma Rabia Fidan, Gözde Merve Türksoy, Nur Su Çakır, Ahmet Körpınar, Serena Mahnoor and Enise Nalli Sezer for their endless patience and support.

I am thankful for my life long friend and love Onur Durhan for his mental support, guide and helps.

Most importantly I am thankful for my mother Neşin Balkan, my father Ertuğrul Balkan , my brother Altuğ Balkan and my sister Sedef Balkan for their endless guidance and help. I am dedicating all my achievements to my family.

With special thanks, this work is partially funded by Scientific and Technological Research Council of Turkey under grant number TUBİTAK 117Z868.

“If one day, my words are against science, choose science.”

“Science is the most reliable guide for civilization, for life, for success in the world. Searching a guide other than science means carelessness, ignorance and heresy.”

“Heroic Turkish woman, you are worthy not to crawl on the ground, but to rise to the sky on your shoulders.”

–Mustafa Kemal Atatürk

## TABLE OF CONTENTS

ABSTRACT .....	v
ÖZ.....	vii
ACKNOWLEDGMENTS .....	x
TABLE OF CONTENTS .....	xii
LIST OF TABLES .....	xvi
LIST OF FIGURES .....	xvii
LIST OF ABBREVIATIONS .....	xxi
INTRODUCTION .....	1
1.1 GTP Binding Proteins.....	1
1.1.1 Small GTPases.....	1
1.1.2 Heterotrimeric G-proteins .....	2
1.1.2.1 G $\alpha$ subunits:.....	4
1.2 GPCR signaling.....	7
1.2 .....	8
1.2.1 Classical GPCR Interaction Model .....	8
1.2.2 GPCR oligomerization .....	9
1.3 G-protein signaling.....	9
1.3.1 Signaling of Small GTPases .....	10
1.3.2 Signaling of Heterotrimeric G protein.....	11

1.4	Protein-Protein Interactions.....	12
1.4.1	Protein-protein Interaction detection Methods in vivo.....	13
1.4.1.1	Förster Resonance Energy Transfer (FRET) .....	14
1.4.1.1.1	Confocal microscopy fluorescent imaging .....	18
1.4.1.1.2	Monochromator Plate Reader .....	20
1.3.1	.....	21
1.4.1.2	Minigenes.....	21
1.5	Aim of Study .....	22
MATERIALS AND METHODS.....		25
2.1	Materials.....	25
2.1.1	Mammalian Cell Culture.....	25
2.1.2	Bacteria culture .....	26
2.1.3	Cloning.....	27
2.2	Methods.....	28
2.2.1	Cloning.....	28
2.2.2	Mammalian Cell culture .....	36
2.2.3	Fluorescence Measurements .....	38
2.2.4	Image Analysis with Pix-FRET Program .....	39
2.2.5	Functional Analysis with cAMP-Glo™ Assay .....	40
2.2.6	Statistical analysis .....	42
RESULTS AND DISCUSSION .....		43
3.3	Investigation of Interaction Between G $\alpha$ i and G $\alpha$ s Proteins with FRET by Using Confocal Microscope.....	48

3.4	Investigation of G $\alpha$ i and G $\alpha$ s Interaction with FRET Technique Using Fluorescence Plate Reader.....	53
3.5	Preparation and Sequence Analysis of G $\alpha$ i and G $\alpha$ s Specific Minigenes	56
3.6	Investigation of the Receptor Dependency of G $\alpha$ i and G $\alpha$ s Interaction by Using Minigenes.....	59
3.6.1	Investigation by Using Confocal Microscopy .....	59
3.6.2	Investigation by Using Fluorescence Plate Reader .....	64
3.7	Investigation of G $\alpha$ i and G $\alpha$ s Interaction with Agonist Treatment for D2R and A2R Receptor Signaling Pathway Activation by Using Fluorescence Plate Reader.....	68
3.8	Future Studies .....	72
3.9	Discussion.....	73
	CONCLUSION .....	75
	REFERENCES .....	77
A.	COMPOSITIONS OF SOLUTIONS .....	87
B.	MAMMALIAN EXPRESSION MAPS .....	91
C.	DESIGNED PRIMERS .....	92
D.	FUSION PROTEIN CODING SEQUENCES .....	93
E.	cAMP GLO ASSAY STATISTICAL ANALYSIS .....	105
F.	STATISTICAL ANALYSIS OF THE CONFOCAL MICROSCOPY RESULTS Of G $\alpha$ i-G $\alpha$ s FRET PAIRS .....	106
G.	MONOCHROMATOR PLATE READER RESULT STATISTICAL ANALYSYS OF G $\alpha$ i-G $\alpha$ s FRET PAIRS.....	107

H. STATISTICAL ANALYSIS OF THE CONFOCAL MICROSCOPY RESULTS Of $G_{\alpha i}$ - $G_{\alpha s}$ FRET PAIRS WITH $G_{\alpha i}$ and $G_{\alpha s}$ PROTEIN SPECIFIC MINIGENES .....	108
I. MONOCHROMATOR PLATE READER RESULT STATISTICAL ANALYSYS OF $G_{\alpha i}$ - $G_{\alpha s}$ FRET PAIRS WITH $G_{\alpha i}$ and $G_{\alpha s}$ PROTEIN SPECIFIC MINIGENES .....	109
J. WITH/WITHOUT CGS+QUINPIROLE TREATMENT RESULT ANALYSIS OF $G_{\alpha i}$ - $G_{\alpha s}$ FRET GROUP WITH/WITHOUT MINIGENE ....	110
K. CURVE FITTING STATISTICAL ANALYSIS .....	111

## LIST OF TABLES

### TABLES

<b>Table 2. 1:</b> Optimal PCR conditions for G $\alpha$ tagging .....	29
<b>Table 2. 2:</b> Optimal PCR conditions for G $\alpha$ i Minigene Preparation .....	30
<b>Table 2. 3:</b> Optimal PCR conditions for G $\alpha$ s Minigene Preparation.....	30
<b>Table 2. 4:</b> PCR mixture for G $\alpha$ minigene Preparation .....	30
<b>Table 2. 5:</b> Optimized integration PCR protocol .....	31
<b>Table A. 1:</b> DMEM High Glucose Composition .....	87
<b>Table A. 2:</b> Composition of TFB I Solution .....	90
<b>Table A. 3:</b> Composition of TFB II Solution.....	90
<b>Table C. 1:</b> Minigene Cloning Primers .....	92



## LIST OF FIGURES

### FIGURES

<b>Figure 1. 1:</b> G $\alpha$ protein family members, expression patterns and % amino acid identities with each other .....	3
<b>Figure 1. 2:</b> G $\beta$ and G $\gamma$ protein family members , expression patterns and % amino acid identities with each other.....	4
<b>Figure 1. 3:</b> G $\alpha$ protein molecular structure and domains .....	4
<b>Figure 1. 4:</b> G $\alpha$ i protein structure.....	6
<b>Figure 1. 5:</b> Schematic representation of Classical model of GPCR and heterotrimeric G protein interaction.....	8
<b>Figure 1. 6:</b> Small G protein signal transduction. ....	10
<b>Figure 1. 7:</b> K-Ras signaling pathways. ....	11
<b>Figure 1. 8:</b> A1 and A2A receptor heterotetrameric model coupling with G $\alpha$ i and G $\alpha$ s proteins. ....	12
<b>Figure 1. 9:</b> Protein-protein interaction types.....	13
<b>Figure 1. 10:</b> EGFP and mCherry fluorophore excitation and emission spectum	17
<b>Figure 1. 11:</b> Imaging principles of A)widefield epifluorescence and B)Confocal microscope .....	19
<b>Figure 1. 12:</b> Spinning disc microscope component schematic representation. ...	20
<b>Figure 1. 13:</b> Monochromator plate reader component schematic representation.	21
<b>Figure 1. 14:</b> G protein alpha subunit specific minigenes and sequence domains.	22
<b>Figure 2. 1:</b> Overlapping extension PCR representation. ....	32
<b>Figure 2. 2:</b> cAMP-Glo™ Assay kit working principle. ....	41
<b>Figure 3. 1:</b> cAMP-Glo Assay results of G $\alpha$ proteins labeled with EGFP and mCherry fluorophores. ....	43
<b>Figure 3. 2:</b> Membrane targeted organelle marker Gap43 sequence labeled with A) mCherry and B) EGFP.....	46
<b>Figure 3. 3:</b> Fluorescent protein labeled G $\alpha$ s $\Delta$ 73-85 protein visualization. ....	47
<b>Figure 3. 4:</b> Fluorescent protein labeled G $\alpha$ i 91 protein visualization.....	47

<b>Figure 3. 5:</b> EGFP Fluorescent protein labeled Gai 121 protein visualization..	48
<b>Figure 3. 6:</b> Confocal FRET imaging of Gai(91)-EGFP and Gas(73-85)-mCherry..	50
<b>Figure 3. 7:</b> Confocal FRET imaging of Gai(121)-EGFP and Gas(73-85)-mCherry. ....	51
<b>Figure 3. 8:</b> Confocal FRET imaging of Gap43 EGFP and Gap43-mCherry..	52
<b>Figure 3. 9:</b> Confocal FRET imaging of Gap43mCherry-L-EGFP. 300ng of plasmid transfected into N2a cell line..	52
<b>Figure 3. 10:</b> Pix FRET analysis of confocal images. ....	53
<b>Figure 3. 11:</b> Spectral area normalization of FRET spectrum of the Gai and Gas FRET pairs.....	55
<b>Figure 3. 12:</b> Acceptor / Donor ratio of normalized spectrum of Gai-Gas and FRET control groups. ....	56
<b>Figure 3. 13:</b> Restriction sites for PstI double cutter for pcDNA 3.1(-).....	57
<b>Figure 3. 14:</b> Gai and Gas minigene cloning scheme.ö m56 .....	58
<b>Figure 3. 15:</b> Gai minigene cloning agarose gel results. ....	58
<b>Figure 3. 16:</b> Gas minigene cloning agarose gel results. ....	59
<b>Figure 3. 17:</b> LSM Airy scan Confocal FRET imaging of Gai(91)-EGFP and Gas(73-85)-mCherry. 500ng of Gai(91)-EGFP and Gas(73-85)-mCherry co-transfected into N2a cell line .....	61
<b>Figure 3. 18:</b> LSM Airy scan Confocal FRET imaging of Gai(121)-EGFP and Gas(73-85)-mCherry..	62
<b>Figure 3. 19:</b> LSM Airy scan Confocal FRET imaging of Gai(121)-EGFP and Gas(73-85)-mCherry + Gai and Gas minigenes..	63
<b>Figure 3. 20:</b> Pix FRET analysis of confocal images. ....	64
<b>Figure 3. 21:</b> Spectral area normalization of FRET spectrum of the Gai-Gas and minigene added Gai-Gas FRET pairs. ....	66
<b>Figure 3. 22:</b> Acceptor / Donor ratio of normalized spectrum of Gai-Gas and FRET control groups .....	67

<b>Figure 3. 23:</b> Spectral area normalization of FRET spectrum of the G $\alpha$ i-G $\alpha$ s and minigene added G $\alpha$ i-G $\alpha$ s FRET pairs with and without CGS+Quinpirole treatment..	69
<b>Figure 3. 24:</b> Acceptor / Donor ratio of the normalized spectrum of G $\alpha$ i-G $\alpha$ s and FRET control groups with CGS and Quinpirole treatment.	71
<b>Figure 3. 25:</b> Location-dependent curve fitting results with MATLAB.....	<b>Error!</b>
<b>Bookmark not defined.</b>	
<b>Figure B. 1:</b> pcDNA3.1(-) expression vector map.....	91
<b>Figure E. 1:</b> Statistical analysis of G $\alpha$ i fusion protein functional assay results...	105
<b>Figure F. 1:</b> Ordinary One way ANOVA analysis of G $\alpha$ i(121) EGFP-G $\alpha$ s(73-85)mCherry , G $\alpha$ i(91) EGFP-G $\alpha$ s(73-85)mCherry and Gap43 EGFP+ Gap43 mCherry negative control group confocal microscope results calculated with Pix FRET.....	106
<b>Figure G. 1:</b> G $\alpha$ i(121) EGFP-G $\alpha$ s(73-85)mCherry , G $\alpha$ i(91) EGFP-G $\alpha$ s(73-85)mCherry and Gap43 FRET control groups mCherry spectral peak region result analysis with Ordinary One way ANOVA .....	107
<b>Figure G. 2:</b> G $\alpha$ i(121) EGFP-G $\alpha$ s(73-85)mCherry , G $\alpha$ i(91) EGFP-G $\alpha$ s(73-85)mCherry and Gap43 FRET control groups Acceptor/Donor peak area result analysis with Ordinary One way ANOVA .	107
<b>Figure H. 1:</b> LSM Confocal microscope result from G $\alpha$ i(121) EGFP-G $\alpha$ s(73-85)mCherry , G $\alpha$ i(91) EGFP-G $\alpha$ s(73-85)mCherry and G $\alpha$ i(121) EGFP-G $\alpha$ s(73-85)mCherry with minigene FRET groups analyzed with Ordinary One Way Anova analysis.....	108
<b>Figure I. 1:</b> Monochromator plate reader results of G $\alpha$ i(121) EGFP-G $\alpha$ s(73-85)mCherry, G $\alpha$ i(91) EGFP-G $\alpha$ s(73-85)mCherry and G $\alpha$ i(121) EGFP-G $\alpha$ s(73-85)mCherry with minigene FRET groups Ordinary One Way Anova analysis...	109

**Figure I. 2:** Acceptor/Donor spectral peak area results of G $\alpha$ i(121) EGFP-G $\alpha$ s(73-85)mCherry, G $\alpha$ i(91) EGFP-G $\alpha$ s(73-85)mCherry and G $\alpha$ i(121) EGFP-G $\alpha$ s(73-85)mCherry with minigene FRET groups Ordinary One Way Anova analysis.... 109

**Figure J. 1:** Ordinary One Way ANOVA analysis of mCherry spectrum peak normalized area comparison of G $\alpha$ i-G $\alpha$ s FRET pairs with/without G $\alpha$  protein specific minigenes and with/without CGS+Quinpirole treatment..... 110

**Figure J. 2:** One way ANOVA analysis of Acceptor/Donor spectral area normalized peak results of G $\alpha$ i-G $\alpha$ s FRET pairs with/without G $\alpha$  protein specific minigenes and with/without CGS+Quinpirole treatment..... 110

**Figure K. 1:** Signal localization curve fit Two way ANOVA analysis results of FRET pairs. .... 111

**Figure K. 2:** Membrane curve fit result One Way ANOVA analysis of FRET pairs ..... 111

## LIST OF ABBREVIATIONS

### ABBREVIATIONS

A2A	Adenosine 2A
AC	Adenylyl Cyclase
ADP	Adenosine Diphosphate
AMP	Adenosine Monophosphate
ATP	Adenosine Triphosphate
$\beta_2$ AR	Beta-2 Adrenergic Receptor
Barr2	Beta-Arrestin 2
bp	base pair
cAMP	cyclic AMP
D-MEM	Dulbecco's Modified Eagle Medium
DMSO	Dimethyl sulfoxide
DNA	Deoxyribonucleic Acid
EDTA	Ethylenediamine tetraacetic acid
EE	Early Endosomes
FBS	Fetal Bovine Serum
FRET	Förster Resonance Energy Transfer
GFP	Green Fluorescent Protein
GPCR	G Protein Coupled Receptors

kb	kilo base pair
LB	Luria Bertani
MAPK	Mitogen-Activated Protein Kinase
mCherry	Monomeric Cherry
mEGFP	Monomeric Enhanced Green Fluorescent Protein
N2a	Neuro2a
PBS	Phosphate Buffered Saline
PCR	Polymerase Chain Reaction
PPIs	Protein-protein interactions
SBT	Spectral bleed-through

# CHAPTER 1

## INTRODUCTION

### 1.1 GTP Binding Proteins

In multicellular organisms, homeostasis mainly depends on signal transduction, which allows the organism to respond properly to changes that originate from both the organism and the environment. Signal transduction in such organisms includes Guanine binding proteins (G-proteins) and G protein coupled receptors (GPCRs). G-protein family is an extensive family, and their members have evolutionarily conserved domains, which bind GTP/GDP and their receptors. GPCRs are one of the most abundant receptors on cell membrane. When a GPCR binds to its ligand, the G-protein is activated, then GDP-GTP exchange from G-protein transduces the extracellular signal to the intracellular response. G protein signal transduction is required for cellular responses, including cell growth, protein synthesis, and membrane vesicle transport. In general, G-proteins are classified under two main classes as small G proteins (small GTPases) and heterotrimeric G proteins.

#### 1.1.1 Small GTPases

Members of small G-protein sub family are homologous of the alpha subunit of heterotrimeric G proteins. Small GTPases are key proteins in cellular signal transductions and cellular responses such as sustaining cell polarity, progressing cell cycle, and reorganizing cytoskeleton of the cell in eukaryotic cells. Considering their 3D structure, sequence, and function, despite containing over 150 members, small G protein family have only five main groups: Ras, Rho, Arf/Sar, Rab, and Ran. Among those groups, Ras proteins are the most studied member of these groups (Song et al.,

2019). H-Ras, K-Ras4A and 4B, and N-Ras are Ras family members and are responsible for regulating cell growth, division, differentiation, and death by utilizing signaling pathways (Repasky et al., 2010).

### **1.1.2 Heterotrimeric G-proteins**

Apart from Small G proteins and Ras family, heterotrimeric G proteins were reported firstly by Alfred Gilman and Martin Rodbell 30 years ago. Members of heterotrimeric G proteins have three subunits; alpha, beta, and gamma. Alpha subunit of heterotrimeric G proteins has a binding affinity to GTP and GDP. Various subtypes of this subunit is present a such as  $G\alpha_i$ ,  $G\alpha_s$ ,  $G\alpha_q$  and  $G\alpha_{12}$ , where each has different signal transduction paths. Similarly, beta-gamma subunits have many different sub-types, and these subunits act as a dimer that target different effectors. Together with alpha subunit, this family trigger many effectors that regulate ion channels, adenylyl cyclase, phosphoinositide-specific phospholipase C (PI-PLC) and phosphodiesterase (PDE) (Zachariou et al., 2012).

$G\alpha$  protein family members in the human genome have 35-95% homology with each other. In addition, 23 types of  $G\alpha$  proteins are divided into four main subclasses:  $G\alpha_s$ ,  $G\alpha_i$ ,  $G\alpha_q$  and  $G\alpha_{12/13}$ .  $G\alpha_s$  family includes  $G\alpha_s$  and  $G\alpha_{olf}$ . While  $G\alpha_s$  expressed by many cells of the body,  $G\alpha_{olf}$  expression is mainly from olfactory sensory neurons.  $G\alpha_{i1}$ ,  $G\alpha_{i2}$ ,  $G\alpha_{i3}$ ,  $G\alpha_o$ ,  $G\alpha_{it-rod}$ ,  $G\alpha_{it-cone}$ ,  $G\alpha_{igust}$  and  $G\alpha_{iz}$  belong to  $G\alpha_i$  family diagrams are presented in Figure 1.1.  $G\alpha_i$  family is the most variegated family among others. The main effect of  $G\alpha_i$  family, is the inhibition of the cAMP-dependent protein kinase (Boullaran & Gales, 2015).



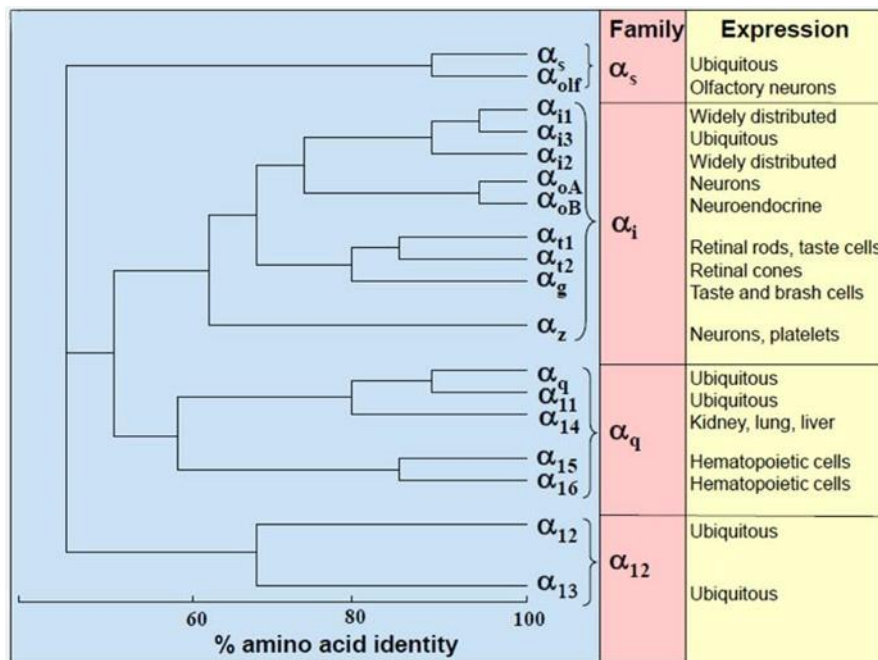


**Figure 1. 1:** G $\alpha$  protein family members, expression patterns and % amino acid identities with each other (Taken from (Syrovatkina et al., 2016)).

The beta-gamma dimer of heterotrimeric G proteins has a variety of members. G $\beta$  family has five members that have homology around 80-90% with each other. G $\beta_5$  member of the family shows 50% sequence matching and is expressed at the brain cells. In addition, G $\beta_1$  expression is seen in retinal rods and G $\beta_4$  expression is seen in retinal cones while other members' expression location is widely distributed to all body cells. G $\gamma$  family has 12 members and the members have 30-70% sequence identity as given in Figure 1.2 (Syrovatkina et al., 2016).

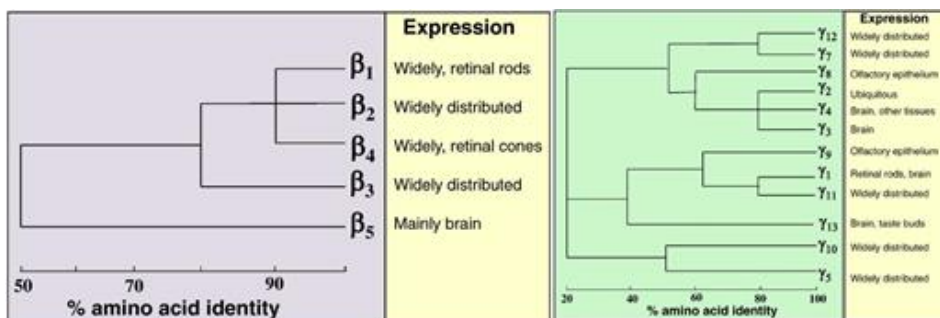


**Figure 1. 2:** G $\beta$  and G $\gamma$  protein family members , expression patterns and % amino acid identities with each other (Taken from (Syrovatkina et al., 2016)).

### 1.1.2.1 G $\alpha$ subunits:

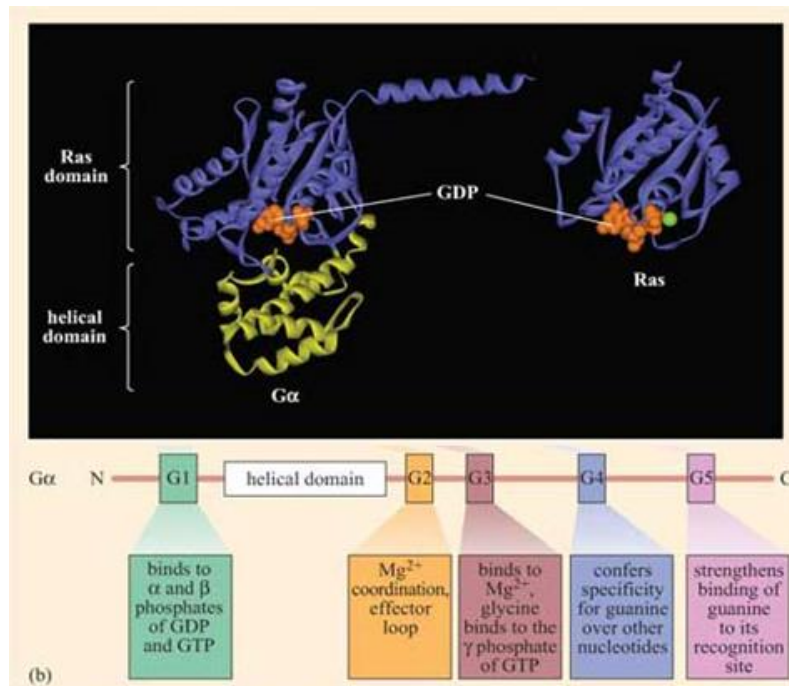


**Figure 1. 3:** G $\alpha$  protein molecular structure and domains. A) G $\alpha$  protein 3D molecular structure, B) G $\alpha$  protein domains and functionalities (Adapted from (*Cell Signalling: 3.5 Monomeric G Proteins - OpenLearn - Open University - S377\_4*, n.d.)).

G $\alpha$  proteins consist of 2 main domains: helical domain and Ras-like domain, also known as the G domain. Helical domain of G $\alpha$  proteins is shared and belongs to G $\alpha$  proteins, whereas the Ras-like domain is shared by all GTPases. G domain consists of 5 main sub-domains; G1, G2, G3, G4, and G5 (Figure 1.3). While the G4 domain

gives  $G\alpha$  a specificity to bind to GTP/GDP, G1 and G3 domains have a function to bind to phosphates belong to GTP/GDP nucleotide. G2 is acting as an effector loop and coordinating  $Mg^{+2}$  ions. G5 domain act as a helper by strengthening GTP/GDP binding with its recognition sites (Cell Signalling: 3.5 Monomeric G Proteins - OpenLearn - Open University - S377\_4, n.d.). Ras-like domain functions as GTP binding domain that binds to  $G\alpha$  subunit after receptor activation and signal transduction. The helical domain of  $G\alpha$  proteins specifies the  $G\alpha$  binding proteins. After activation of  $G\alpha$ , the helical domain changes its conformation and loops displaced by Ras-like domain (Dohlman & Jones, 2012).

$G\alpha_i$  signaling is through inhibiting adenylyl cyclase by extracellular activation and conformational change of its specific GPCRs, thus cAMP cannot be produced from ATP. Moreover, this inhibition causes activation of PKA. cAMP pathways regulate processes in the body like heart rate, cortisol secretion, and breakdown of glycogen and fat. It is required to maintain memory, heart relaxation, water absorption in the kidney. Mainly,  $G\alpha_i$  couples with acetylcholine M2 and M1, Adenosine A1 & A3 receptors, Cannabinoid receptors, Dopamine D2, D3, D4, serotonin and opioid receptors.  $G\alpha_i$  signaling-related activation of Phospholipase C(PLC) and inhibition of adenylyl cyclase may cause an increase in vascular tone, and the diameter of vessels. Smooth muscle relaxation is also related to  $G\alpha_i$  signaling. Signal transductions from endothelial cells via  $G\alpha_i$  protein cause Nitric Oxide release and prostaglandins and endothelium-derived hyperpolarizing factors (EDHFs). This action causes relaxation in smooth muscle cells. Via adrenergic receptor Beta,  $G_i$  signal transduction decreases PKA activity resulting in calcium inhibition, which reduces contractile force (Hendriks-Balk et al., 2008) .

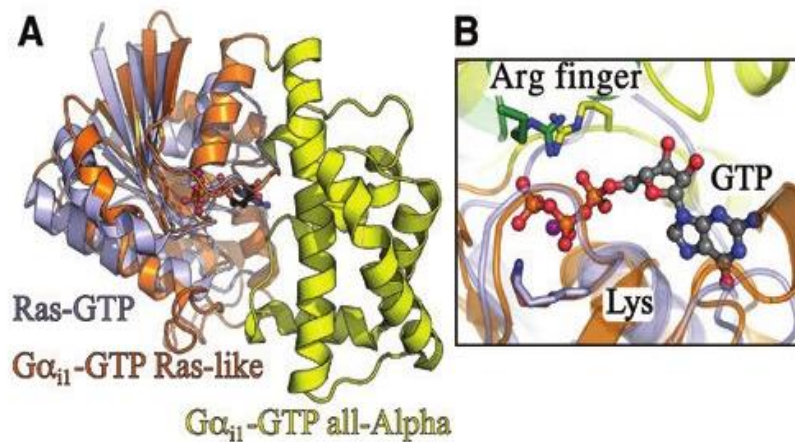


**Figure 1. 4:** *Gα<sub>i</sub>* protein structure, A) overall 3D structure and domains and , B) GTP binding domain representation.(*Structural Similarities between Ras and Gα<sub>i</sub>*. (A) *The Gα Subunit of...* | *Download Scientific Diagram*, n.d.)

In contrast, the *G<sub>αs</sub>* mechanism stimulates cAMP production when its GPCR is activated. ATP to cAMP production increases, so PKA gets activated. Related GPCRs to *G<sub>αs</sub>* signaling are mainly; ACTH receptors, Adenosine receptor types A2a and A2b, Arginine vasopressin receptor 2, β-adrenergic receptors types β1, β2 and β3, Cannabinoid receptor 2, Dopamine receptors D1-like family. *G<sub>αs</sub>* subunit related signaling via beta adrenergic receptors mediate contraction in cardiomyocytes via PKA phosphorylation and Ca<sup>+2</sup> channel (Hendriks-Balk et al., 2008). Activity increases Ca<sup>+2</sup> leading to increase of positive charge intracellularly(London et al., 2004).

*Gαq* family members are *Gαq*, *Gα11*, *Gα14* and *Gα16*. While *Gαq* and *Gα11* show ubiquitous expression patterns and having 90 % sequence identity with each other, *Gα14* express from kidney, liver, and lung cells and has 80 % sequence identity with *Gαq*. In addition, *Gα16* express from hematopoietic cells and has 57 % identity with

Gαq(Mizuno & Itoh, 2009). Gα12 family consists of Gα12 and Gα13 and express by most human cells(Kelly et al., 2006) .

## 1.2 GPCR signaling

G protein-coupled receptors (GPCRs), which are integral membrane proteins, are the largest family of signaling receptors. 1/3 of all produced clinical drugs on the market target GPCRs (Hauser et al., 2017). While inactive GPCR signal transduction phase, GPCR and its heterotrimeric G protein locates from cell membrane. There are two main hypothesis for GPCR-G protein coupling. The first one claims that G protein-GPCR interaction occurs after ligand binding and then Gα and Gβγ subunit dissociates due to GDP-GTP exchange (*GPCR / Learn Science at Scitable*, n.d.). The second one claims that there is a GPCR-G protein precoupled complex. After ligand interaction, Gα and Gβγ subunit dissociation occurs due to GDP-GTP exchange.(Matúš & Prömel, 2018). Ligand interaction with GPCRs results in GPCR signalling activation and Gα dissociation from Gβγ. Last 11 amino acid of Gα subunit is required for heterotrimeric G protein GPCR interaction (Gilchrist et al., 2002). When the extracellular part of GPCR interacts with its ligand, change in its conformation triggers Gα subunit GDP-GTP exchange and heterotrimeric G protein is activated. Gα subunit separates from beta-gamma dimer, Gα subunit transduces signal via its effector interactions while beta-gamma dimer regulating other effectors (Nestler & Duman, 1999). This heterotrimeric G protein based secondary messenger system is required to transform extracellular signals to cellular responses (Morris & Malbon, 1999) (Tsvetanova et al., 2015).

### 1.2.1 Classical GPCR Interaction Model

The classical GPCR-G protein interaction model states one GPCR can interact with one heterotrimeric G protein. This model of GPCR signaling has seven steps. Firstly, GPCR, G protein, and adenylyl cyclase locate on the cell membrane with no interaction except random interactions. Then, agonist ligand of the GPCR bind and change GPCR conformation. Then, GDP-GTP exchange occurs at the alpha subunit of the heterotrimeric G protein. Activation of G protein causes  $G\alpha$  and  $G\beta\gamma$  separation. Separated  $G\alpha$  protein interacts and activates adenylyl cyclase. Adenylyl cyclase binding site overlaps with  $G\beta\gamma$  binding site. Thus, separation of  $G\beta\gamma$  dimer from  $G\alpha$  is required for the interaction with adenylyl cyclase. Activated adenylyl cyclase produces cyclic AMP. Finally, GTPase activity triggers GTP-GDP hydrolysis causing the termination of the signaling and heterotrimeric G protein reunites as presented in Figure 1.5.

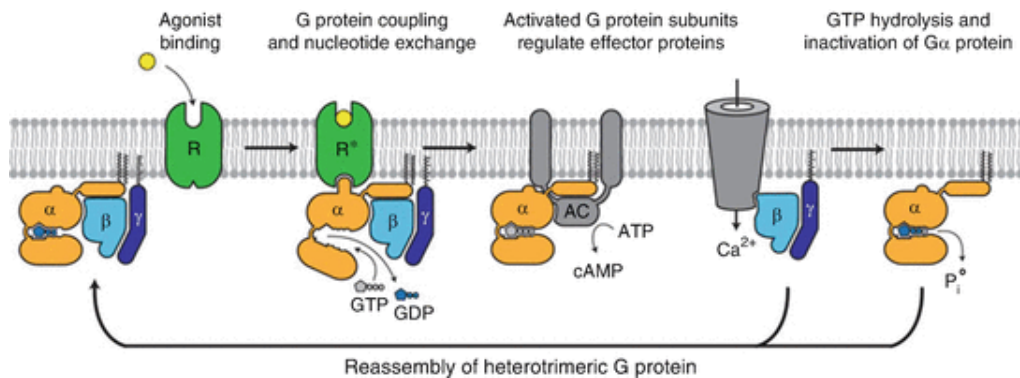


**Figure 1.5:** Schematic representation of Classical model of GPCR and heterotrimeric G protein interaction. (Taken from (Pincas et al., 2018))

### 1.2.2 GPCR oligomerization

The classical GPCR signaling model is still used, but recent studies have reported that GPCRs can oligomerize and share heterotrimeric G proteins while signaling (Ferré et al., 2016). This interaction type enables cell to control the signal intensity, enlarge transduced signal, modify the signal and cellular response as well. Oligomers could be homomeric with same kind of GPCR interaction or heteromeric more than one kind of GPCR interaction. Navarro and his group showed that A1 Receptor homodimer and A2A receptor homodimer interact with each other and form heterotetrameric structure. This heterotetramer allows  $G_{\alpha i}$  and  $G_{\alpha s}$  protein interaction, theoretically. Furthermore, crosstalk between A2A homodimer and D2R homodimer was recognized in 1991, and interaction of these receptors was shown in 2015 (Ferré et al., 2016). According to this interaction model, it is not known whether  $G_{\alpha i}$  and  $G_{\alpha s}$  are interacting or not.

### 1.3 G-protein signaling

G protein family, containing two subfamily as small G proteins and heterotrimeric G proteins, binds GTP and GDP molecules, act as a key role for signal transduction, cell growth and division, protein synthesis, and vesicular transportation (Wettschureck & Offermanns, 2005). G protein  $\alpha$  subunit and small G proteins have structural similarities with each other and bind GTP and GDP similarly. In contrast with  $G_{\alpha}$  subunits, small G proteins can act independently as hydrolase enzymes (Sprang, 2016). While the monomeric structure is observed for small G proteins, heterotrimeric G proteins have subunits called  $G_{\alpha}$ ,  $G_{\beta}$  and  $G_{\gamma}$ . When GPCR is activated by ligand and change its conformation,  $G_{\alpha}$  binds to GTP and then separates from  $G_{\beta}$ - $G_{\gamma}$  heterodimer. While the  $G_{\alpha}$  subunit interacts with its effectors,  $G_{\beta}$ - $G_{\gamma}$  dimer act on other effectors (Oldham & Hamm, 2008) As a result, activation of

GTPases activates various pathways as presented in Figure 1.6 (Dohlman & Campbell, 2019).

Effectors of the heterotrimeric G proteins are mainly GIRK, MAPK, PLC $\beta$ , PI3K, and adenylyl cyclase. In addition, small GTPase effectors are TIAM1, PI3K and RAF mainly. Both of these families has a role of cell growth, division and tumorigenesis since PI3K interaction. However, heterotrimeric G proteins regulates ion channels by interacting with GIRK and small GTPases regulates bipolar spindle assembly, chromosome congression and mitotic progression by interacting with TIAM1 (Monfort, 2018).

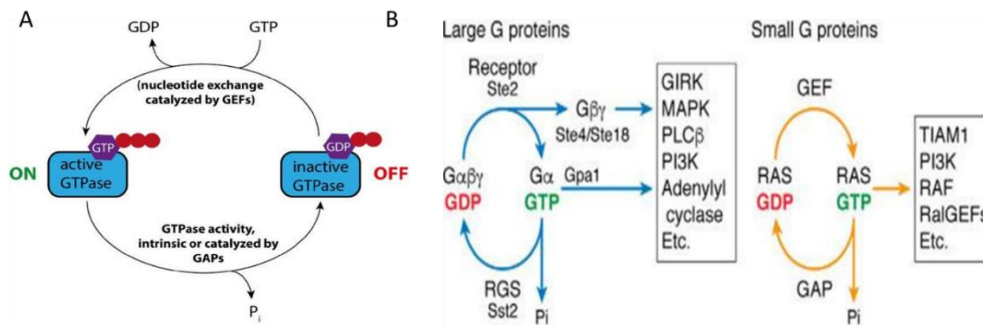


**Figure 1. 6:** Small G protein signal transduction. A) Schematic representation of Small GTPase signal transduction. B) Comparison of Small GTPase member Ras signal transduction with heterotrimeric G protein pathways. (Taken and adapted from (Monfort, 2018))

### 1.3.1 Signaling of Small GTPases

Small GTPases can act as monomeric hydrolase enzymes, bind their receptors and transduce signals. Ras proteins can be activated by Tyrosine kinase receptors, and GTP bound Ras protein transduces signal pathways like MAPK, PI3K that are important for cell differentiation and division as presented in Figure 1.7 (Vasan et



al., 2014). Mutants of Ras proteins destroy the balance between differentiation and division. If cell division cannot be controlled, it could cause malignancy, and lead to cancer. K-Ras 4B mutants are seen widely on colorectal cancer. Recently, scientific contributions about K-Ras 4B protein have been reported. K-Ras 4B mutant form can be seen with GNA12 protein wild type overexpression (H et al., 2015) and belongs to small GTPase family Ras group, binds each other, and creates dimers (Chung et al., 2016)(Nan et al., 2015).

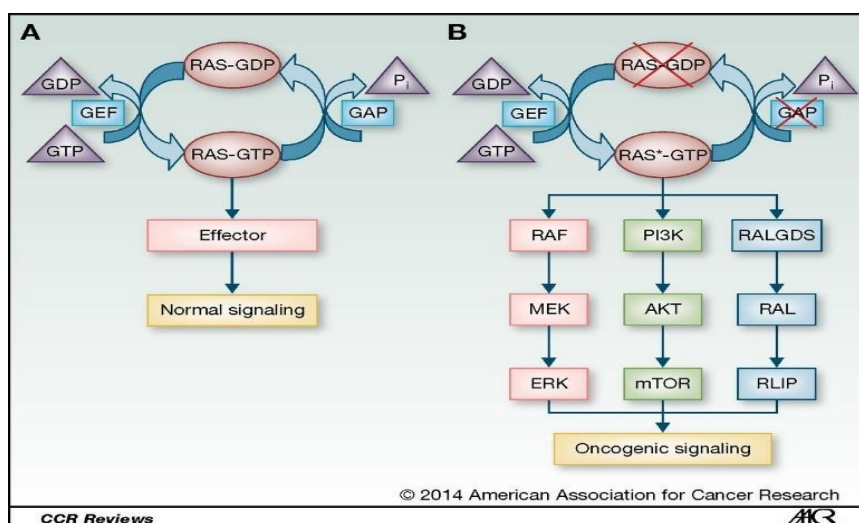


**Figure 1. 7:** K-Ras signaling pathways. A) Wild type Ras signalling pathways and, B) Oncogenic mutated Ras pathways (Taken from (Vasan et al., 2014))

### 1.3.2 Signaling of Heterotrimeric G protein

Heterotrimeric G protein  $\alpha$  subunits also bind to their GPCRs, and GDP-GTP exchange system allows them to transduce signals. In addition, Navarro and his study group indicated that a heterotetramer structure of GPCR A1 homodimer and A2A homodimer interacts with each other and forms heterotetrametric GPCR oligomer (Navarro et al., 2016). In this heterotetrametric interaction, G $\alpha$ i protein is shared by A1 homodimer and G $\alpha$ s protein is shared by A2A homodimer. This system theoretically shows that, G $\alpha$ i and G $\alpha$ s proteins are close each other enough for a

possible dimerization. A1 and A2A receptor heterotetramer model is schematically represented in Figure 1.8 (Franco et al., 2021)

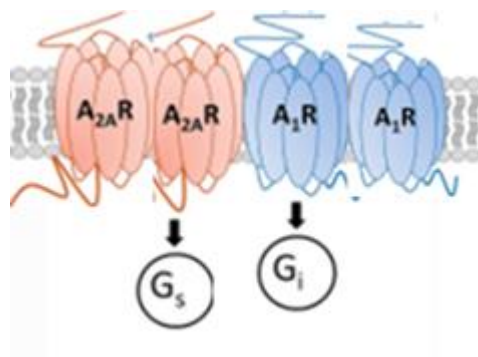


**Figure 1. 8:** A1 and A2A receptor heterotetrameric model coupling with G<sub>ai</sub> and G<sub>as</sub> proteins (Adapted from (Franco et al., 2021)).

#### 1.4 Protein-Protein Interactions

Cellular pathways and responses from extracellular and intracellular events are mostly depend on proteins. In order to transduce signals that are responsible for such events via signaling pathways, proteins should interact with other molecules, mostly with other proteins. In order to say that two proteins are interacting, they should be closer than 10 nanometers (Xing et al., 2016a). These interactions between proteins are various, and proteins can interact with other proteins via random interactions. To be able to say that the two proteins are interacting specifically, there should be permanent or transiently contact to another molecule physically with a specific position and/or interface. Furthermore, in order to say that two proteins are interacting with each other specifically, interaction between two protein should have specific purpose as well , such as gene expression, protein degradation etc. (de Las Rivas & Fontanillo, 2010). According to their binding affinity, interaction can be obligate, which means one of the proteins from the complex is useless, so the complex form is required for the functionality. Whereas proteins can interact and form a complex, and also act independently in non-obligate interactions. According to interaction stability, interacting proteins can bind each other permanently or

transiently, but most of the time, obligate interactions are permanent as given in Figure 1.9 (Acuner Ozbabacan et al., 2011).

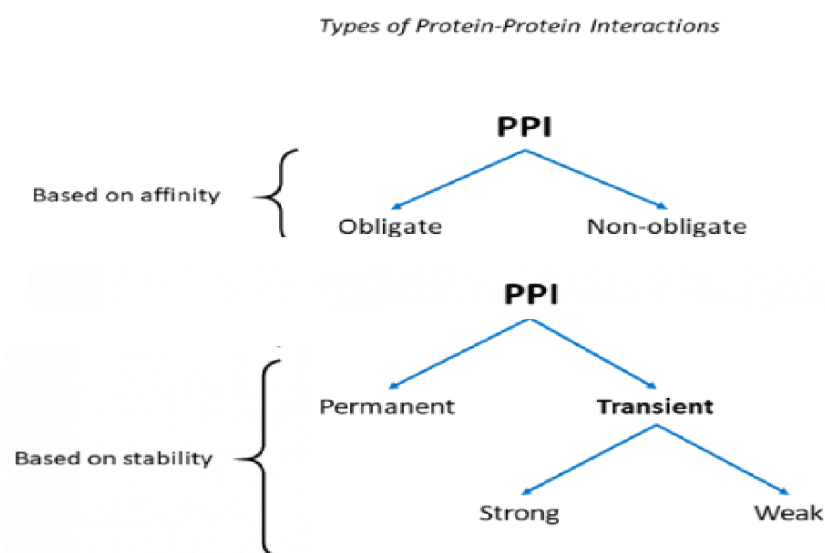


**Figure 1. 9:** Protein-protein interaction types. (Adapted from (Acuner Ozbabacan et al., 2011)).

#### 1.4.1 Protein-protein Interaction detection Methods in vivo

Cellular events to sustain homeostases like synthesis, maturation, vesicle budding, trafficking, and degradation are controlled protein-protein interactions (PPIs) (Xing et al., 2016). Thus, tracking and detecting PPIs is an opened and essential field for systems biology. Especially in drug development and pharmaceutical fields, in order to detection of target molecules and their modification and affection , it is essential to know relevant protein-protein interaction outcomes *in vivo*(de Las Rivas & Fontanillo, 2010).

To detect PPIs *in vivo* there are two classes of methods that can be used. First class is high throughput techniques that include Yeast two-hybrid and affinity purification.

The second class is low throughput techniques, that include devices as nuclear magnetic resonance (NMR) spectroscope, atomic force microscope, and electron microscope. Furthermore confocal fluorescent microscope could be used for FRET studies with proper fluorophore labeling while analyzing *in vivo* and *in vitro* protein-protein interactions (Peng et al., 2017).

#### **1.4.1.1 Förster Resonance Energy Transfer (FRET)**

Recent studies indicates that investigating interactions by using advanced fluorescent microscopy techniques is very popular and reliable (Ishikawa-Ankerhold et al., 2012). The advantage of such techniques is allowing the researcher to work *in vivo* and record and/or track live responses after certain treatments. FRET technique that belongs to advanced fluorescent microscopy techniques, is used widely to study for protein dynamics, protein-protein interaction and other biological molecules, such as DNA (Okamoto & Sako, 2017). Innovations in the fluorescence microscopy field, such as developing new fluorescent probes, allow scientists to use FRET technique more sensitively to be able to detect PPIs. Thus, FRET is a powerful tool to detect interactions and dynamics of proteins via its capability of detection sensitivity in nanosecond time range and angstrom distances with high resolutions in very broad and very narrow ranges.

FRET technique was developed in 1948 by Theodore Försters while he was aiming to study photosynthesis efficiency (Lemke & Deniz, 2011). FRET technique depends on nonradiative energy transfer between donor fluorophore and acceptor fluorophore. When donor fluorophore excited with its specific wavelength, it excites ground state non-excited acceptor fluorophore by long-range dipole-dipole interaction between donor and acceptor fluorophore that are located in between 10-100 angstrom distance (Sekar & Periasamy, 2003). In order to use FRET technique correctly, there are some requirements about donor and acceptor fluorophore selection. Firstly, the emission spectrum of donor fluorophore should have an

overlapping region with the excitation spectrum of acceptor. Secondly, donor and acceptor fluorophore distance should be more than the collision diameter. Lastly, dipole position between donor and acceptor should not be positioned.

Försters Theory suggests that energy nonradiative energy transfer rate  $k_T(r)$  between donor and acceptor pair can be calculated by using the equation below:

$$k_T(r) = \frac{1}{\tau_D} \left( \frac{R_0}{r} \right)^6$$

From the equation, r means the distance between donor and acceptor,  $R_0$  means Förster distance, and  $\tau_D$  means the rate of decay of donor when acceptor fluorophore is absent. Thus, FRET efficiency calculation can be explained with the equation below:

$$E_{\text{FRET}} = \frac{1}{1 + \left( \frac{r}{R_0} \right)^6}$$

Efficiency of the FRET formula enables to detect donor and acceptor distance, so its usage enables to calculate donor and acceptor distances in nanoscales(Wallace & Atzberger, 2017).

There are many ways to measure FRET Efficiency for example: Donor photobleaching (FLIM), Acceptor photobleaching, Spectral Imaging, and 3Cube method (Sensitized Emission). In this study, 3 cube method was used.

3 cube method is also referred as two-color ratio imaging (*Fluorescence Resonance Energy Transfer (FRET) Microscopy - Introductory Concepts | Olympus LS, n.d.; Wallace & Atzberger, 2017*). Overlaps between donor excitation-acceptor excitation and donor emission-acceptor emission are significant problems. The donor excitation with its specific wavelength should not excite the acceptor and the signal that is collected from acceptors emission spectrum should not overlap with donors emission spectrum ideally. Thus, 3 groups should be analyzed using proper filters to calculate FRET and eliminate the spectral bleed-through (SBT) from FRET data. First group is donor fluorophore expression only group, second group is acceptor fluorophore expression only group and the final one is FRET group with both donor and acceptor expression. Donor fluorophore expressed and excited groups emission signal that is collected from acceptor emission spectral region should be minimized and acceptor expressed groups donor excitation and acceptor emission signal should be minimized to collect ideal data. In this study, EGFP and mCherry fluorescent proteins are used as a FRET pair. Since overlaps between donor emission and acceptor emission and also donor excitation and acceptor excitation are very limited, by using certain regions for excitation and emission, crosstalk can be eliminated and ideal data can be collected (Figure 1.10).

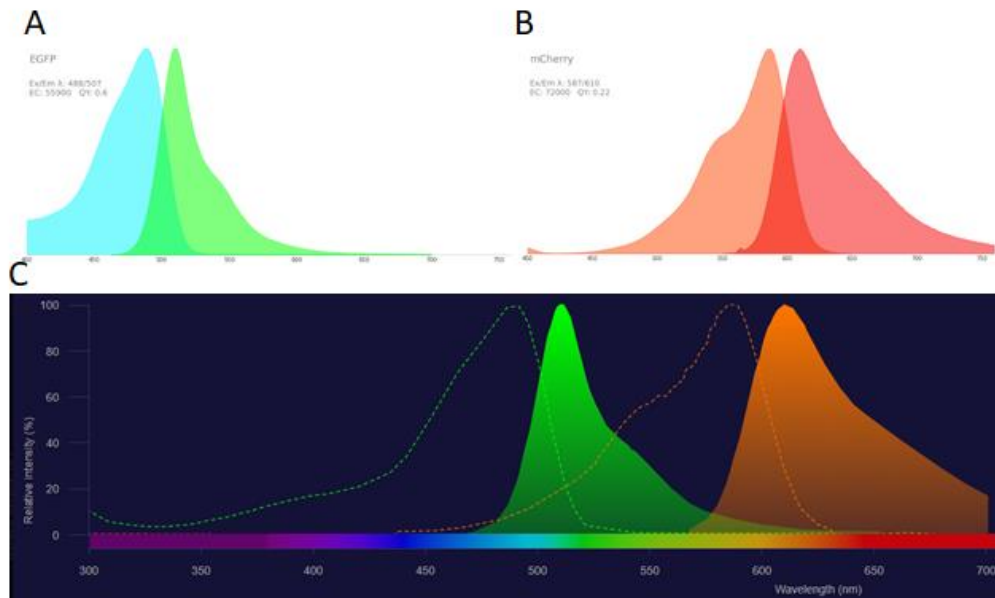


**Figure 1. 10:** EGFP and mCherry fluorophore excitation and emission spectrums. A) EGFP fluorophore excitation (blue) and emission (green) spectral graph, B) mCherry fluorescent protein excitation (orange) and emission(red) spectral graph, C) EGFP and mCherry spectral regions with overlaps. (Adapted from [www.fpbases.org](http://www.fpbases.org) and <https://www.thermofisher.com/order/fluorescence-spectraviewer#!/> )

In this thesis, confocal fluorescent microscopy and monochromator plate reader were used for protein-protein interaction detection with FRET technique. Data taken from FRET experiments were calculated with FRET formula below.

$$\text{FRET} = \frac{I_{\text{FRET}} - \text{BT}_{\text{Donor}} * I_{\text{Donor}} - \text{BT}_{\text{Acceptor}} * I_{\text{Acceptor}}}{N}$$

$$\text{NFRET} = \frac{I_{\text{FRET}} - \text{BT}_{\text{Donor}} * I_{\text{Donor}} - \text{BT}_{\text{Acceptor}} * I_{\text{Acceptor}}}{N} * 100$$

$$\text{BT}_{\text{acceptor}} = \frac{I_{\text{FRET}}}{I_{\text{Acceptor}}}$$

$$\text{BT}_{\text{donor}} = \frac{I_{\text{FRET}}}{I_{\text{Donor}}}$$

#### 1.4.1.1.1 Confocal microscopy fluorescent imaging

Most commonly used fluorescent microscope design in life sciences is epifluorescence design. Confocal microscope is an electronic system that is combined with a widefield epi-fluorescence instrument. This combination has laser illuminators, an electronic and optical component included scanning head, a computer system in order to display and monitor image and appropriate software to tune signal, process and analyze the images (Figure 1.11). Due to low signal to noise ratio of confocal microscope, it is one of the best device options to apply FRET technique.



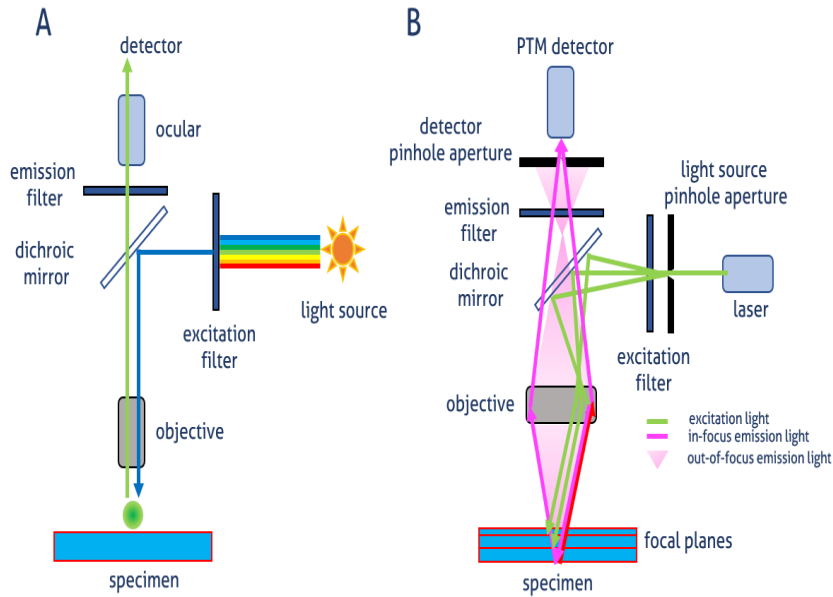


**Figure 1. 11:** Imaging principles of A)widefield epifluorescence and B)Confocal microscope (Taken from <https://www.ptglab.com/news/blog/if-imaging-widefield-versus-confocal-microscopy/>)

The sequential light collection is the main point of confocal imaging. Scanning of signal point by point by using Nipkow disc is one way to take an image with a confocal microscope. Nipkow disc enables the system to eliminate non-focused light by spinning and rotating the small holes. Thus, only focused light is expected to reach to the specimen, theoretically. As a result, both stage and beam stay stable, and also, the captured image is sharper and more detailed. In this thesis spinning disc confocal microscope was used for FRET imaging experiments (Figure 1.12).

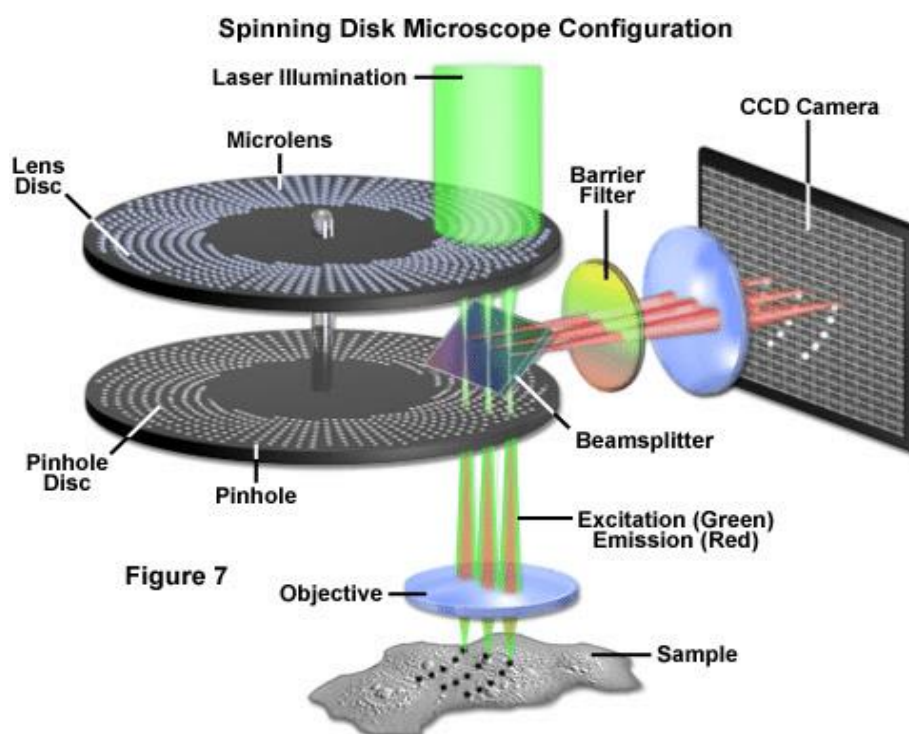


**Figure 1. 12:** Spinning disc microscope component schematic representation. (ZEISS Microscopy Online Campus | *Introduction to Spinning Disk Microscopy*, n.d.)

#### 1.4.1.1.2 Monochromator Plate Reader

Monochromator plate reader diffracts light that is produced by the light source and enables the user to select specific wavelength excitation with the capacity of its slit width. The light for exciting the specimen passes from the excitation slit and reaches to the well containing sample. Later, emitted signal from the sample passes from the emission slit. In this thesis, using monochromator fluorescence micro plate reader for FRET applications enabled us to record FRET emission spectra and FRET spectral changes. In order to compare acceptor peaks and collect signals from FRET pair emission spectral regions, a negative control group was used.

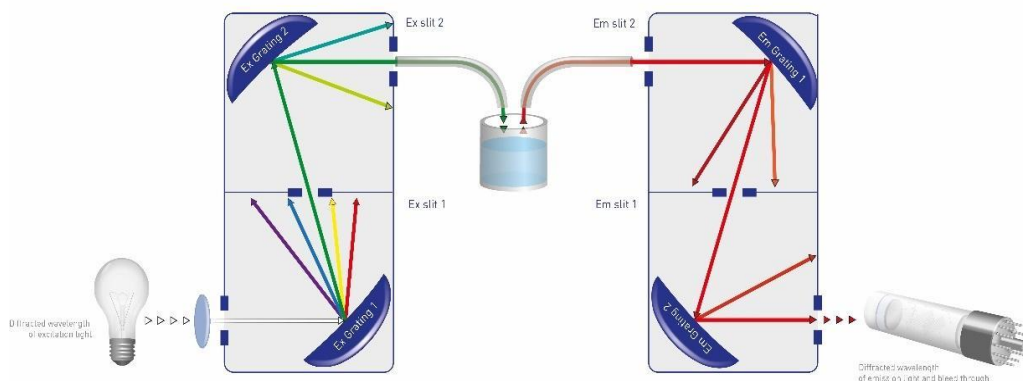
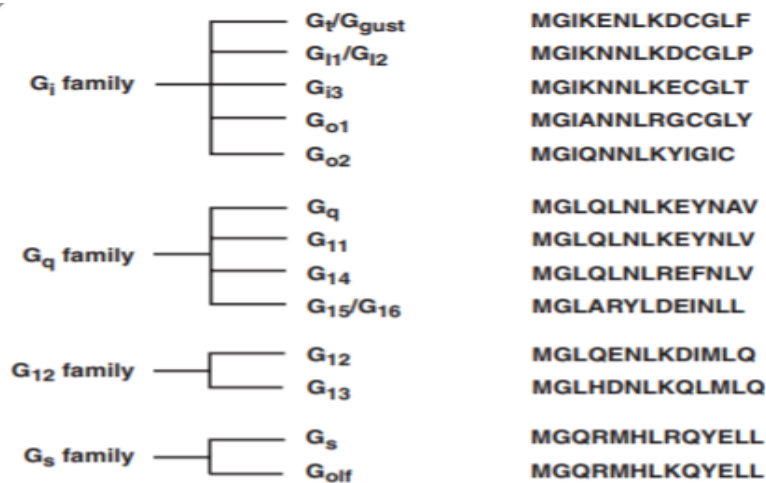


**Figure 1. 13:** Monochromator fluorescence microplate reader component schematic representation. (*Monochromator vs Filter-Based Plate Reader: Which Is Better?* - Promega Connections, n.d.)

#### 1.4.1.2 Minigenes

G proteins interact with their GPCRs in order to transmit signals and initiate proper cellular responses. This interaction occurs via the last 11 amino acids of G $\alpha$  subunit. Many approaches has been developed in order to intentionally prevent this signal transduction for analysing the important components of the pathways. One of those approaches is minigenes. Minigenes used in this study are small cassettes that include ribosome binding sequence, stabilizing glycine amino acids and last 11 amino acid of relevant G $\alpha$  protein (Gilchrist et al., 2002). The function of ribosome binding sequence in this casset is for the recruitment of the mRNA transcript of the minigene to a ribosome for minigene synthesis. Glycine amino acids at the beginning and the end in this cassette stabilize the peptide (Figure 1.14) (Gilchrist et al., 2002).



GCCGCCACCATGGGACAGCGCATGCACCTTCGTCAGTACGAGCTGCTCGGATAA

RED: Ribosome binding sequence

YELLOW: Start codon and stop codon

PURPLE: Protective Glycine amino acid

BLACK: Last 11 amino acid coding sequence of G alpha protein

**Figure 1. 14:** G protein  $\alpha$  subunit specific minigenes and sequence domains (Adapted from (Gilchrist et al., 2002)).

In this thesis, minigenes were used in order to inhibit the interaction between GPCRs and fluorescent protein labeled G $\alpha$  proteins. This approach enabled the investigation of receptor dependency on G $\alpha_i$  and G $\alpha_s$  protein interaction.

## 1.5 Aim of Study

Classical GPCR signaling suggests that, one GPCR can interact with one heterotrimeric G protein. However, recent studies reveal that GPCRs can form dimers and oligomers. GPCR oligomerization allows the cell to tune signaling and give an ability to the cell to respond more precisely. Many GPCR oligomer models were proposed by recent publications such as; A1-A2A heteromer and A2A-D2R

heteromer. In these oligomers, while A2A receptor has binding affinity to G $\alpha$ s protein, both A1 and D2R receptors has binding affinity to G $\alpha$ i protein.

Recent studies show K-Ras protein that belongs to small GTPase family activated by homodimerization (Muratcioglu et al., 2015; Nussinov et al., 2019). Muratcioglu *et al.* also studied this interaction in more details and represented two predicted interfaces for the dimer (Muratcioglu et al., 2015, 2020). In addition, Navarro *et al.* showed A1 and A2A GPCR heterotetramer model with theoretical G $\alpha$ s and G $\alpha$ i protein interaction. This interaction was shown by BRET method in their 2018 study (Navarro et al., 2018).

This study aims to analyze G $\alpha$ i and G $\alpha$ s protein interaction by using FRET technique. Effect of G protein - GPCR interaction on G $\alpha$ i-G $\alpha$ s interaction by the use G $\alpha$  protein specific minigenes and effect of ligand activation via A2A-D2R heterotetramer on G $\alpha$ i-G $\alpha$ s interaction was tested.



## CHAPTER 2

### MATERIALS AND METHODS

#### 2.1 Materials

##### 2.1.1 Mammalian Cell Culture

##### 2.1.1.1 Mouse Neuroblastoma Neuro2a (N2a) Cell Line

In this study, to visualize and investigate the physical interaction between fluorescently tagged G $\alpha$ i and G $\alpha$ s proteins, the N2a cell line was used. N2a cell line cultivation and proliferation processes can be maintained and completed in 2-3 days. Furthermore, transfection applications can easily be performed by using the N2a cell line. In this thesis, an N2a cell line product called CCL-13 *Mus musculus* brain neuroblastoma was purchased from the ATCC company, ENGLAND.

##### 2.1.1.2 Cell Media

N2a growth media was prepared by using OptiMEM®I Reduced Serum Medium with L-glutamine (Invitrogen, Cat#31985047) that makes 44.5% of the media, Dulbecco's Modified Eagle Medium DMEM including high glucose with L-glutamine (Invitrogen, Cat#41966029) that makes 44.5% of the media, 10% of the media is Fetal Bovine Serum (Biological industries, Cat#04127-1B) and 1% of the media is Penicillin/Streptomycin solution (Biological industries, Cat# 03-031-1B). The prepared N2a media was filtered using a 0.22  $\mu$ m filter. The formulation of DMEM is given in Appendix A.

### **2.1.1.3 Maintenance**

Maintenance of the N2a cell culture required an incubator that can be used at 5 % CO<sub>2</sub> and 37 °C. In addition, passage and transfection processes were performed by using Nuve® LN 120 laminar flow cabinet. The passage of the cells was performed every 3 days after reaching 80 % confluency. During the passage, before removing cells from the attached surface, the washing step was performed by using PBS. The passage of N2a cells required Trypl-E Express with phenol red (Invitrogen, Cat#12605-028) and the passage of the cells was performed in the T25 flask. Formulation of PBS was given in Appendix A.

### **2.1.1.4 Other Chemicals and Materials**

Transfection protocol performed by using Lipofectamine™ LTX and Plus™ Reagent purchased from Invitrogen (MA, USA), using the optimized protocol below.

## **2.1.2 Bacteria culture**

### **2.1.2.1 Strain of Bacteria and Bacterial Growth Media**

Bacterial transformation experiments were performed by using *Escherichia coli* XL1-Blue strain. As bacterial growth culture media, Luria Bertani solution was prepared and autoclave sterilized for 20 minutes by using 121 °C from Nuve® OT 40L autoclave machine. In order to apply bacterial selection with antibiotics, ampicillin (100 µg/ml) was used. Transformation of bacterial colonies was collected from LB agar plates incubated after transformation protocol at 37 °C for 16 hours from the ZHWY-200B incubation machine by Zhicheng Instruments. The incubation process of the collected colony inoculation was performed by using liquid LB



solution and incubated into rotary shaker ZHWY-200B by Zhicheng Instruments at 200 rpm for 16h at 37 °C.

### **2.1.3 Cloning**

#### **2.1.3.1 Plasmids, Primers, and Sequencing**

Plasmids containing *Homo sapiens* Gai1 and Gas protein genes and also EGFP and mCherry labeled versions prepared within the scope of TÜBİTAK project numbered 117Z868 and titled as “Investigation of G $\alpha$  protein dimerization mechanisms in live cells”. Unlabeled (carrying wild-type genes) versions of these plasmids were purchased from Addgene. FRET control groups were prepared in our laboratory by a former Master student Hüseyin Evci. EGFP and mCherry plasmids were kindly gifted by Prof. Dr. Henry Lester, California Institute of Technology (CA, USA). The mammalian expression vector containing CMV promoter used in this thesis is pcDNA3.1(-) that was kindly gifted by Prof. Dr. Ayşe Elif Erson Bensen, Middle East Technical University (Ankara /TURKEY).

Primers used in this study were purchased from Integrated DNA Technologies (IDT) (IO, USA) and PRZ Biotech (Ankara, TURKEY). All constructs were sequenced by BMLabosis (Ankara/TURKEY).

#### **2.1.3.2 Other Chemicals and Materials**

Chemical materials were purchased from Sigma Chemical Company (NY, USA). Molecular cloning enzymes like Phire Green Master Mix DNA polymerase, T4 ligase, and 6X DNA dye purchased from Thermo Scientific (MA, USA) and restriction enzymes purchased from New England Biolabs (MA, USA). Generuler

was purchased from Fermentas. Plasmid Miniprep and Gel extraction kits were purchased from Thermo Scientific (MA, USA).

## **2.2 Methods**

### **2.2.1 Cloning**

#### **2.2.1.1 Preparation of Competent *E. coli* Cells by Rubidium Chloride Method**

In order to prepare competent *E. coli* XL1-Blue cells, firstly, cells were streaked on an antibiotic-free LB agar plate and incubated for 16 hours at 37 °C. After the incubation period, a single colony was picked and inoculated with 2 ml antibiotic-free liquid LB media. Inoculated growth tube was incubated from shaker for 16 hours at 37 °C, 200 rpm. Then the overnight grown culture was inoculated into antibiotic-free LB culture media containing 20 mM MgSO<sub>4</sub> with a 1:100 (v:v) ratio. Prepared inoculation flask incubated into shaker at 37 °C, 200 rpm until reaching 0.4-0.6 OD 600. When the subculture reach to OD 0.4-0.6 at 600 nm, the culture was separated into 50 ml falcons and centrifugated at 4000 rpm at 4 °C for 5 minutes. After the centrifugation process, the supernatant was discarded, and the pellet was gently dissolved in 20 ml TFB1 solution then incubated for 5 minutes on ice. After that, the pellet dissolved in TFB1 solution and centrifued at 2000 rpm for 5 minutes at 4 °C. The supernatant was discarded and pellet gently dissolved by using 2 ml TFB2 solution. The falcons incubated on ice for 45 minutes. After the incubation, cells were aliquoted as 50 µl into 1.5 ml Eppendorf tubes and quickly transferred into liquid nitrogen. The competent cell containing Eppendorf tubes were then stored at -80 °C. TFB1 and TFB2 solution preparation was explained in Appendix A.

### 2.2.1.2 Polymerase Chain Reaction (PCR)

In this study, the PCR method was used for EGFP and mCherry fluorescent protein amplifications for  $G\alpha$  tagging and minigene sequence amplification.

For  $G\alpha$  tagging, fluorescent protein amplicants include 24bp overlapping regions with  $G\alpha$  and  $G\beta$  proteins from both 5' and 3' regions. Between overlapping region and EGFP/mCherry sequence, there are 18bp linker sequences (TCTGGAGGAGGAGGATCT). Primer designs were given in Appendix C. Optimal PCR condition was given in Table 1.

For  $G\alpha$  specific minigene construction, gene cassette with the last 11 amino acid sequence of  $G\alpha$  proteins amplified by using PCR mixture given in Table 2.4 and conditions in Table 2.2 and 2.3. Since G-C content was very high, no annealing step was used in PCR for  $G\alpha$  minigene.

**Table 2. 1:**Optimal PCR conditions for  $G\alpha$  tagging

Reagent	Amount			
5X Phire Reaction Buffer	10 $\mu$ l	Pre-	98 °C	30 sec
Phire HS II DNA Polymerase	1 $\mu$ l	denaturation		
DNA Template(EGFP/mCherry)	250-300ng	Denaturation	98 °C	10 sec
10Mm dNTPs	1 $\mu$ l	Annealing	58 °C	30 sec
Forward Primer	1.25 $\mu$ l(20pmol)	Extension	72 °C	1 min
Reverse Primer	1.25 $\mu$ l(20pmol)	Final	72 °C	5 min
DMSO	1.5 $\mu$ l(3%)	Extension		

X 34

Nuclease Free Water	Up to 50 μl
Total	50 μl

**Table 2. 2:** Optimal PCR conditions for *Gai* Minigene Preparation

Pre-Denaturation	98°C	30 sec.
Denaturation	98°C	10sec.
Annealing	55°C	30 sec.
Extension	72°C	10sec.
Final Extension	72°C	1 min.

**Table 2. 3:** Optimal PCR conditions for *Gas* Minigene Preparation

Pre-Denaturation	98°C	30 sec.
Denaturation	98°C	10sec.
Extension	72°C	10sec.
Final Extension	72°C	1 min.

**Table 2. 4:** PCR mixture for *Gα* minigene Preparation

Reagent	Amount
Phire Green Master Mix	10 μl
<i>Gai</i> / <i>Gas</i> wt in pcDNA3.1 (-)	100ng
Forward Primer	0.25μl from 20 μM stock
Reverse Primer	0.25μl from 20 μM stock
Nuclease free water	Up to 20μl

### 2.2.1.3 PCR Integration Method (Overlap Extension PCR Method)

Fluorescent protein amplicants with overhanging regions that match with G protein  $\alpha$  subunits were inserted into  $G\alpha$  proteins. Confirmed amino acid positions of the insertions are A121-E122 and L91-K92 for  $G\alpha_i$  and E73-S85 for  $G\alpha_s$  proteins. For this insertion method, fluorescent proteins with proper overhang regions that match the appropriate  $G\alpha$  gene should produce and amplified by using PCR. For the second PCR reaction, those amplicants were used as megaprimers with a 1:5 template primer ratio. Matched regions of the mega primer bind the  $G\alpha$  gene matching region and produce a whole new artificially produced non-methylated plasmid. All methylated unlabeled template plasmids were digested via DpnI. The conditions of the method and a schematic figure about the method were given in Table 2.5 and Figure 2.1.

**Table 2. 5:** Optimized integration PCR protocol

Reagent	Amount				
Phire Green HS II Master Mix	10 $\mu$ l	Pre-denaturation	98 $^{\circ}$ C	3 min	} X 18
DNA Template( $G\alpha_i/s$ in pcDNA 3.1(-))	100ng	Denaturation	98 $^{\circ}$ C	30 sec	
1st PCR products	500ng	Annealing	51-65 $^{\circ}$ C	1min	
DMSO	1.5 $\mu$ l(3%)	Extension	72 $^{\circ}$ C	2 min/kb	
Nuclease Free Water	Up to 50 $\mu$ l	Final Extension	72 $^{\circ}$ C	5 min	
Total	50 $\mu$ l				

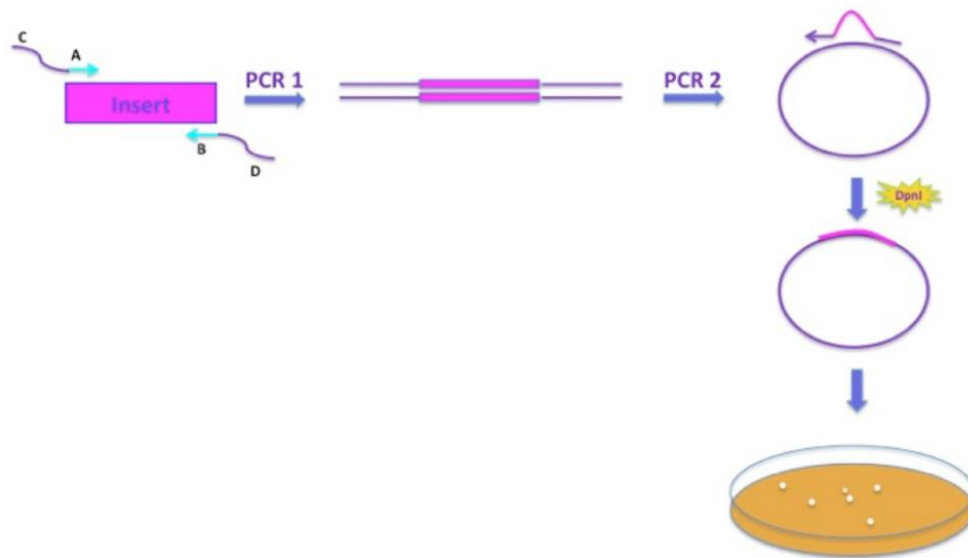


**Figure 2. 1:** Overlapping extension PCR representation. A and B parts of PCR primer representation fit with the insertion sequence, while C and D parts fit the vector that insertion was performed. (Taken from <https://bitesizebio.com/20958/overlap-extension-pcr-cloning/>)

#### 2.2.1.4 Agarose Gel Electrophoresis

DNA samples amplified via PCR and restriction products for fluorescent protein tagging were visualized to control and validate amplification by using 1 % agarose gel. On the other hand, samples of DNA for minigene preparation were visualized via 2 % agarose gel. The agarose gels were prepared as 100 ml volume and 36  $\mu$ l Ethidium Bromide (EtBr) added into the gel as DNA chelator to visualize using UV light. Firstly, 1 gram of agarose for 1 % or 2 grams of agarose for 2 % gel was weighted and added into 100 ml 1X TAE buffer. The mixture was heated with microwave until the agarose pieces were dissolved. Then liquid agarose gel mixture was cooled with tap water for 30 seconds, and after cooling, 36  $\mu$ l EtBr was added and mixed well. The gel was poured into a gel box with appropriate combs. After polymerization, DNA samples were prepared via diluting loading dye (Thermo

Scientific, #R0611) from 6X to 1X. The samples were loaded into wells, and Generuler (Fisher, Product code:11803983) was used as a DNA marker. The Samples run for 35 minutes with 110V. 50X TAE buffer stock solution preparation protocol can be found in Appendix A.

#### **2.2.1.5 Extraction from Agarose Gel**

Amplification of PCR products and restriction products were loaded to agarose gel and visualized via UV. Comparing with the appropriate position of the DNA ladder, DNA bands were cut and placed into 1.5 ml Eppendorf tubes. The gel contained Eppendorf tube weight was measured, and empty Eppendorf tube weight was subtracted from it. GeneJET Gel Extraction Kit (Thermo Fisher Scientific, #K0691) was used to extract DNA from agarose gel, and the protocol given by the kit was applied. In the final step, 30  $\mu$ l preheated nuclease-free water was used for DNA elution from the column membrane instead of the 50  $\mu$ l Elution Buffer provided by the kit to increase eluted DNA yield.

#### **2.2.1.6 Determination of DNA Amount**

In order to detect the yield of DNA products, BioDrop  $\mu$ LITE device was used. Before measurement, the sample loading space was washed via distilled water to clean the remaining samples from other measurements. Then device opened and calibrated itself. Life sciences section and DNA subsection were selected and 1 $\mu$ l nuclease-free water was used as blank. After blank measurement, 1 $\mu$ l DNA sample was loaded on sample loading space, and the measurement was taken.

#### **2.2.1.7 Restriction Enzyme Digestion**

New England Biolabs Inc. (NEB) (MA,USA) restriction digestion enzymes were purchased for this study. Sticky ended products were obtained after the restriction

process. As NEB's instruction manual suggested, the restriction process was performed with 1 unit of enzyme for 1 µg of DNA. In this study, at least 1000 ng DNA was used for the restriction processes with 1 µl enzyme and 1.5 µl CutSmart® NEB buffer, and the final volume was completed to 20 µl. The final mixture mixed well and incubated for 4 hours at 37 °C.

#### **2.2.1.8 PCR Purification**

In order to remove restriction components and purify the DNA product, PCR purification was applied by using the Thermo Scientific GeneJet Purification kit (#K0702). The protocol given by the kit was applied, but the elution step was performed by using 30 µl nuclease-free water instead of 50 µl EB to increase yield.

#### **2.2.1.9 Ligation**

Ligation reaction was used to covalently bind the DNA products and the vector plasmid that are restricted compatibly. In this study, the ligation process was applied to insert sticky-ended restriction products into expression vector pcDNA3.1(-). Vector to insert ligation ratio as 1:3, 1:5, 1:10, and 1:15 was calculated according to the 150 ng restricted vector. 20 µl ligation reaction includes at least 150 ng restricted vector, insert, 1µl T4 DNA Ligase enzyme (NEB, Cat#0202T) and 1X 2 µl T4 DNA ligase buffer, and then the total volume was completed to 20 µl by using nuclease-free water. The ligation reaction was incubated at room temperature for 16 hours.

#### **2.2.1.10 Transformation of Competent *E. coli* Cells**

Bacterial transformation protocol applied for transferring a vector that carries desired gene into a bacterial host. In this study, this protocol was applied to ligation products and plasmids that need to be amplified. RbCl competent *E. coli* XL1 blue strain used



as a bacterial host that was stored at -80 °C. Competent cells were taken from -80 °C and kept on ice for 15 minutes. After 15 minutes of incubation time, 7 µl ligation product and 1 µl circular plasmid were added into a competent cell tube, pipetted well under sterile conditions. The mixture of DNA and bacteria was incubated on ice for 30 minutes. Later, the tube containing DNA and competent cells were heat-shocked at 42 °C for 45 seconds. Then the tube was incubated on ice for 3 minutes. After incubation, 750 µl SOC was added into the tube, and the tube was incubated for 1 hour on shaker at 37 °C, 180 rpm. After the tube was centrifuged at 4000 rpm, 600 µl supernatant was discarded and the pellet was dissolved with the remaining SOC. The dissolved pellet was spread on LB agar plate prepared with ampicillin since the vector used in this study (pcDNA3.1(-)) has an ampicillin resistance gene. Agar plates were incubated at 37 °C for 14-16 hours for bacterial colony growth.

#### **2.2.1.11 Plasmid Isolation from *E. coli***

Plasmid DNA isolation protocol was performed by using Thermo Scientific's GeneJET plasmid miniprep kit and protocol provided by the kit(#K0503). Single colony was selected on the agar plate and inoculated into 5ml LB with 5 µl ampicillin and worked sterile. LB with antibiotic and bacteria colony was incubated at 37 °C for 16 hours with 180 rpm. Later, the LB tube centrifugated at 4000 rpm. Supernatant discarded and protocol provided by the kit was applied on the pellet. The elution step was performed by using 70 µl nuclease-free water instead of 100 µl EB to increase yield.

## **2.2.2 Mammalian Cell culture**

### **2.2.2.1 Passage And Cell Seeding**

In this study, Neuro2A (N2A) cell line from *Mus musculus* was used as a mammalian cell line. N2A cells have approximately 70 hours of doubling time, so passage protocol was applied after 3-4 days of incubation. During the incubation time, N2A cells were grown into a T25 flask and incubated at 37 °C and 5% CO<sub>2</sub>. For passaging process, the flasks were taken into the laminar flow, the cell media in flask was suctioned, and cells were washed gently by using warm 1X PBS. Later, PBS was suctioned and 500 µl Trypl-E was added to the top of the cells. The flask was transferred into 37 °C incubator with 5% CO<sub>2</sub> for 5 minutes. Then 8ml N2A media was added into the incubated flask in the laminar flow, pipetted gently. New T25 flask labeled and 8ml N2A media was added into it. 400 µl cell media with N2A cells were taken from the old flask and added into the prepared flask. The new flask was incubated at 37 °C incubator with 5% CO<sub>2</sub> until the next passage. These cells were used until the 45<sup>th</sup> passage.

The cells from the old flask were kept, and 10 µl of the cell suspension was transferred onto hemocytometer with a coverslip. Under microscope (100X), the cells were counted from the 4 corners, and then total number was divided to 4 and multiplied to 10.000 to find the cell number in 1ml suspension. 120.000 cells for 35mm plastic dishes and 60.000 cells for 35mm glass bottom dishes were calculated and seeded. Glass bottom dishes were used for microscope imaging and plastic bottom dishes were used for plate reader experiments.

For plate reader experiments, after 1 day of transfection incubation, cells were lifted and 10.000 cells were seeded into 96 well plates.

#### **2.2.2.2 Transfection of mammalian expression vector to N2a cells**

In order to artificially introduce DNA samples into mammalian cells, a transfection protocol was used. Transient transfection performed by using Lipofectamine™ LTX with Plus™ Reagent purchased from Invitrogen (MA, USA) for this thesis study since it this product has more than 80 % transfection efficiency rate (Maurisse et al., 2010). For the transfection process, 60.000 and 120.000 cells were seeded on glass and plastic dishes, respectively, followed by 2 ml media addition. The dishes were incubated for 24 hours before transfection process for cell attachment. Following day, 100-300 ng of plasmid DNA for microscope imaging and 100-500 ng of plasmid DNA for plate reader experiments was added into 100 µl OptiMEM™ and mixed. 4 µl Plus™ reagent was added into a plasmid and 100 µl OptiMEM™ containing tubes. The mixture was incubated for 15 minutes at room temperature. During the incubation time, a new set of 100 µl OptiMEM™ tubes were prepared. 4 µl Lipofectamine™ LTX was added into tubes that were contained only OptiMEM™. After the incubation time, the tubes containing lipofectamine and added 100 µl OptiMEM™ were mixed with the tubes containing Plus™ Reagent contained and 100 µl OptiMEM™ with plasmid DNA. The final mixture was incubated for 15 minutes at room temperature. During incubation, dishes with cells were taken from the incubator, and the media was suctioned from the dishes. The cells were gently washed with 1ml 1X PBS. 1ml PBS was suctioned, and 680 µl OptiMEM™ was added on top of the cells. When the incubation time ended, 200 µl transfection mixture was dropped into cells with 680 µl OptiMEM™. The dishes were incubated at 37 °C with 5% CO<sub>2</sub> for 3 hours and 2ml media was added afterward. For confocal microscopy experiments, the dishes were incubated for 2 days for imaging and were used afterwards. For plate reader experiments, dishes were incubated 1 day and then cells were lifted and seeded into 96 well plate.

## **2.2.3 Fluorescence Measurements**

### **2.2.3.1 Imaging with Spinning Disc Confocal Microscope**

After transfection of EGFP and mCherry tagged  $G\alpha$  proteins to N2A cells, and following incubation time, glass-bottom dishes were imaged by using Leica DMI 4000 equipped with Andor DSD2 spinning disc confocal microscope. The reason for the usage of the Andor DSD2 spinning disc microscope is that it has a frame rate maximum of 22 frames per second with 370 – 700 nm excitation range and 410 – 750 nm emission range. The spinning disc enables the rejection of non-focused light and gives sharper images. The imaging process was performed by using 63X immersion oil NA 1.4 objective lens.

For confocal microscopy FRET experiments, 3-Cube method was used. Plasmids were transfected into 60.000 N2a cells on the 35mm glass bottom dishes. For each FRET pair, three dishes were prepared. The first dish contained only  $G\alpha$  protein gene tagged with EGFP sequence, the second one contained  $G\alpha$  protein gene tagged with mCherry sequence, and the third one contained both EGFP and mCherry tagged  $G\alpha$  protein genes. First and second dishes used for bleed through calculations.

For bleed through dishes, two imaging setups were used, and images were taken as stacks of both images. Only EGFP tagged  $G\alpha$  protein containing dishes were excited with 470-500 nm wavelengths, and emission spectrums were set as 500-550 nm that collects green signal (donor channel) and 600-650nm that collects red signal (FRET channel). Only mCherry tagged  $G\alpha$  protein containing dishes were excited with 560-600 nm (Acceptor Channel) and 470-500nm, and the emission spectrum was set as 600-650 nm that collects red signal. All three imaging setups were used for FRET dish, and images were taken as stacks containing three images.

### **2.2.3.2 Measurement with Monochromator plate reader**

After imaging and visualization with a confocal fluorescent microscope, Fluorescence microplate reader measurements were taken. While imaging with a confocal fluorescent microscope, approximately 50-100 cell images were collected, but 96 well plate measurements can give a signal combination of 10.000 cells; therefore, the results would more accurately represent the whole population of transiently transfected cells. In addition, the fluorescence plate reader enables to arrange specific excitation wavelengths according to its slit width. In this study, SpectraMax iD3 Multi-Mode Microplate Reader (Thermo Scientific) was used as a monochromator plate reader with 450 nm excitation for donor fluorophore EGFP, and 490-750nm spectral emission to collect overall EGFP and mCherry emission spectrum signals. For FRET measurements, only donor, only acceptor, and FRET groups were transfected to N2A cells and 10.000 cells seeded into SPL black 96 well plates. If there is an energy transfer between donor and acceptor fluorophores EGFP and mCherry, normalized spectrum gives lower EGFP peak and increased mCherry peak. Therefore, spectral emission signals were normalized and EGFP and mCherry peaks were compared to investigate if there is an energy transfer or not.

### **2.2.4 Image Analysis with Pix-FRET Program**

The physical interaction of proteins can be investigated by using the FRET technique. Although many advantages of FRET over other methods like enabling live-cell investigations, spectral bleed-through should be in consideration. When donor and acceptor excitation and emission spectrum overlap, excitation of the donor may also excite the acceptor, and donor emission spectra may leak to acceptor fluorophore emission spectra. These situations cause false FRET signals and are called spectral bleed through. For FRET experiments, three groups were used; the first one expresses only donor fluorophore tagged protein, the second one expresses only the acceptor fluorophore tagged protein, and the last group is the FRET group

that expresses both of these proteins. In this thesis study, the Pix FRET plug-in of ImageJ was used for FRET calculations of confocal microscope images (Ro<sup>^</sup>mero<sup>^</sup> *et al.*, n.d.). PixFRET allows to eliminate false FRET signals by analyzing signals from the only donor expressing and only acceptor expressing cell images used (Ro<sup>^</sup>mero<sup>^</sup> *et al.*, n.d.). During analysis to determine spectral bleed-through, only donor and only acceptor images were loaded into ImageJ program PixFRET plug-in. Ten FRET group images were analyzed, and FRET efficiencies were determined cell by cell (Ro<sup>^</sup>mero<sup>^</sup> *et al.*, n.d.)

### **2.2.5 Functional Analysis with cAMP-Glo™ Assay**

The functionality of fluorescent protein labeled G $\alpha$  proteins produced in TÜBİTAK 1001 project 117Z868 and titled “Investigation of G $\alpha$  protein dimerization mechanisms in live cells” analyzed with cAMP-Glo™ assay produced by Promega (WI, USA). The assay principle depends on cAMP concentration measurement in a cell. If cAMP concentration increases in cells, cAMP binds to protein kinase A(PKA). There are two catalytic and two regulatory domains of PKA. If there is no cAMP in the cellular environment, PKA remains in the inactive form. During activation and cAMP production, the regulatory component changes its conformation, and the catalytic component is released. The released catalytic subunit catalyzes ATP transfer terminal and produces PKA substrate. Therefore, unused ATP level measured with cAMP-Glo assay with Kinase Glo reagent, which is a luciferase-based reagent. Concentration changes of ATP can be determined as light intensity. In addition, the cAMP level is inversely proportional to the luminescence signal. When cAMP increase, the luminescence signal decrease (Figure 2.2).

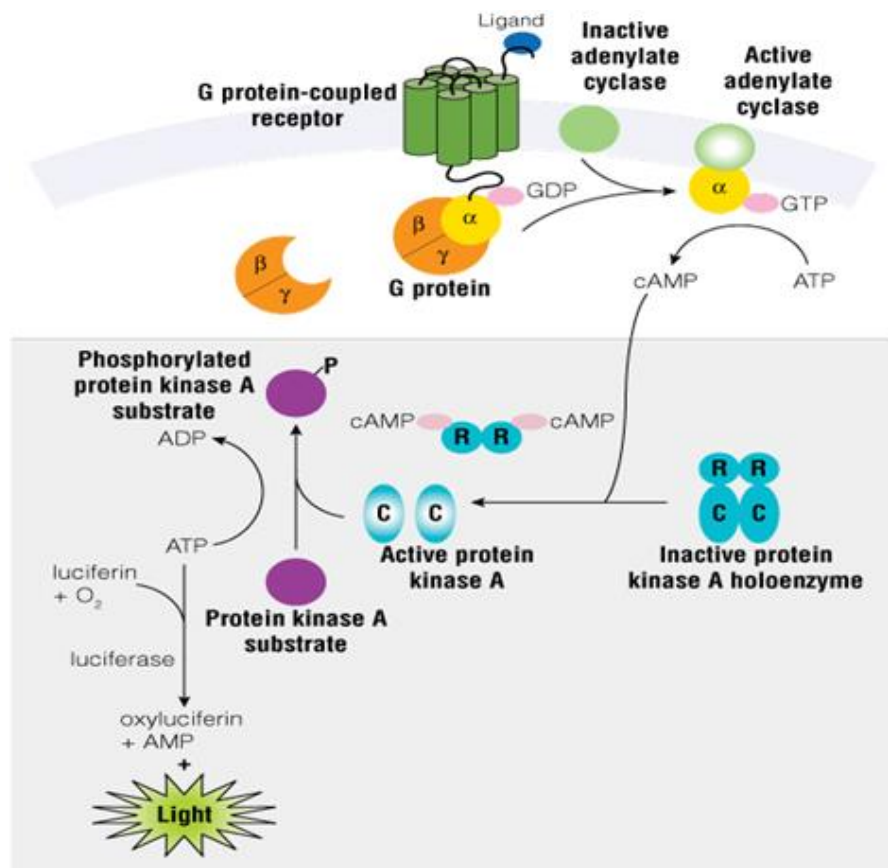


**Figure 2. 2:** cAMP-Glo™ Assay kit working principle. (Taken from [www.promega.com](http://www.promega.com))

Gai protein activation with D2R results in inhibition of cAMP level while Gas protein activation with A2A receptor increases cAMP concentration. Therefore, the activity of Gai protein causes an increase of luminescence signal while Gas protein activity results in a decrease.

In this study, 120.000 N2A cells were seeded onto 35 mm plastic bottom dishes and incubated for 24 hours. After incubation time, 500 ng plasmids of fluorescently labeled Gα proteins were transfected via Lipofectamine LTX with Plus Reagent, and incubated for 24 hours. Then, cells were lifted and counted. 10.000 cells were seeded on 96 well white SPL immunoplate. The next day, before kit protocol, Gαi transfected cell containing wells were treated with 20 µl of 20 µM forskolin (Sigma-Aldrich, #66575-29) for the cAMP increase and incubated for 30 minutes at 37 °C

with 5% CO<sub>2</sub>. Then, forskolin was removed and 10 μM Quinpirole (Sigma-Aldrich, #73625-62) dissolved into 1X induction buffer (formulation in Appendix A) added into wells as D2R agonist, incubated at 37 °C with 5% CO<sub>2</sub> for 20 minutes (DM et al., 2014). For G<sub>αs</sub> expressing cells, 15.5 μM 20μl CGS 21680 (Sigma Aldrich, product# 119137) dissolved into 1X induction buffer added as A2A receptor agonist and incubated for 20 minutes at 37 °C with 5 % CO<sub>2</sub> (D *et al.*, 2011). After the A2A receptor and D2R activation with proper agonists, assay protocol was performed according to the manual given by the supplier.

### **2.2.6 Statistical analysis**

Graphpad Prism is computer software used by scientists for basic statistical analysis of scientific data. The program enables its users to combine graphs, calculate statistical analysis, and organize data. In this thesis study, data analyses were performed by using Graphpad prism 8. To analyze the data with Graphpad Prism 8, One Way ANOVA was used to analyze more than two groups with one condition. T-Test used to compare two different groups with one condition. Results were presented as mean ± standard error of the mean (SEM). P values less than or equal to 0.05 are considered significantly different.



## CHAPTER 3

### RESULTS AND DISCUSSION

#### 3.1 Functional Analysis of EGFP and mCherry Tagged $G\alpha$ proteins by cAMP-Glo Assay Kit

In this thesis,  $G\alpha i$  proteins that were labeled between 91<sup>st</sup>-92<sup>nd</sup> and 121<sup>st</sup>-122<sup>nd</sup> positions and  $G\alpha s$  protein that was labeled from 73-85 position with mCherry and EGFP were used as FRET pairs. These constructs were prepared by a former Lab. member Ms. Özge Atay. The functionality of  $G\alpha s$  protein that was labeled with EGFP and mCherry proteins, and  $G i$  121 EGFP were tested with cAMP -Glo Assay Kit purchased from Promega (WI, USA) in our laboratory during previous studies.  $G\alpha i$  91-92 EGFP and mCherry and  $G\alpha i$  121 mCherry functionalities were tested with the same kit during this thesis period. The results obtained from these functionality analysis presented in Figure 3.1.

##### Functional analysis of Fluorescently Labeled $G\alpha$ Proteins

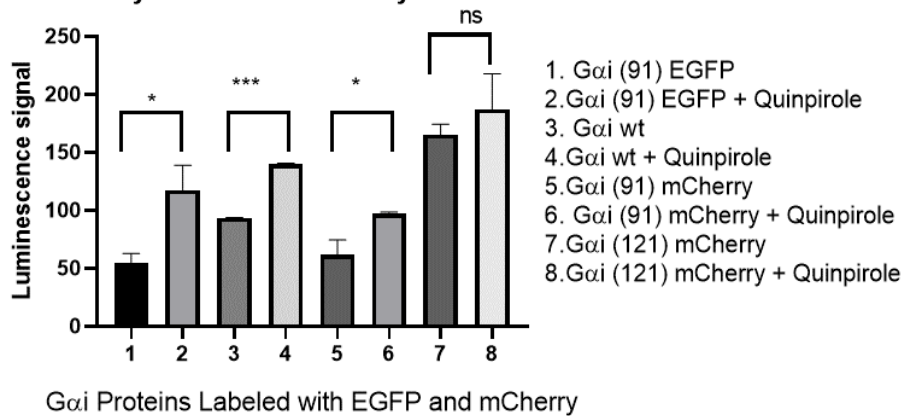


**Figure 3. 1:** cAMP-Glo Assay results of  $G\alpha$  proteins labeled with EGFP and mCherry fluorophores. (Unpaired T-test applied for determination of the luminescence difference after ligand treatment,  $G\alpha$  91 EGFP p value:  $0.0323 < 0.05$ ,

Gα 91 mCherry p value: 0.0347<0.05, Gα wild type p value: 0.0003<0.05, Gα 121 mCherry p value: 0.4627>0.05)

As mentioned in Chapter 1, Gαi proteins inhibit cAMP production in the cell and Gαs proteins are cAMP stimulatory proteins. The principle of cAMP-Glo Assay Kit is based on detection of cAMP via luminescent signal, which has an inverse proportion with cAMP concentration in the cell. Thus, according to the assay principle and Gαi protein activity, luminescence signal increase was expected due to reduced cAMP concentration upon Gi coupled GPCR stimulation via an agonist ligand, Quinpirole. The assay was performed with the wild-type Gαi control group, and luminescence increase was compared.

Before Quinpirole treatment of the cells transfected with Gαi plasmids, Forskolin treatment was applied to increase basal cAMP concentration to observe Gαi effect much clearly. After ligand treatments, assay protocol was performed, and luminescence measurements were taken. T-test was applied to the groups that include cells transfected with the same plasmids for statistical analysis. Functionality of Gαi 91 EGFP and mCherry plasmid luminescence increase after Quinpirole treatment shows the functionality of these plasmids compared to only Forskolin treated group. However, Gαi 121 mCherry plasmid luminescence increase between Quinpirole treated and only forskolin treated group was not found significant according to T-test. The reason for this observation could be the constitutive activity of Gαi 121 mCherry protein due to a conformational change that could arise because of the tagging position and maturation time of mCherry. (See Appendix E)

### **3.2 Confirmation of Membrane localization of G $\alpha$ Proteins and FRET Control Groups with Membrane Targeted Organelle Marker**

Biological activity controlled EGFP and mCherry labeled G $\alpha$ i and G $\alpha$ s plasmids were transiently transfected into 60.000 N2A cells (for 35mm glass dishes 300 ng DNA was used). Since G $\alpha$ i 121 mCherry protein showed constitutive function this construct was not used in further experiments. Instead, EGFP labeled version of this construct was used. The expected cellular membrane expression pattern of G $\alpha$  proteins was validated by using plasma membrane marker Gap43 labeled with EGFP and mCherry fluorophores. Gap43 protein is a membrane-targeted protein (Huang *et al.*, 2015). Gap43 was labeled with EGFP and mCherry fluorescent protein by a former student of our laboratory Mr. Hüseyin Evci. Furthermore, a positive FRET control group with Gap43 mCherry (RGSLVPR) EGFP prepared by Mr. Hüseyin Evci was used during this thesis work (Albertazzi *et al.*, 2009).

Confocal microscope localization validation experiments showed G $\alpha$ i and G $\alpha$ s fusion proteins and Gap43 control group were located at the plasma membrane. Confocal images can be seen from Figure 3.2, Figure 3.3, Figure 3.4 and Figure 3.5.

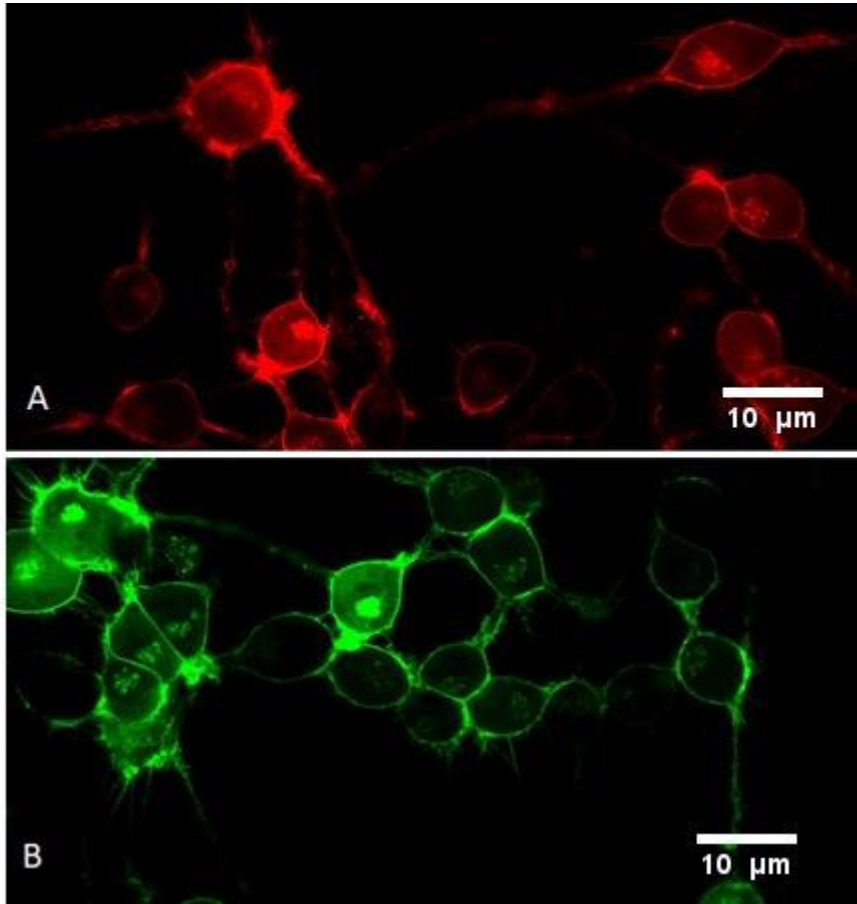


**Figure 3. 2:** Membrane targeted organelle marker Gap43 sequence labeled with A) mCherry and B) EGFP. mCherry protein samples were excited with 583 nm for 1000 ms, 100 % light intensity. EGFP protein samples excited with 482 nm for 1000 ms with 50 % light intensity, 63x and NA 1.4. objective was used for both channels.

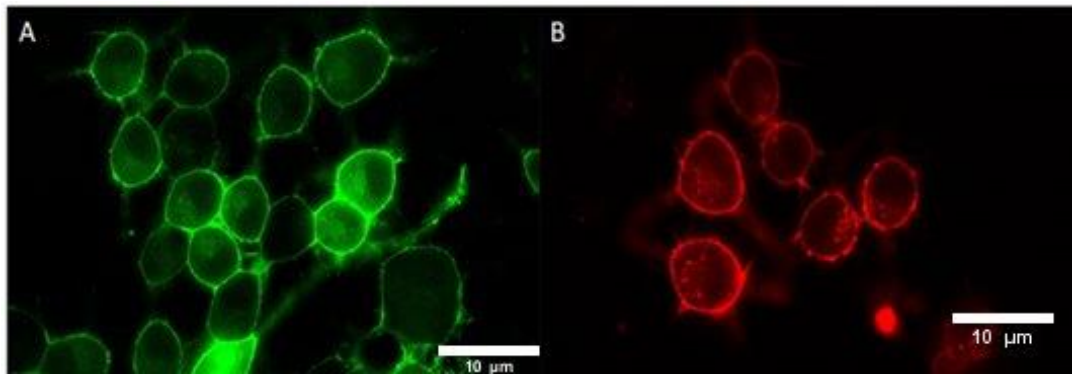


**Figure 3. 3:** Fluorescent protein labeled *Gas*  $\Delta$ 73-85 protein visualization. A)EGFP labeled *Gas*  $\Delta$ 73-85 protein, and B) mCherry labeled *Gas*  $\Delta$ 73-85 protein visualization. EGFP protein samples excited with 482nm for 1000 ms with intensity 50 % , 63x and NA 1.4. mCherry protein samples excited with 583nm, intensity 100% , 63x and NA 1.4.

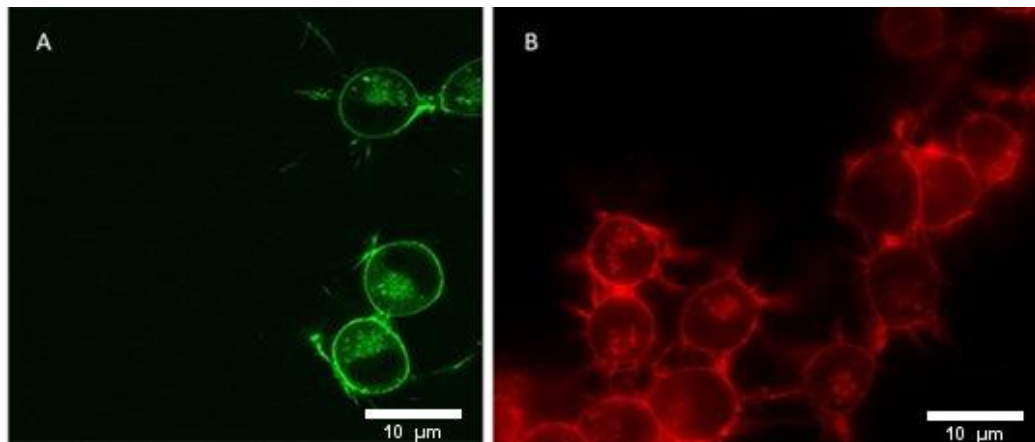


**Figure 3. 4:** Fluorescent protein labeled *Gai* 91 protein visualization. A)EGFP labeled *Gai* 91 protein, and B) mCherry labeled *Gai* 91 protein visualization. EGFP protein samples excited with 482nm for 1000 ms with intensity 50% , 63x and NA 1.4. mCherry protein samples excited with 583nm for 500ms. with intensity 100%, 63x and NA 1.4.

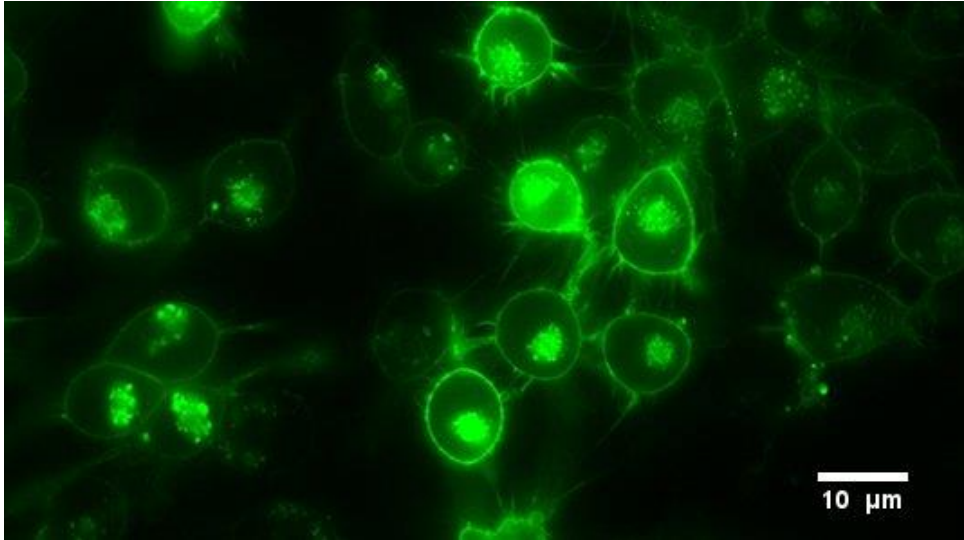


**Figure 3. 5:** EGFP Fluorescent protein labeled *Gai* 121 protein visualization. EGFP protein samples excited with 482 nm for 1000 ms with intensity 50 %, 63x and NA 1.4.

### **3.3 Investigation of Interaction Between *Gai* and *Gas* Proteins with FRET by Using Confocal Microscope**

After localization confirmation of the EGFP and mCherry labeled  $G\alpha$  protein constructs, interactions between *Gai* and *Gas* proteins were investigated using *Gai*(91) and *Gai*(121) EGFP and *Gas*(73-85) mCherry plasmids. Constructs were transfected into N2a cells as 300 ng for 60.000 cells after the optimization process

for FRET study with spinning disc confocal microscopy imaging. 300 ng Gap43 EGFP and Gap43 mCherry plasmids were co-transfected to 60,000 N2a cells used as negative control group. In addition to this, Gap43 mCherry(RGSLVPR)EGFP fusion protein (Gap43 mCherry-L-EGFP) was used as the positive control group (Albertazzi *et al.*, 2009).

Imaging was performed with three sets of imaging tracks; FRET, EGFP, and mCherry. The reason for using EGFP and mCherry tracks is to calculate Spectral Bleed Through (SBT) that is used in PixFRET plug-in to calculate net FRET. The number of cells imaged in each set was approximately 20. Images from each set were SBT normalized and analyzed by using PixFRET plug-in of ImageJ. FRET efficiency ranges (1-10%, 11-20%, 21-30%, 31-40% and 41-50%) were determined and visualized via 5-ramp option with color code ruler and presented in Figure 3.6, Figure 3.7 and Figure 3.8.

Gap43 EGFP and Gap43 mCherry co-transfection group FRET efficiency value was calculated between 0-10% as shown in Figure 3.8 and Figure 3.9. The reason for this FRET value is long range (9-10 nm) random interactions between Gap43 EGFP and Gap43 mCherry fusion protein interactions at the N2a cell membrane. Gap43mCherry-L-EGFP positive FRET control group %FRET efficiency value was calculated between 3-30%. G $\alpha$ i(91) EGFP and G $\alpha$ s(73-85)mCherry fusion protein interaction FRET efficiency value was also calculated between 0-30% as presented in Figure 3.6 and Figure 3.9. Similarly, G $\alpha$ i(121) EGFP and G $\alpha$ s(73-85)mCherry fusion protein interaction FRET efficiency value was calculated as 0-30%.

It was found that up to 10% FRET efficiency, % pixel number of G $\alpha$ i – G $\alpha$ s FRET pairs are significantly different than Gap43 negative control group as shown in Figure 3.10( $p < 0.05$ ), (See Appendix F). This result indicates, a physical interaction between G $\alpha$ i and G $\alpha$ s as close as the positive control where the donor and the acceptor are physically linked to each other.

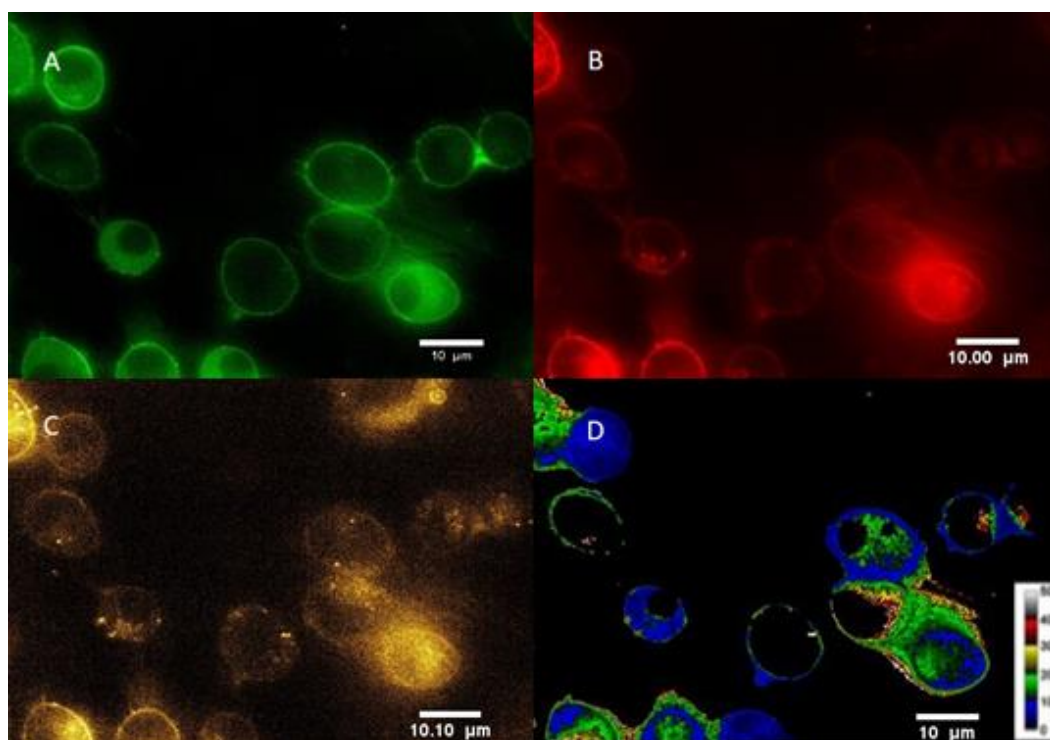


**Figure 3. 6:** Confocal FRET imaging of *Gai*(91)-EGFP and *Gas*(73-85)-mCherry. 300ng of *Gai*(91)-EGFP and *Gas*(73-85)-mCherry co transfected into N2a cell line. A) Image of EGFP channel; channel excitation at 482 nm with exposure time 0.5 s and intensity 50%. B) Image of mCherry channel; channel excitation at 586 nm with exposure time 1s and intensity 100%. C) Image of FRET channel; channel excitation at 482 nm with exposure time 0.5 s and intensity 50%. D) FRET efficiency in color scale; blue ,green, yellow,red and whire colors represent 0-10%, 11-20%, 21-30%, 31-40%, and 41-50% efficiencies of FRET, respectively.



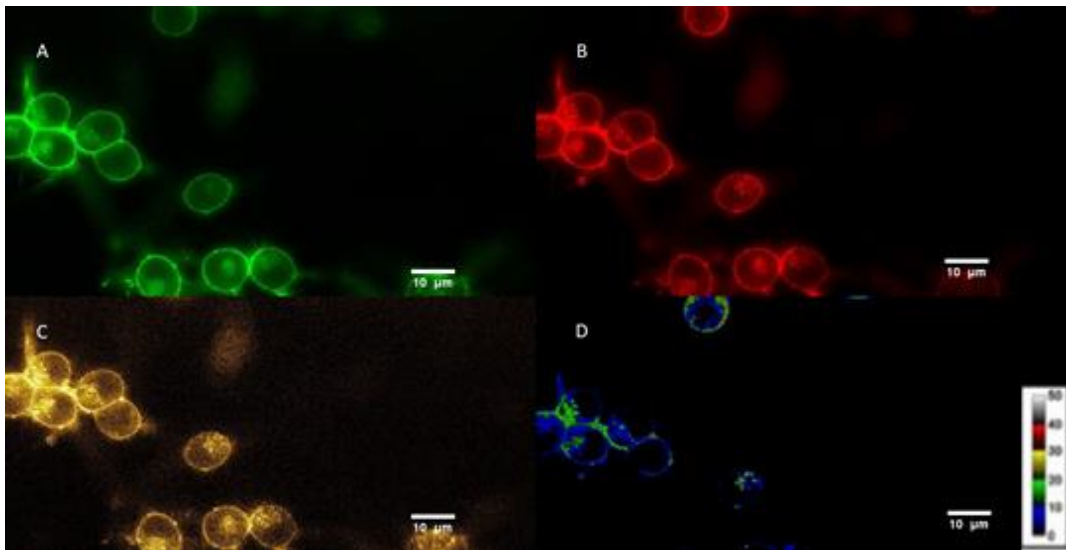


**Figure 3. 7:** Confocal FRET imaging of Gai(121)-EGFP and Gas(73-85)-mCherry. 300ng of Gai(121)-EGFP and Gas(73-85)-mCherry co transfected into N2a cell line. A) Image of EGFP channel; channel excitation at 482 nm with exposure time 0.5 s and intensity 50%. B) Image of mCherry channel; channel excitation at 586 nm with exposure time 1s and intensity 100%. C) Image of FRET channel; channel excitation at 482 nm with exposure time 0.5 s and intensity 50%. D) FRET efficiency in color scale; blue ,green, yellow,red and white colors represent 0-10%, 11-20%, 21-30%, 31-40%, and 41-50% efficiencies of FRET, respectively.

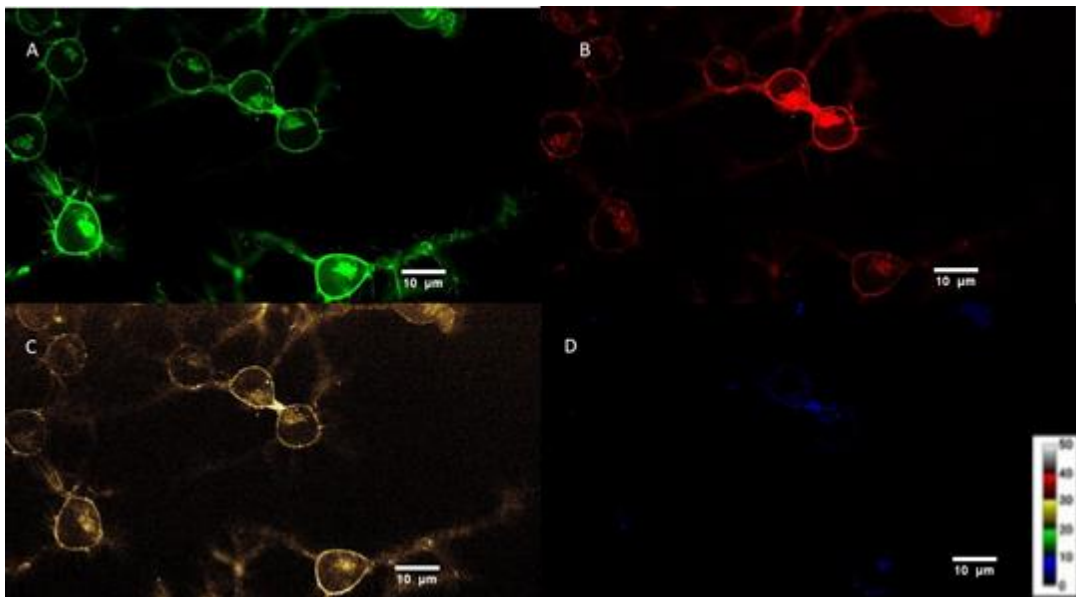


**Figure 3. 8:** Confocal FRET imaging of Gap43 EGFP and Gap43-mCherry. 300ng of Gap43 EGFP and Gap43mCherry co transfected into N2a cell line. A) Image of EGFP channel; channel excitation at 482 nm with exposure time 0.5 s and intensity 50%. B) Image of mCherry channel; channel excitation at 586 nm with exposure time 1s and intensity 100%. C) Image of FRET channel; channel excitation at 482 nm with exposure time 0.5 s and intensity 50%. D) Image of FRET efficiency; blue represents 0-10%, green 11-20%, yellow 21-30%, red 31-40%, and white 41-50% efficiency of FRET.

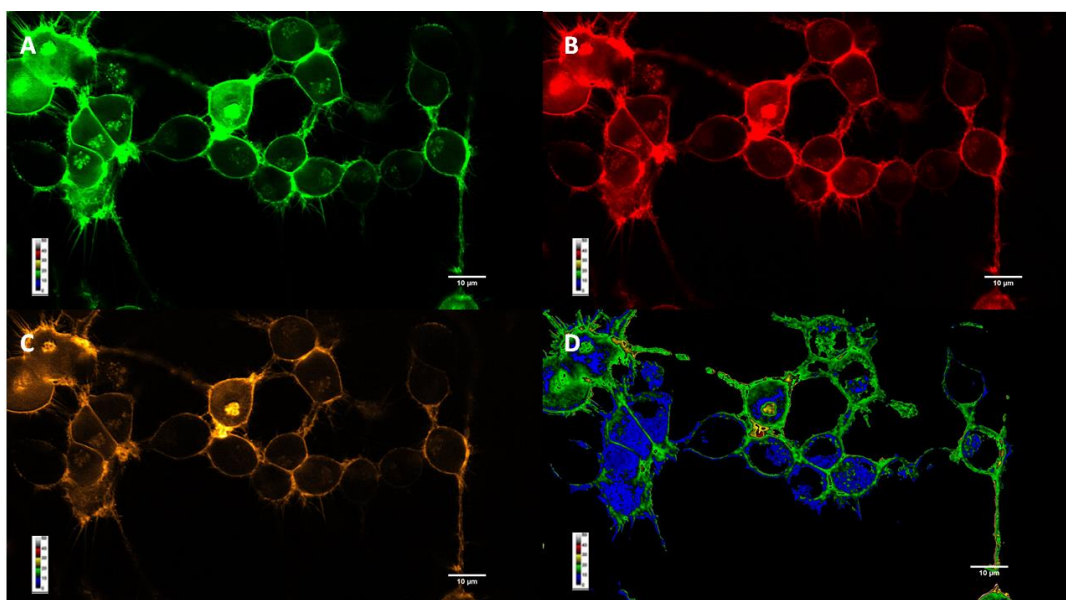


**Figure 3. 9:** Confocal FRET imaging of Gap43mCherry-L-EGFP. 300ng of plasmid transfected into N2a cell line. A) Image of EGFP channel; channel excitation at 482 nm with exposure time 0.5 s and intensity 50%. B) Image of mCherry channel; channel excitation at 586 nm with exposure time 1s and intensity 100%. C) Image of FRET channel; channel excitation at 482 nm with exposure time 0.5 s and intensity 50%. D) FRET efficiency in color scale; blue ,green, yellow,red and whire colors represent 0-10%, 11-20%, 21-30%, 31-40%, and 41-50% efficiencies of FRET, respectively.

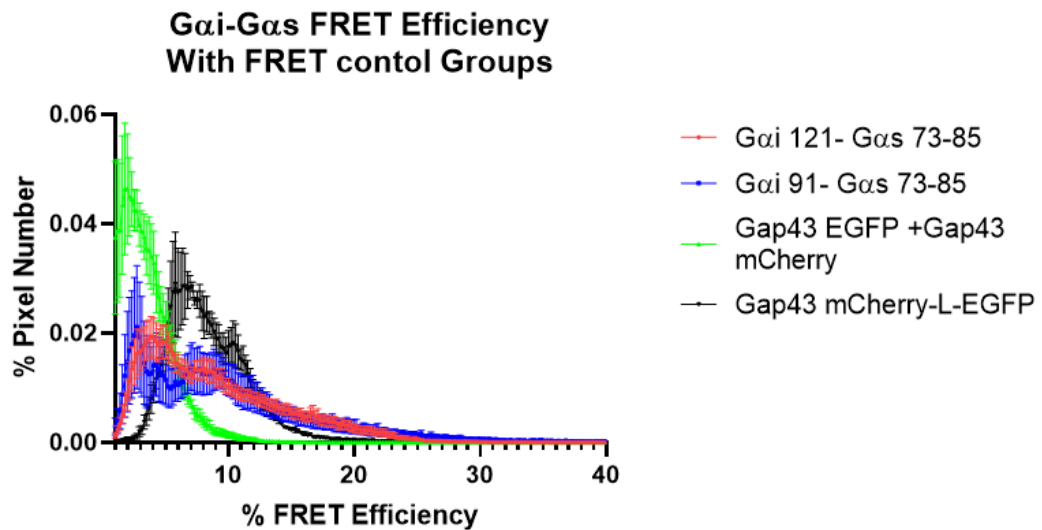


**Figure 3. 10:** Pix FRET analysis of confocal images. Green represents G $\alpha$ i(121)-EGFP and G $\alpha$ s(73-85)-mCherry, blue represents G $\alpha$ i(91)-EGFP and G $\alpha$ s(73-85)-mCherry and black represents Gap43 EGFP and Gap43-mCherry (negative control), Gap43mCherry-L-EGFP (positive control).

### 3.4 Investigation of G $\alpha$ i and G $\alpha$ s Interaction with FRET Technique Using Fluorescence Plate Reader

After confocal microscopy studies, G $\alpha$ i-G $\alpha$ s FRET pairs with G $\alpha$ i 121 EGFP- G $\alpha$ s (73-85) mCherry and G $\alpha$ i 91 EGFP - G $\alpha$ s (73-85) mCherry physical interactions were investigated by using a fluorescence plate reader to collect signals from a larger sample size. G $\alpha$  constructs with fluorescent proteins and FRET control groups were transfected into N2A cells and seeded into black 96 well plates. Spectral measurements were taken following 450 nm EGFP excitation after the optimization process to reduce mCherry spectral bleed through. The area below the spectral signal was collected using Spectramax ID3 was calculated and normalized for all

measurements. Overall spectral region area was normalized to 1. The signal distribution plotted as line graph was presented in Figure 3.10-A. EGFP peak reduction and mCherry peak increase were expected when there is an energy transfer from donor fluorophore EGFP to acceptor fluorophore mCherry. As shown in Figure 3.10-A EGFP spectral peak (400-420 nm) of negative control group Gap43 EGFP + Gap43 mCherry was higher than positive control group Gap43 EGFP-L-mCherry and G $\alpha$ i-G $\alpha$ s FRET pairs. Furthermore, the mCherry peak of the negative control group does not exist since there were only random interactions between the donor and the acceptor fluorophores. Moreover, acceptor fluorophore mCherry spectral region (600-630nm) peaks were focused and analyzed with One way ANOVA since they had one categorical independent variable and one quantitative dependent variable with more than 3 groups. The negative FRET control group was found to be significantly different from positive FRET control, G $\alpha$ i 121 EGFP- G $\alpha$ s (73-85) mCherry and G $\alpha$ i 91 EGFP - G $\alpha$ s (73-85) mCherry FRET pairs ( $p < 0.0001$ ). No significant differences were found between the positive FRET control group and G $\alpha$ i-G $\alpha$ s FRET pairs ( $p > 0.05$ ). Furthermore, no significant difference was found between G $\alpha$ i 121 EGFP- G $\alpha$ s (73-85) mCherry and G $\alpha$ i 91 EGFP - G $\alpha$ s (73-85) mCherry FRET pairs ( $p > 0.05$ ) (See Appendix G for overall data analysis).

Furthermore, to get rid of the cumulative results of the spectral combining of each well value and each dataset, acceptor (600-630nm) and donor (510-520nm) region ratio were calculated for normalized spectral area well measurements individually as shown in Figure 3.11. According to one way ANOVA analysis, no significant difference was found between G $\alpha$ i 121 EGFP- G $\alpha$ s (73-85) mCherry and G $\alpha$ i 91 EGFP - G $\alpha$ s (73-85) mCherry FRET pairs. On the other hand, G $\alpha$ i 121 EGFP- G $\alpha$ s (73-85) mCherry, G $\alpha$ i 91 EGFP - G $\alpha$ s (73-85) mCherry and Gap43 mCherry-L-EGFP FRET pairs were found significantly different from Gap43 EGFP, and Gap43 mCherry cotransfected group ( $p < 0.05$ ). This experiment validates the interaction between G $\alpha$ i and G $\alpha$ s proteins.

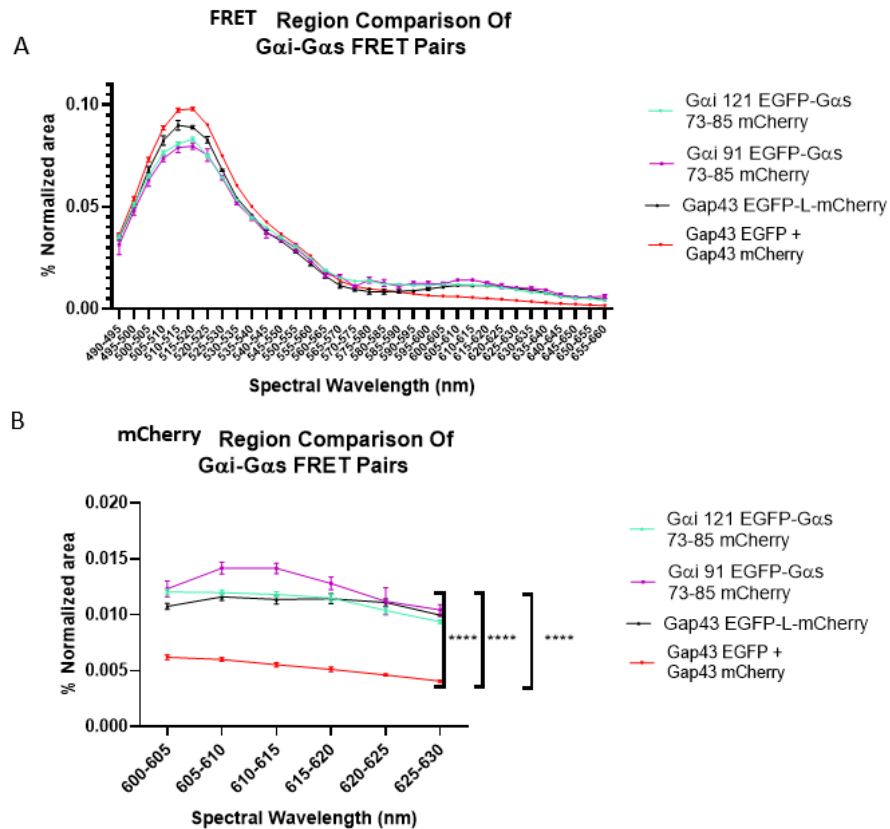


**Figure 3. 11:** Spectral area normalization of FRET spectrum of the Gai and Gas FRET pairs. A) Overall spectral region normalization, B) mCherry energy transfer region focused comparison between FRET control groups and Gai and Gas FRET pairs ( Gai 121 EGFP-Gas 73-85 mCherry, Gai 91 EGFP-Gas 73-85 mCherry , Gap43 mCherry-L-EGFP, and Gap43 EGFP + Gap43mCherry presented as blue, pink, black and red, respectively. One way ANOVA used as statistical analysis. Gai 121 EGFP-Gas 73-85 mCherry vs. Gap43 EGFP + Gap43 mCherry  $p < 0.0001$  , Gai 91 EGFP-Gas 73-85 mCherry vs. Gap43 EGFP + Gap43 mCherry  $p < 0.0001$  and Gap43 EGFP-L-mCherry vs. Gap43 EGFP + Gap43 mCherry  $p < 0.0001$ , there are no significant difference between Gai 91 EGFP-Gas 73-85 mCherry, . Gai 121 EGFP-Gas 73-85 mCherry and Gap43 EGFP-L-mCherry  $p > 0.05$ ).

### Acceptor/Donor Peak Area Ratio Comparison Of G $\alpha$ i-G $\alpha$ s FRET Pair Spectrum

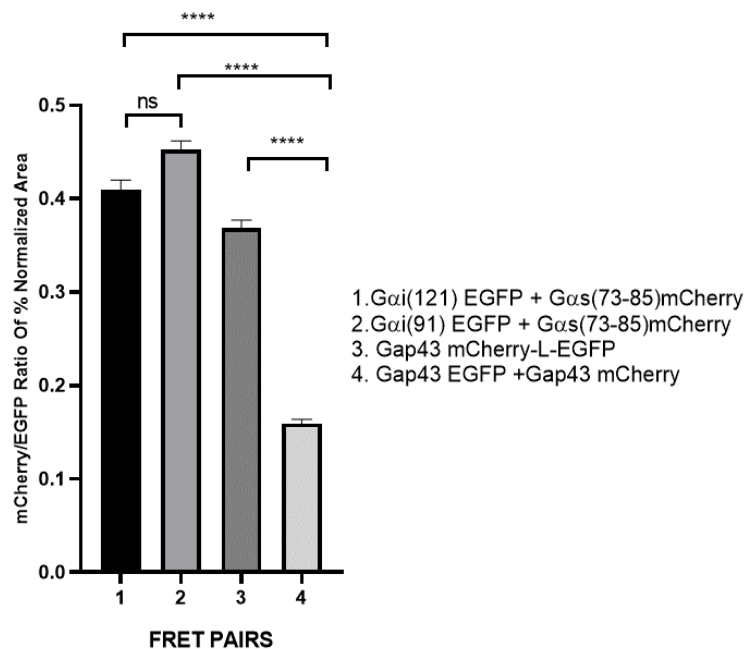


**Figure 3. 12:** Acceptor / Donor ratio of normalized spectrum of G $\alpha$ i-G $\alpha$ s and FRET control groups. (One way ANOVA applied results for groups; G $\alpha$ i 121 EGFP-G $\alpha$ s 73-85 mCherry vs. Gap43 EGFP + Gap43 mCherry  $p < 0.05$ , G $\alpha$ i 91 EGFP-G $\alpha$ s 73-85 mCherry vs. Gap43 EGFP + Gap43 mCherry  $p < 0.05$  and Gap43 EGFP-L-mCherry vs. Gap43 EGFP + Gap43 mCherry  $p < 0.05$  respectively.)

After these results, the study was continued using G $\alpha$ i (121) EGFP-G $\alpha$ s (73-85) mCherry FRET pair due to results that were given under Future Studies section.

### 3.5 Preparation and Sequence Analysis of G $\alpha$ i and G $\alpha$ s Specific Minigenes

G $\alpha$  protein-specific minigenes mainly include last 11 amino acids of specific G $\alpha$  protein and blocks receptor binding sites to inhibit G $\alpha$  protein GPCR interaction competitively. As it was mentioned in Chapter 1, in this study, G $\alpha$ i and G $\alpha$ s specific minigenes were used to inhibit receptor binding.

In order to insert *Gai* protein-specific minigenes, proper cut sites were selected. Since minigene size is smaller than the Multiple Cloning Site of the pcDNA3.1(-), restriction control with double digestion was not considered as an option. Thus, the PstI double cutter was used as control digestion. The diagram of restriction sites is depicted in Figure 3.13. For this strategy, primers design to delete PstI cut site inside the Multiple Cloning Site of the pcDNA3.1(-). For *Gai* minigene NheI and EcoRI cut sites, for *Gas* minigene NheI and HindIII cut sites selected.

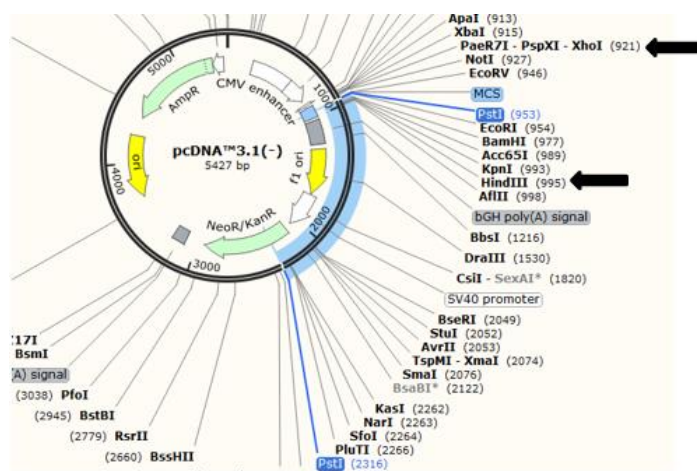


**Figure 3. 13:** Restriction sites for PstI double cutter for pcDNA 3.1(-)

For *Gai* and *Gas* minigenes, PCR mixture and optimal annealing conditions were set to 55 °C for Polymerase Chain Reaction (PCR). PCR product size was validated by loading 2X agarose gel and performing electrophoresis as presented in Figure 3.14A and Figure 3.15 A gel images. *Gai* and *Gas* minigene PCR amplicants size were found to be 66 bp as expected. No template control band from *Gas* minigene reaction was due to two reasons. The first reason was that the primers had high GC content and the second reason was that primers had overlapping regions.

After restriction, ligation, and transformation protocol, colonies were grown from agar plates inoculated into LB. Isolated plasmids were then cut by using PstI and



empty pcDNA3.1(-) was used as a negative control. From empty pcDNA3.1(-) and false-positive colony plasmids, it is expected that plasmid piece drop with 1363bp size and positive colonies were expected to be only linearize .

As expected, both G $\alpha$ i minigene and G $\alpha$ s minigene positive plasmids were linearized by comparing both empty pcDNA3.1(-) cut with PstI as a double cutter and empty pcDNA3.1(-) cut with HindIII as single cutter as presented from Figure 3.14 C and Figure 3.15 C gel images. After sequencing and analyzing the sequence results, no mutation was detected for both minigene samples.

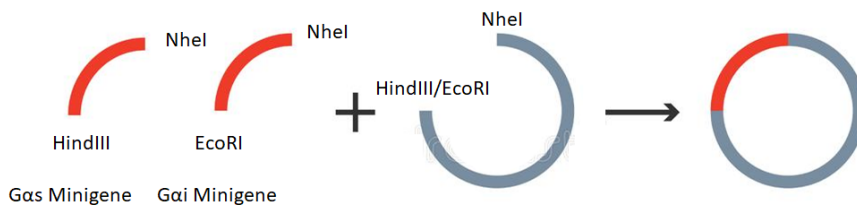


**Figure 3. 14:** G $\alpha$ i and G $\alpha$ s minigene cloning scheme.ö m56

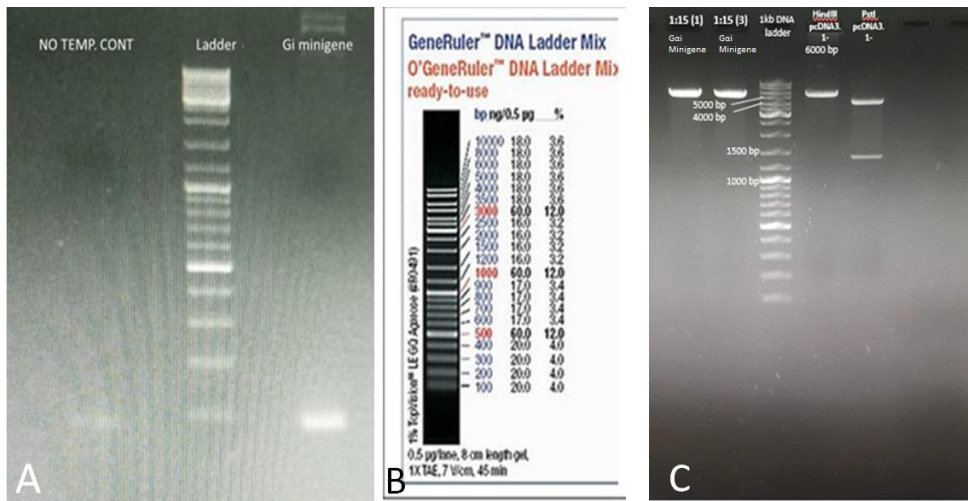


**Figure 3. 15:** G $\alpha$ i minigene cloning agarose gel results. A) PCR amplification B) Generuler DNA Ladder Mix map and C) Control restriction images. 1X Agarose gel



run with 110 V for 30 minutes for control restriction. For PCR products, 2X Agarose gel ran for 100 V for 45 minutes.

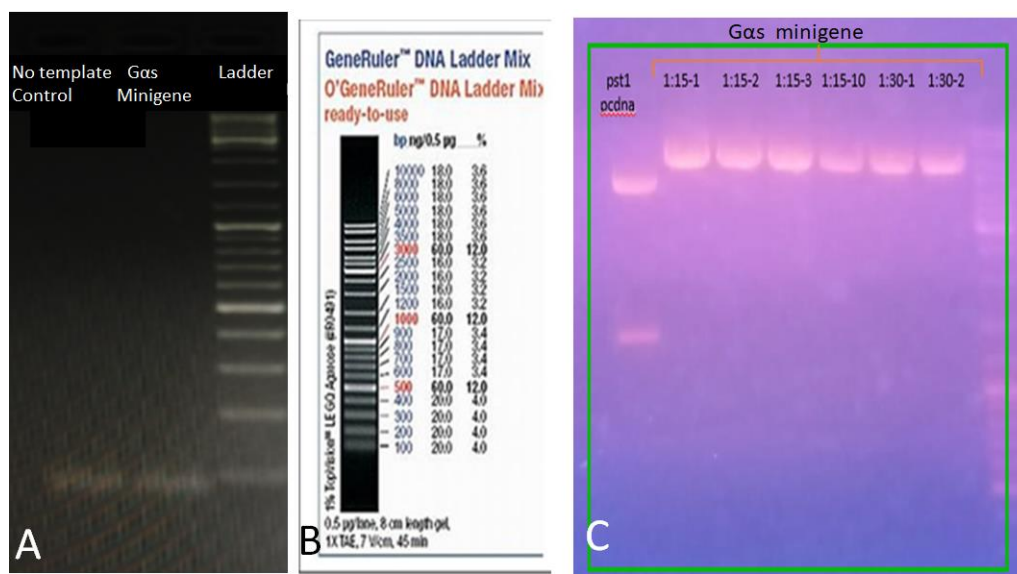


**Figure 3.16:** Gas minigene cloning agarose gel results. A) PCR amplification, B) Generuler DNA Ladder Mix map, and C) Control restriction images. 1X Agarose gel run with 110 V for 30 minutes for control restriction. For PCR products, 2X Agarose gel ran for 100 V for 45 minutes.

### 3.6 Investigation of the Receptor Dependency of Gai and Gas Interaction by Using Minigenes

#### 3.6.1 Investigation by Using Confocal Microscopy

After detection and validation of Gai-Gas interaction, receptor dependency of this interaction was investigated by using Gai and Gas specific minigene expression. Since there was no significant difference between Gai(121)EGFP-Gas(73-85)mCherry and Gai(91)EGFP-Gas(73-85)mCherry FRET efficiency,

Gai(121)EGFP-Gas(73-85)mCherry FRET pair was selected for the minigene experiment.

Gai(121)EGFP-Gas (73-85)mCherry with Gai and Gas minigenes, Gai(121)EGFP-Gas(73-85)mCherry and Gai(91)EGFP-Gas(73-85)mCherry groups were transfected into 100.000 N2a cells as 500 ng each. Since the DSD2 spinning disc confocal microscope from the lab was not working at this time, experiments were performed with Zeiss LSM 900, which is a laser scanning confocal microscope.

FRET efficiency calculations were performed using PixFRET plug-in. Gai(91)EGFP-Gas(73-85)mCherry FRET efficiencies calculated were found consistent with the previous results reported in this thesis using spinning disc confocal microscope. Membrane FRET efficiency signal was found in the 0-30% range as shown in Figure 3.17 and Figure 3.20. Gai(121)EGFP-Gas(73-85)mCherry and Gai(121)EGFP-Gas(73-85)mCherry + Gai and Gas minigene expressing group FRET efficiencies were found in the 0-35% range as shown in Figure 3.18, Figure 3.19 and Figure 3.20. The reason for this 5% increase for Gai(121)EGFP-Gas(73-85)mCherry group for laser scanning microscope data could be the transfection efficiency between spinning disc samples and laser scanning microscope samples. Low FRET efficiency calculated cell number could be more in spinning disc microscope samples.

In order to analyze the data, One-way ANOVA was used to compare 0-10% %FRET efficiency values between the two datasets. According to %FRET efficiency graph statistical analysis, all groups were found significantly different from each other ( $p < 0.05$ ). Slight spectral shift to the left side of the Gai(121)EGFP-Gas(73-85)mCherry + Gai and Gas minigene group compared to Gai(121)EGFP-Gas(73-85)mCherry and Gai(91)EGFP-Gas(73-85)mCherry FRET pairs could mean that receptor interaction blocked Gai(121)EGFP-Gas(73-85)mCherry FRET pairs are capable of physical interaction (See Appendix H).

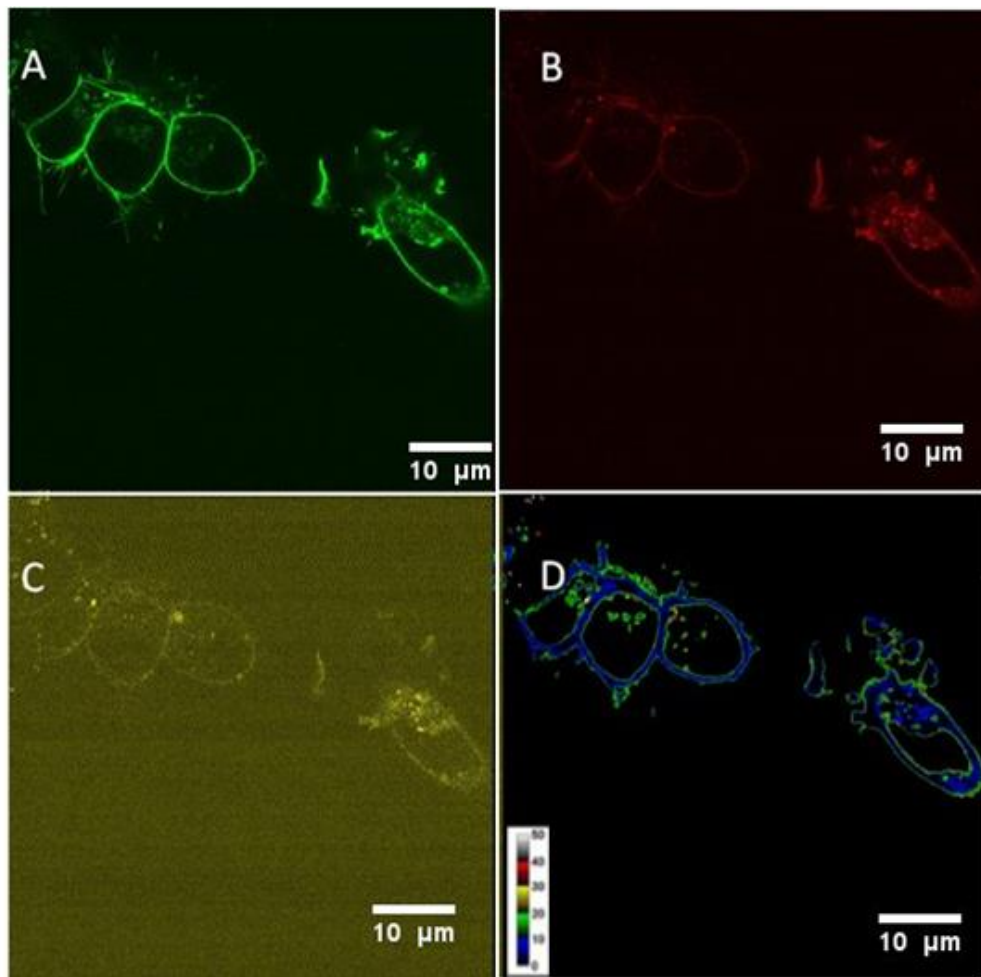


**Figure 3. 17:** LSM Airy scan Confocal FRET imaging of *Gαi(91)-EGFP* and *Gαs(73-85)-mCherry*. 500ng of *Gαi(91)-EGFP* and *Gαs(73-85)-mCherry* co-transfected into N2a cell line. A) Image of EGFP channel excited from 488nm with 800V and emission was taken from 510 nm by taking 490-575nm spectral region. B) Image of mCherry channel excited from 587 nm with 800V and emission was taken from 610 nm by taking 620-700 nm spectral region. C) Image of FRET channel excited from 488 nm with 800V and emission was taken from 610 nm by taking 620-700nm spectral region. D) FRET efficiency in color scale; blue ,green, yellow,red and white colors represent 0-10%, 11-20%, 21-30%, 31-40%, and 41-50% efficiencies of FRET, respectively.

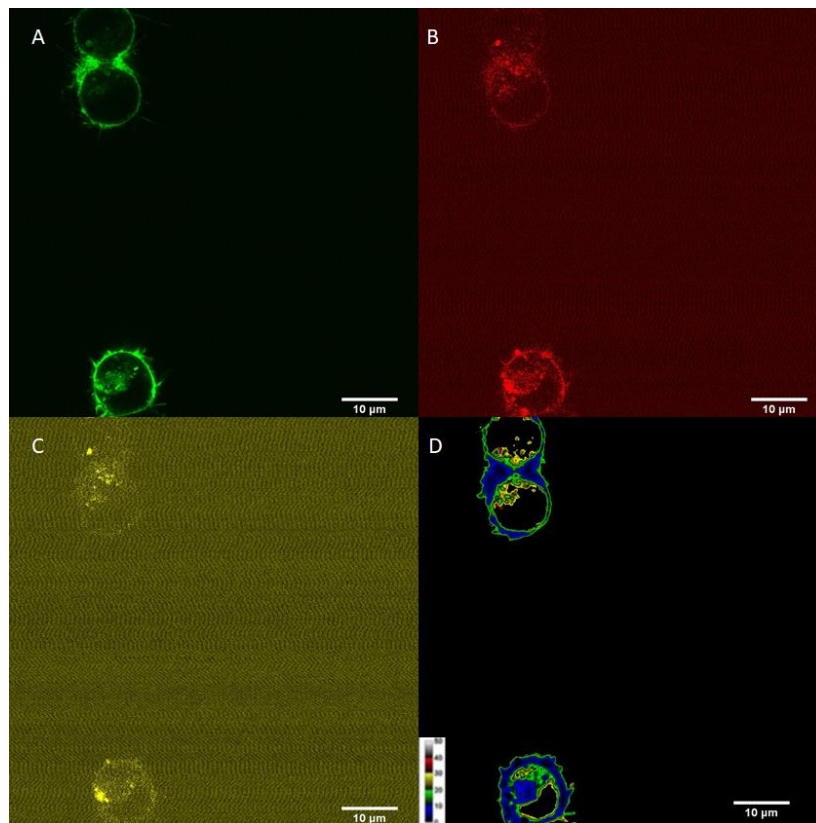


**Figure 3. 18:** LSM Airy scan Confocal FRET imaging of Gai(121)-EGFP and Gas(73-85)-mCherry. 500ng of Gai(121)-EGFP and Gas(73-85)-mCherry co-transfected into N2a cell line. A) Image of EGFP channel excited from 488nm with 800V and emission was taken from 510nm by taking 490-575nm spectral region. B) Image of mCherry channel excited from 587 nm with 800V and emission was taken from 610nm by taking 620-700nm spectral region. C) Image of FRET channel excited from 488 nm with 800V and emission was taken from 610nm by taking 620-700nm spectral region. D) FRET efficiency in color scale; blue ,green, yellow,red and whire colors represent 0-10%, 11-20%, 21-30%, 31-40%, and 41-50% efficiencies of FRET, respectively.

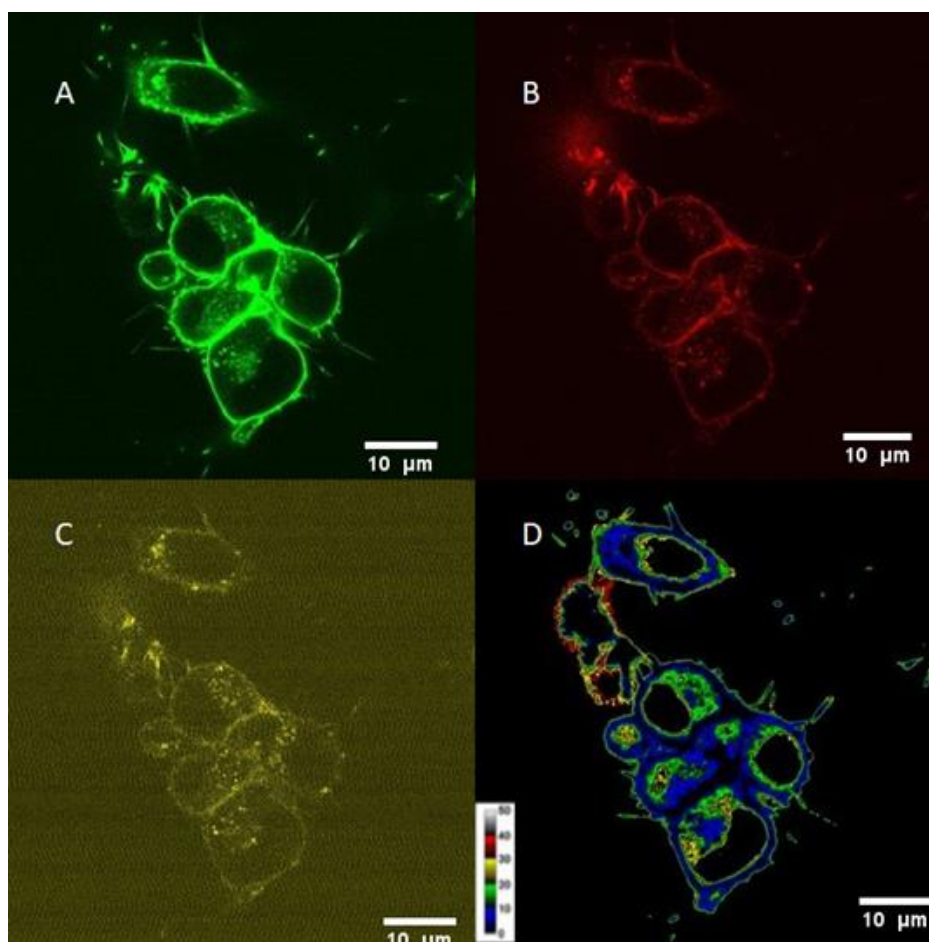


**Figure 3. 19:**LSM Airy scan Confocal FRET imaging of *Gai*(121)-EGFP and *Gas*(73-85)-mCherry + *Gai* and *Gas* minigenes. 500 ng of *Gai*(121)-EGFP, *Gas*(73-85)-mCherry with *Gai* and *Gas* minigenes co-transfected into N2a cell line. A) Image of EGFP channel excited from 488nm with 800V and emission was taken from 510nm by taking 490-575 nm spectral region. B) Image of mCherry channel excited from 587 nm with 800V and emission was taken from 610nm by taking 620-700nm spectral region. C) Image of FRET channel excited from 488 nm with 800V and emission was taken from 610nm by taking 620-700nm spectral region. D) FRET efficiency in color scale; blue ,green, yellow,red and white colors represent 0-10%, 11-20%, 21-30%, 31-40%, and 41-50% efficiencies of FRET, respectively.

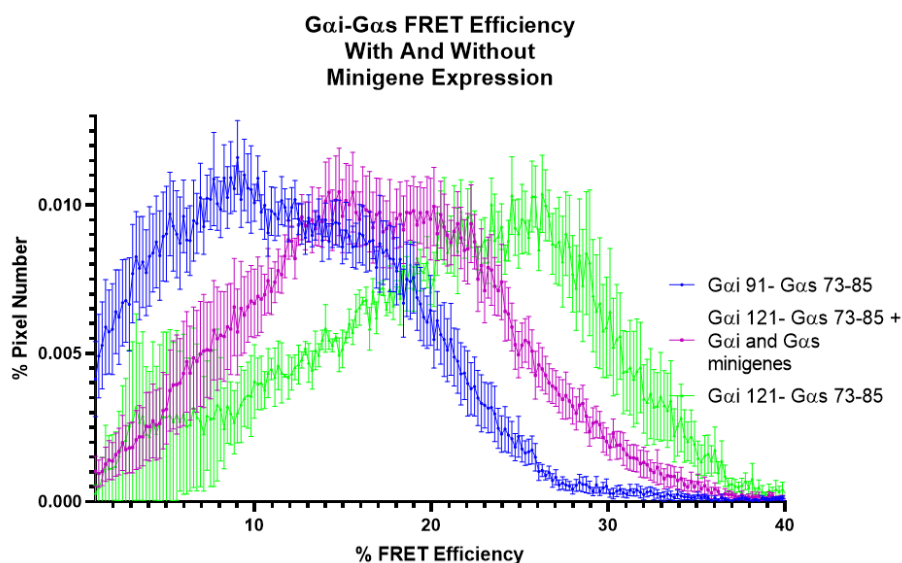


**Figure 3. 20:** Pix FRET analysis of confocal images. Green represents G $\alpha$ i(121)-EGFP and G $\alpha$ s(73-85)-mCherry, blue represents G $\alpha$ i(91)-EGFP and G $\alpha$ s(73-85)-mCherry and pink represents G $\alpha$ i(121)-EGFP and G $\alpha$ s(73-85)-mCherry + G $\alpha$ i and G $\alpha$ s minigene (One Way ANOVA performed to first 10% efficiency values,  $p < 0.05$ )

### 3.6.2 Investigation by Using Fluorescence Plate Reader

The classical GPCR-heterotrimeric G protein signaling model suggests that one GPCR binds one heterotrimeric G protein after ligand binding and secondary messenger system becomes activated. However, recent studies showed that GPCR oligomers, such as A2A-D2R heterotetramer, one heterotrimeric G protein  $\alpha$  subunit can be shared by two GPCRs (Ferré *et al.*, 2016). Furthermore, studies showed that Ras family members, that belong to small G protein family, can form homodimers independent from their receptor (Inouye *et al.*, 2000). Thus, we investigated whether G $\alpha$ i-G $\alpha$ s physical interaction has receptor-independent property or not. For this purpose, G $\alpha$ i 121 EGFP-G $\alpha$ s 73-85 mCherry FRET pair interaction was further investigated in the presence of G $\alpha$ i and G $\alpha$ s specific minigenes. As it was stated in Chapter 1, minigenes block G $\alpha$  protein interaction with GPCRs.

In order to collect signals from a larger sample size, G $\alpha$ i 121 EGFP-G $\alpha$ s 73-85 mCherry FRET pairs and G $\alpha$ i 121 EGFP-G $\alpha$ s 73-85 mCherry FRET pairs with G $\alpha$ i and G $\alpha$ s specific minigenes FRET groups were investigated with a fluorescence plate reader. The constructs were transfected into N2A cell line with FRET control groups as 500 ng for 100.000 cells. G $\alpha$ i 91 EGFP-G $\alpha$ s 73-85 mCherry FRET pair were not included in this experiment since earlier plate reader experiments gave no significant difference between G $\alpha$ i 91 EGFP-G $\alpha$ s 73-85 mCherry and G $\alpha$ i 121 EGFP-G $\alpha$ s 73-85 mCherry FRET pairs.

Spectral measurement was taken by using 450 nm excitation and taking emission signals in the 490-750 nm range for every 5 nm. From the raw forms of the measured spectral signal, area under the spectral signal line calculated and normalized. Acceptor peak region (600-630nm) was compared by using one-way ANOVA. No significant difference was found between G $\alpha$ i 121 EGFP-G $\alpha$ s 73-85 mCherry, G $\alpha$ i 121 EGFP-G $\alpha$ s 73-85 mCherry FRET pairs with G $\alpha$ i and G $\alpha$ s specific minigenes and Gap43mCherry-L-Gap43 EGFP ( $p > 0.05$ ). Compared to Gap43 EGFP and Gap43 mCherry co-transfection group, G $\alpha$ i 121 EGFP-G $\alpha$ s 73-85 mCherry, G $\alpha$ i 121 EGFP-G $\alpha$ s 73-85 mCherry FRET pairs with G $\alpha$ i and G $\alpha$ s specific minigenes and Gap43mCherry-L-Gap43 EGFP were found to be significantly different as presented in Figure 3.21 ( $p < 0.05$ ) (See Appendix I).



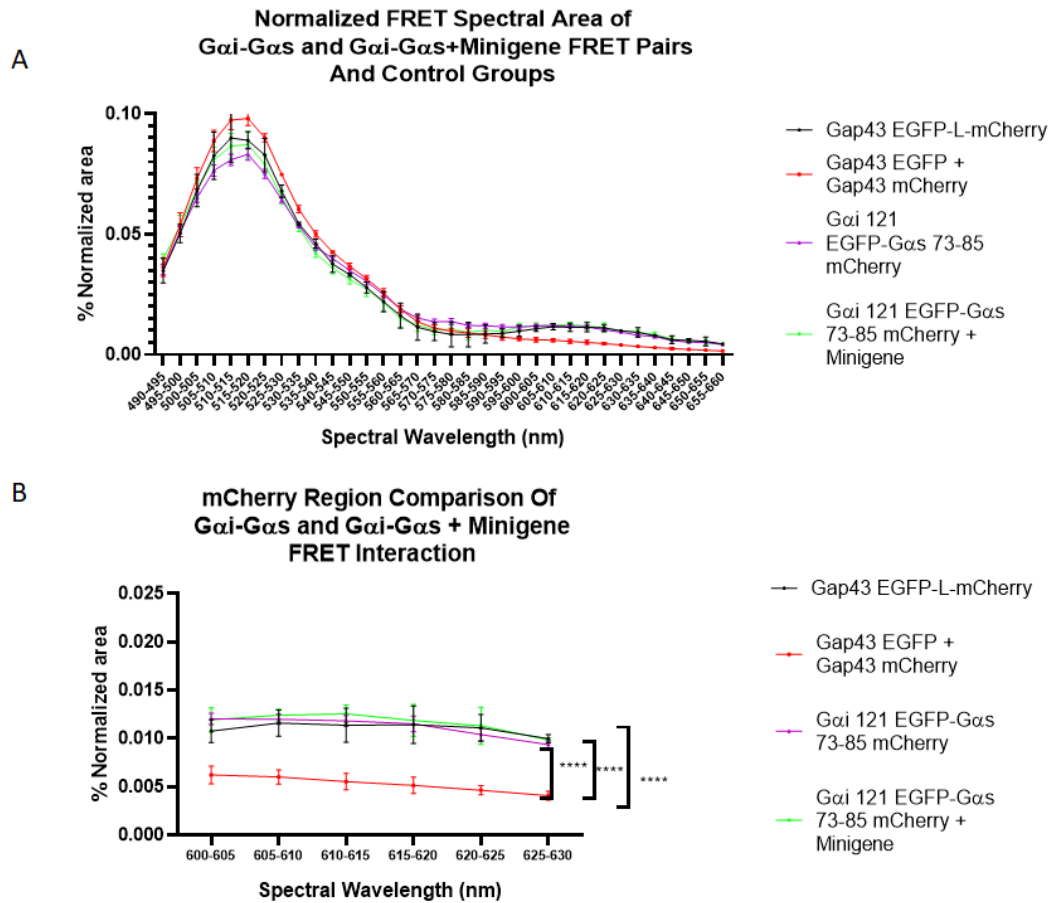


**Figure 3. 21:** Spectral area normalization of FRET spectrum of the G $\alpha$ i-G $\alpha$ s and minigene added G $\alpha$ i-G $\alpha$ s FRET pairs. A) Overall spectral region normalization, B) mCherry energy transfer region focused comparison between FRET control groups and G $\alpha$ i-G $\alpha$ s and minigene added G $\alpha$ i-G $\alpha$ s FRET pairs (One way ANOVA used as statistical analysis. G $\alpha$ i 121 EGFP-G $\alpha$ s 73-85 mCherry vs. Gap43 EGFP + Gap43 mCherry  $p < 0.0001$ , G $\alpha$ i 121 EGFP-G $\alpha$ s 73-85 mCherry + Minigene vs. Gap43 EGFP + Gap43 mCherry  $p < 0.0001$  and Gap43 EGFP-L-mCherry vs. Gap43 EGFP + Gap43 mCherry  $p < 0.0001$ , there are no significant difference between G $\alpha$ i 121 EGFP-G $\alpha$ s 73-85 mCherry + Minigene vs. Gap43 EGFP, G $\alpha$ i 121 EGFP-G $\alpha$ s 73-85 mCherry and Gap43 EGFP-L-mCherry  $p > 0.05$ )

In order to avoid the combination of overall measurements for each wells; acceptor (600-630 nm) and donor (510-520 nm) region ratio was calculated for spectral area



normalized well measurements individually as presented in Figure 3.22. One-way ANOVA was applied to FRET pairs to be able to compare with each other. According to the analysis *Gai* 121 EGFP-*Gas* 73-85 mCherry FRET group was found significantly different from the *Gai* and *Gas* minigene expressing *Gai* 121 EGFP-*Gas* 73-85 mCherry FRET group ( $p < 0.05$ ). Statistical analysis of the fluorescence plate reader was found consistent with the laser scanning confocal microscope after statistical analysis (See Appendix I).

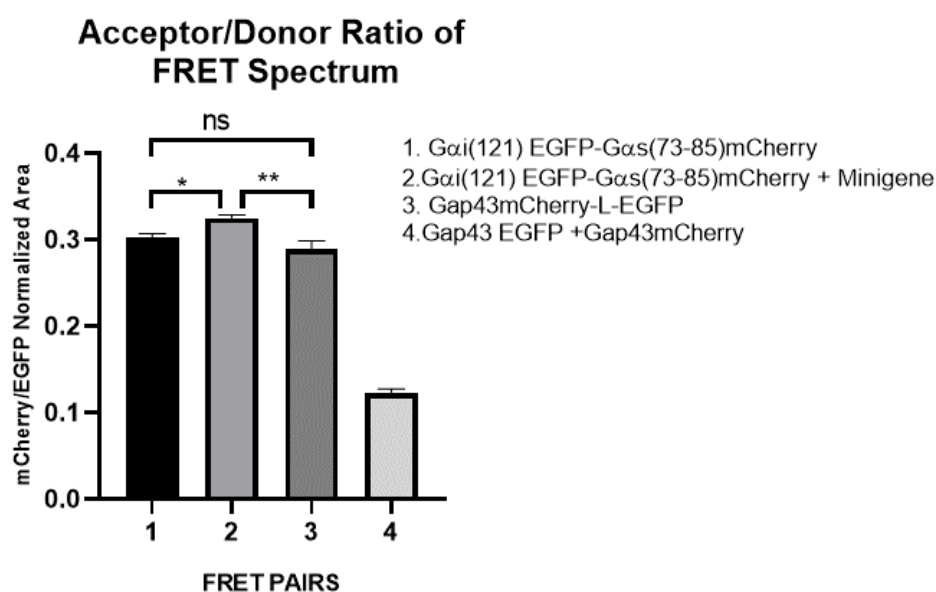


**Figure 3. 22:** Acceptor / Donor ratio of normalized spectrum of *Gai*-*Gas* and FRET control groups (One way ANOVA applied results for groups; *Gai* 121 EGFP-*Gas* 73-85 mCherry vs. *Gai* 121 EGFP-*Gas* 73-85 mCherry + *Gai* and *Gas* minigene  $p < 0.05$ , *Gai* 121 EGFP-*Gas* 73-85 mCherry + *Gai* and *Gas* minigene vs. + *Gai* and *Gas* minigene  $p < 0.05$ , *Gai* 121 EGFP-*Gas* 73-85 mCherry vs. Gap43 EGFP + Gap43 mCherry  $p < 0.05$ , *Gai* 91 EGFP-*Gas* 73-85 mCherry vs. Gap43 EGFP + Gap43 mCherry  $p < 0.05$  and Gap43 EGFP-L-mCherry vs. Gap43 EGFP + Gap43 mCherry  $p < 0.05$  respectively).

### **3.7 Investigation of G $\alpha$ i and G $\alpha$ s Interaction with Agonist Treatment for D2R and A2R Receptor Signaling Pathway Activation by Using Fluorescence Plate Reader**

After the investigation of receptor dependency, characteristics of G $\alpha$ i – G $\alpha$ s protein interaction for A2A -D2R GPCR heterotetramer structure were investigated as well. G $\alpha$ i 121 EGFP-G $\alpha$ s 73-85 mCherry FRET pair and G $\alpha$ i 121 EGFP-G $\alpha$ s 73-85 mCherry FRET pair with G $\alpha$ i and G $\alpha$ s specific minigenes FRET groups was transfected to N2A cell line with Gap43 FRET control groups as 500 ng for 100.000 cells. Before the measurement, 20  $\mu$ l 20  $\mu$ M CGS and 20 $\mu$ l 20 $\mu$ M Quinpirole were added on the cells and incubated at 37 °C at 5 % CO<sub>2</sub> for 20 minutes.

The measurements were performed with 450 nm excitation and 490-750nm emission spectrum with 5 nm steps. Spectral curve area was calculated and normalized for each dataset, as presented in Figure 3.23 A. Then, acceptor peak regions of the FRET pairs were compared by using 600-630 nm mCherry peak area. All G $\alpha$ i-G $\alpha$ s FRET pairs and Gap43 mCherry-L-EGFP positive control groups were found significantly different from the Gap43 EGFP and Gap43 mCherry co-transfected negative control as shown in Figure 3.23 B(p<0.05) (See Appendix J).

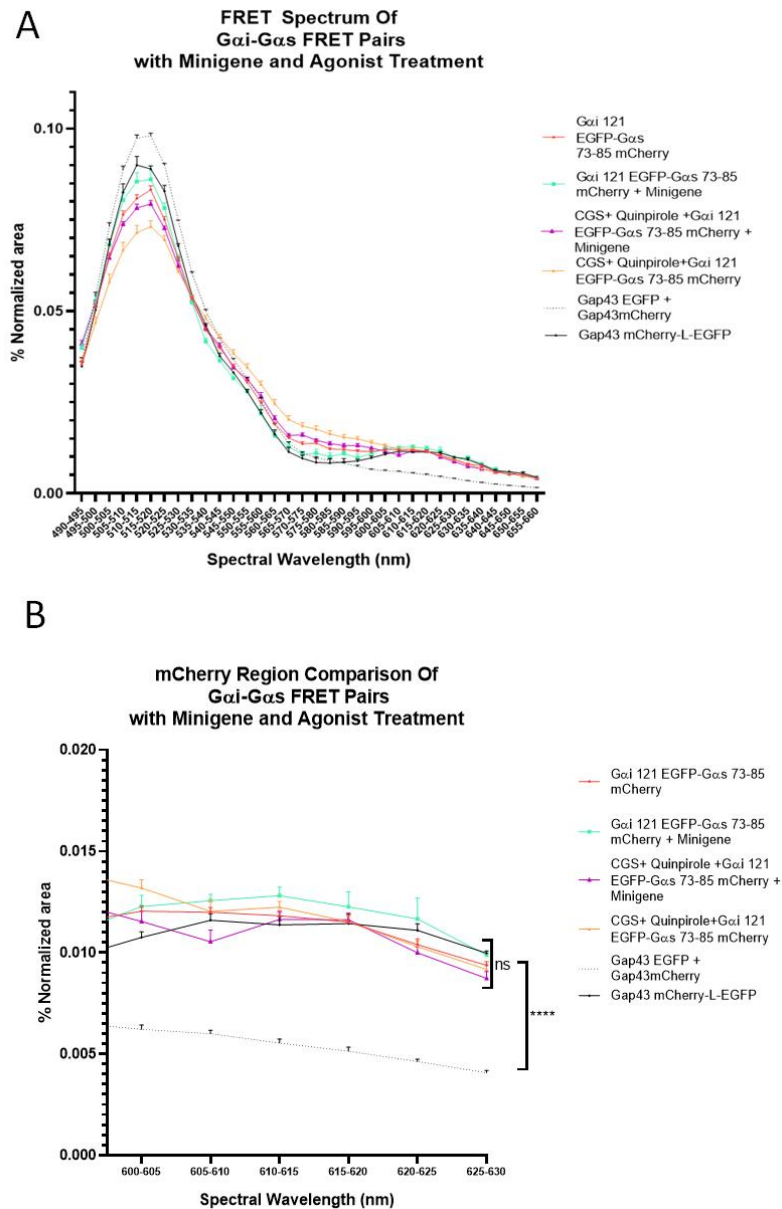


**Figure 3. 23:** Spectral area normalization of FRET spectrum of the  $G_{\alpha i}$ - $G_{\alpha s}$  and minigene added  $G_{\alpha i}$ - $G_{\alpha s}$  FRET pairs with and without CGS+Quinpirole treatment. A) Overall spectral region normalization, B) mCherry energy transfer region focused comparison between FRET control groups and  $G_{\alpha i}$ - $G_{\alpha s}$  and minigene added  $G_{\alpha i}$ - $G_{\alpha s}$  FRET pairs with and without CGS+Quinpirole treatment.

In order to avoid spectral combination of each dataset and each well, the spectral measurement from acceptor (600-630nm) and donor (510-520nm) peak region ratio was calculated for spectral area normalized well measurements individually as shown in Figure 3.24. CGS+Quinpirole treated G $\alpha$ i 121 EGFP-G $\alpha$ s 73-85 mCherry, no treatment applied G $\alpha$ i 121 EGFP-G $\alpha$ s 73-85 mCherry + G $\alpha$ i and G $\alpha$ s minigene and CGS+Quinpirole treated G $\alpha$ i 121 EGFP-G $\alpha$ s 73-85 mCherry + G $\alpha$ i and G $\alpha$ s minigene FRET group acceptor peak ratios were found significantly different from; G $\alpha$ i 121 EGFP-G $\alpha$ s 73-85 mCherry pair ( $p < 0.05$ ). Furthermore, the ligand treatment was significantly increased FRET when compared CGS+Quinpirole G $\alpha$ i 121 EGFP-G $\alpha$ s 73-85 mCherry pair to minigene treated G $\alpha$ i 121 EGFP-G $\alpha$ s 73-85 mCherry ( $p < 0.05$ ). However, there was no significant difference between CGS and Quinpirole treated G $\alpha$ i 121 EGFP-G $\alpha$ s 73-85 mCherry and CGS and Quinpirole treated G $\alpha$ i 121 EGFP-G $\alpha$ s 73-85 mCherry with G $\alpha$ i and G $\alpha$ s minigenes ( $p > 0.05$ )(See Appendix J).

According to the peak area ratio overall for G $\alpha$ i 121 EGFP-G $\alpha$ s, 73-85 mCherry FRET pairs with minigene and ligand treatments, both ligand treatment and minigene treatment increased the FRET individually. However, when both treatments were applied to G $\alpha$ i 121 EGFP-G $\alpha$ s 73-85 mCherry pair and compared to G $\alpha$ i 121 EGFP-G $\alpha$ s 73-85 mCherry with minigenes and CGS+Quinpirole treated G $\alpha$ i 121 EGFP-G $\alpha$ s 73-85 mCherry separately, no significant difference was found ( $p > 0.05$ ). According to these results, there is receptor-independent interaction characteristics of G $\alpha$ i-G $\alpha$ s.

According to treatment characteristics of minigene expression, inhibition of GPCR-G $\alpha$  interaction is expected. Thus, increased peak ratio suggest GPCR independent dimer formation at the cell membrane possibly G $\alpha$  protein at GDP bound form. On the other hand, CGS and Quinpirole treatment activates A2A-D2R heterotetramer and G $\alpha$  protein separation from GPCR oligomers as GTP bound state. Increasing trend of mCherry peak of the ligand treated G $\alpha$ i-G $\alpha$ s FRET pair observed when compared to both minigene expressing G $\alpha$ i-G $\alpha$ s FRET pair and G $\alpha$ i-G $\alpha$ s FRET pair

with no treatment. According to these results, *Gai*-*Gas* interaction with A2A-D2R heterotetrameric structure was found more dominant when compared with minigene treated, possibly GDP bound, form.

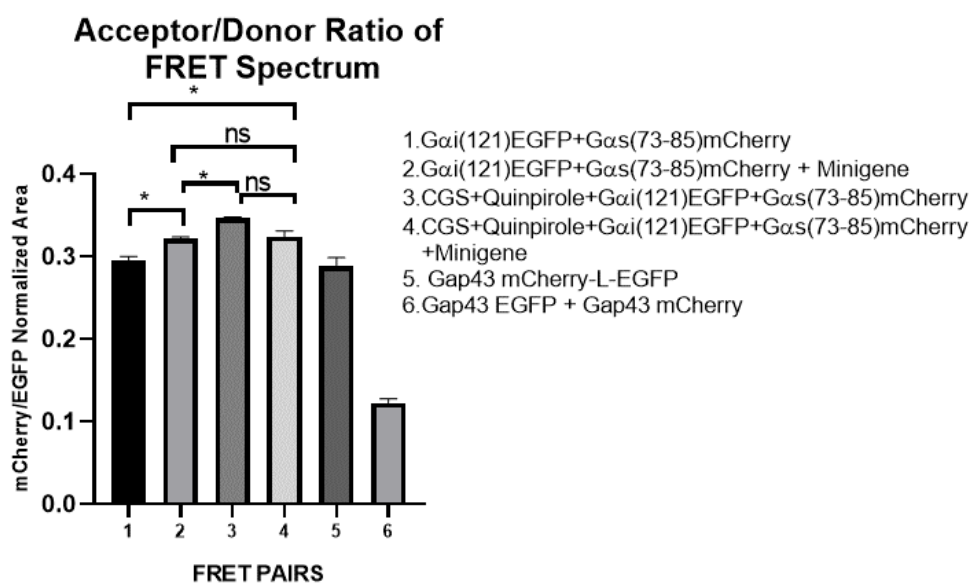


**Figure 3. 24:** Acceptor / Donor ratio of the normalized spectrum of *Gai*-*Gas* and FRET control groups with CGS and Quinpirole treatment. (According to one way ANOVA analysis: *Gai* 121 EGFP-*Gas* 73-85 mCherry vs. *Gai* 121 EGFP-*Gas* 73-85 mCherry + *Gai* and *Gas* minigenes  $p < 0.05$ ; *Gai* 121 EGFP-*Gas* 73-85 mCherry vs. CGS+Quinpirole treated *Gai* 121 EGFP-*Gas* 73-85 mCherry  $p < 0.05$ ; *Gai* 121 EGFP-*Gas* 73-85 mCherry vs. CGS+Quinpirole treated and minigene expressing *Gai* 121 EGFP-*Gas* 73-85 mCherry  $p < 0.05$ ).

### 3.8 Future Studies

Since the FRET results obtained by spinning disc confocal microscopy data has several peaks, it suggests more than one group of interaction. This observation leads us to think fluorescently labeled G $\alpha$  proteins can have different levels of closenes to each other, when the microscope images were examined it is apparent theses different groups localized at different cellular locations. Following careful examination these locations are proposed as various organelles in the cell. In our future studies we plan to investigate various organelles and see if this hypothesis holds true. During this thesis period in order to have some preliminary data 3 different locations for 30 samples were selected and sample curves prepared using the FRET images. The data was kindly analyzed by Dr. Fatma Küçük Baloğlu using MATLAB and locations of curves predicted by a simulation. To analyze the signals, the same image datasets were used again and 30 cells were selected as a whole, not partial (Figure 3.25). Then, this data was fitted to simulated location curves.

The fitted data were analyzed by using One-Way ANOVA. According to statistical analysis results, no significant difference between G $\alpha$ i(121)-G $\alpha$ s(73-85) and G $\alpha$ i(91)-G $\alpha$ s(73-85) on membrane fitting was found ( $p > 0.05$ ). Furthermore, G $\alpha$ i(121)-G $\alpha$ s(73-85) was found to be significantly different than Gap43 EGFP and Gap43 mCherry co-transfection negative FRET pair ( $p < 0.05$ ). However, G $\alpha$ i(91)-G $\alpha$ s(73-85) FRET pair was not found to be significantly different than Gap43 EGFP and Gap43 mCherry co-transfection group ( $p > 0.05$ ) (See Appendix K).

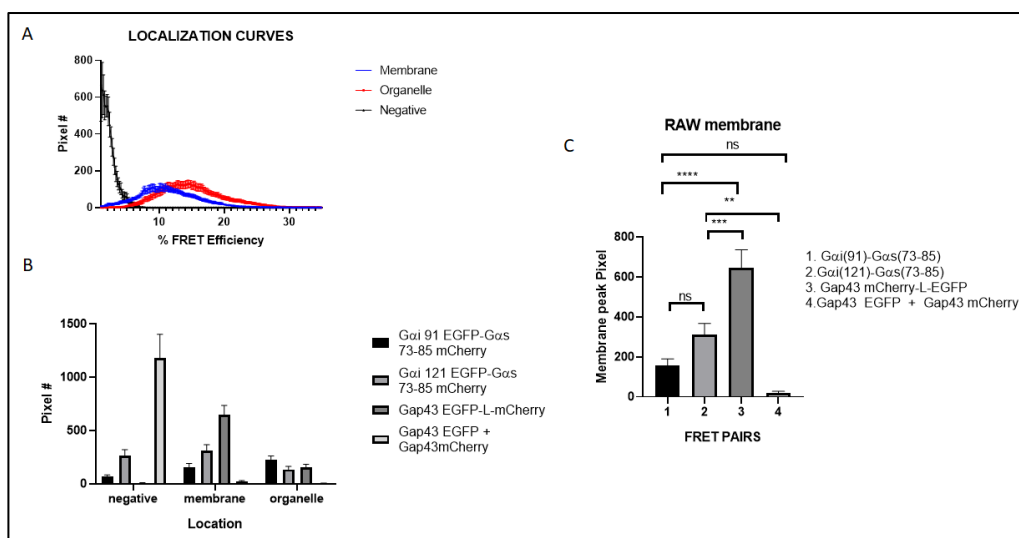


**Figure 3. 25:** Location-dependent curve fitting results with MATLAB. A) Model curves selected from different locations, B) Whole-cell selected FRET pair signal fit to model curves, C) Focusing on membrane signal.

### 3.9 Discussion

Gai and Gas proteins were found in theoretical interaction distance reported by Navarro *et al.* in 2016. In this study, for the first time, Gai and Gas protein interaction was shown using FRET technique. Furthermore, according to minigene expressed Gai and Gas FRET pair results, GPCR interaction interface blocked Gai and Gas interaction found significantly higher than basal Gai and Gas interaction. This finding suggests that there is a GPCR independent Gai and Gas interaction. On the other hand, results obtained following activation of A2A-D2R heterotetrameric structure suggests, possibly GTP bound Gai and Gas protein interaction is dominant in the cellular environment rather than GDP bound Gai and Gas protein interaction. Furthermore, these findings fit to GPCR-G protein interaction hypothesis claiming that both GPCR and the heterotrimeric G protein locates on the cell membrane separately until ligand activation.

The spectral unmixing and curve fitting study, that was applied on FRET efficiency calculated data sets, shows that 91<sup>st</sup> position used G $\alpha$ i and G $\alpha$ s protein interaction trend is more dominant in organelle regions than 121<sup>st</sup> position used G $\alpha$ i and G $\alpha$ s protein interactions.

Constitutively active K-Ras forms could act as oncogenes similarly studies with G $\alpha$  mutantas (especially G $\alpha$ 12) and chimeric G protein family proteins could be extremely useful for cancer studies. According to cAMP-Glo Assay results of ligand-activated and control group luminescence comparisons, using the G $\alpha$ i 121 mCherry construct we showed that some constructs made in this study could be constitutively active. Although these constructs could not be used in this study they could be valuable in further investigations of GTP bound form of G $\alpha$ i and G $\alpha$ s interaction characteristics such as interface, cellular FRET signal localization, and downstream pathways.



## CHAPTER 4

### CONCLUSION

Recent studies suggest that A1-A2A receptor heterotetramer and A2A-D2 receptor heterotetramer structures bring  $G_{\alpha i}$  and  $G_{\alpha s}$  proteins within theoretical interaction distance (Ferre *et al.*, 2008; Navarro *et al.*, 2018). In this thesis, the interaction between  $G_{\alpha i}$  and  $G_{\alpha s}$  proteins was investigated by FRET via both confocal microscopy and fluorescence plate reader measurements. The results from both studies suggest that these proteins interact with each other. Furthermore, the interaction dependency of receptor heterotetramers was investigated by blocking GPCR- $G_{\alpha}$  protein interaction via minigenes (Gilchrist *et al.*, 2002). The increase in the FRET signal from  $G_{\alpha i}$ - $G_{\alpha s}$  FRET pairs in the presence of minigenes suggests that there is a GPCR independent interaction with  $G_{\alpha}$  proteins with possibly GDP bounded form. When focused on  $G_{\alpha i}$ - $G_{\alpha s}$  physical interaction with A2A-D2 receptor heterotetramer specific perspective using A2A receptor-ligand CGS and D2 receptor-specific ligand Quinpirole treatment, normalized acceptor spectral emission peak area over normalized donor spectral emission peak area ratio increased. This suggests that  $G_{\alpha i}$  -  $G_{\alpha s}$  FRET pairs are interacting with GPCR unbound possibly GTP bounded form. This indicates that there are two different receptor-independent interaction types for  $G_{\alpha i}$ - $G_{\alpha s}$  proteins. These interaction types compared with each other by treating  $G_{\alpha i}$ - $G_{\alpha s}$  FRET pair with both minigene and A2A-D2 receptor ligands. Double treatment results were obtained statistically not different when compared with CGS+Quinpirole treatment and minigene treatment results from  $G_{\alpha i}$  -  $G_{\alpha s}$  FRET pairs individually. This can be explained by the limitation of  $G_{\alpha}$  protein binding to GPCR and competitively inhibiting to GTP exchange. According to this, two different  $G_{\alpha i}$ - $G_{\alpha s}$  GPCR independent interaction types were detected, and GTP bound interaction was found to be more dominant to

GDP bound interaction form. These findings fit to GPCR-G protein interaction hypothesis claiming that both GPCR and the heterotrimeric G protein locates on the cell membrane separately until ligand activation.

## REFERENCES

- Acuner Ozbabacan, S. E., Engin, H. B., Gursoy, A., & Keskin, O. (2011). Transient proteinprotein interactions. In *Protein Engineering, Design and Selection* (Vol. 24, Issue 9, pp. 635–648). Oxford Academic.  
<https://doi.org/10.1093/protein/gzr025>
- Addgene: Vector Database - pcDNA3.1(-)*. (n.d.). Retrieved July 11, 2021, from <https://www.addgene.org/vector-database/2097/>
- Albertazzi, L., Arosio, D., Marchetti, L., Ricci, F., & Beltram, F. (2009). Quantitative FRET Analysis With the E0GFP-mCherry Fluorescent Protein Pair. *Photochemistry and Photobiology*, 85(1), 287–297.  
<https://doi.org/10.1111/J.1751-1097.2008.00435.X>
- Boullaran, C., & Gales, C. (2015). Cardiac cAMP: Production, hydrolysis, modulation and detection. In *Frontiers in Pharmacology* (Vol. 6, Issue OCT, p. 203). Frontiers Media S.A. <https://doi.org/10.3389/fphar.2015.00203>
- Cell signalling: 3.5 Monomeric G proteins - OpenLearn - Open University - S377\_4*. (n.d.). Retrieved June 30, 2021, from <https://www.open.edu/openlearn/science-maths-technology/cell-signalling/content-section-3.5>
- Chung, J. K., Lee, Y. K., Lam, H. Y. M., & Groves, J. T. (2016). Covalent Ras Dimerization on Membrane Surfaces through Photosensitized Oxidation. *Journal of the American Chemical Society*, 138(6), 1800–1803.  
<https://doi.org/10.1021/jacs.5b12648>
- D, I., R, D. P., E, E., E, M., I, P., A, M., P, B., F, P., & S, C. (2011). CGS 21680, an agonist of the adenosine (A2A) receptor, decreases acute lung

- inflammation. *European Journal of Pharmacology*, 668(1–2), 305–316.  
<https://doi.org/10.1016/J.EJP HAR.2011.06.049>
- de Las Rivas, J., & Fontanillo, C. (2010). Protein-protein interactions essentials: Key concepts to building and analyzing interactome networks. *PLoS Computational Biology*, 6(6), 1–8.  
<https://doi.org/10.1371/journal.pcbi.1000807>
- DM, E., C, N., LS, d’Angelo, CA, N., JO, D., ML, D., DE, T., AC, M., GP, U., S, M.-Z., & TW, R. (2014). The dopamine D2/D3 receptor agonist quinpirole increases checking-like behaviour in an operant observing response task with uncertain reinforcement: a novel possible model of OCD. *Behavioural Brain Research*, 264(100), 207–229. <https://doi.org/10.1016/J.BBR.2013.12.040>
- Dohlman, H. G., & Campbell, S. L. (2019). Regulation of large and small G proteins by ubiquitination. *Journal of Biological Chemistry*, 294(49), 18613–18623. <https://doi.org/10.1074/jbc.REV119.011068>
- Dohlman, H. G., & Jones, J. C. (2012). Signal activation and inactivation by the G $\alpha$  helical domain: A long-neglected partner in G protein signaling. In *Science Signaling* (Vol. 5, Issue 226, p. re2). NIH Public Access.  
<https://doi.org/10.1126/scisignal.2003013>
- Ferré, S., Bonaventura, J., Tomasi, D., Navarro, G., Moreno, E., Cortés, A., Lluís, C., Casadó, V., & Volkow, N. D. (2016). Allosteric mechanisms within the adenosine A2A-dopamine D2 receptor heterotetramer. In *Neuropharmacology* (Vol. 104, pp. 154–160). Elsevier Ltd.  
<https://doi.org/10.1016/j.neuropharm.2015.05.028>
- Ferre, S., Ciruela, F., Borycz, J., Solinas, M., Quarta, D., Antoniou, K., Quiroz, C., Justinova, Z., Lluís, C., Franco, R., & Goldberg, S. R. (2008). Adenosine A1-A2A receptor heteromers: New targets for caffeine in the brain. In *Frontiers in Bioscience* (Vol. 13, Issue 6, pp. 2391–2399). <https://doi.org/10.2741/2852>

*Fluorescence Resonance Energy Transfer (FRET) Microscopy - Introductory*

*Concepts / Olympus LS.* (n.d.). Retrieved June 30, 2021, from

<https://www.olympus-lifescience.com/en/microscope-resource/primer/techniques/fluorescence/fret/fretintro/>

Franco, R., Cordoní, A., Llinas del Torrent, C., Lillo, A., Serrano-Marín, J., Navarro, G., & Pardo, L. (2021). Structure and function of adenosine receptor heteromers. In *Cellular and Molecular Life Sciences* (Vol. 78, Issue 8, pp. 3957–3968). Springer Science and Business Media Deutschland GmbH. <https://doi.org/10.1007/s00018-021-03761-6>

Gilchrist, A., Li, A., & Hamm, H. E. (2002). G alpha COOH-terminal minigene vectors dissect heterotrimeric G protein signaling. *Science's STKE : Signal Transduction Knowledge Environment*, 2002(118). <https://doi.org/10.1126/stke.2002.118.p11>

*GPCR / Learn Science at Scitable.* (n.d.). Retrieved July 28, 2021, from

<https://www.nature.com/scitable/topicpage/gpcr-14047471/>

H, N., Y, A., Y, T., T, S., A, E., M, K., N, H., F, H., T, U., S, O., N, H., H, O., K, S., T, O., T, K., S, M., & T, S. (2015). Genomic spectra of biliary tract cancer. *Nature Genetics*, 47(9), 1003–1010. <https://doi.org/10.1038/NG.3375>

Hauser, A. S., Attwood, M. M., Rask-Andersen, M., Schiöth, H. B., & Gloriam, D. E. (2017). Trends in GPCR drug discovery: New agents, targets and indications. *Nature Reviews Drug Discovery*, 16(12), 829–842. <https://doi.org/10.1038/nrd.2017.178>

Hendriks-Balk, M. C., Peters, S. L. M., Michel, M. C., & Alewijnse, A. E. (2008). Regulation of G protein-coupled receptor signalling: Focus on the cardiovascular system and regulator of G protein signalling proteins. In *European Journal of Pharmacology* (Vol. 585, Issues 2–3, pp. 278–291). Eur J Pharmacol. <https://doi.org/10.1016/j.ejphar.2008.02.088>

- Ishikawa-Ankerhold, H. C., Ankerhold, R., & Drummen, G. P. C. (2012). Advanced fluorescence microscopy techniques-FRAP, FLIP, FLAP, FRET and FLIM. In *Molecules* (Vol. 17, Issue 4, pp. 4047–4132). Multidisciplinary Digital Publishing Institute (MDPI).  
<https://doi.org/10.3390/molecules17044047>
- Kelly, P., Moeller, B. J., Juneja, J., Booden, M. A., Der, C. J., Daaka, Y., Dewhirst, M. W., Fields, T. A., & Casey, P. J. (2006). The G12 family of heterotrimeric G proteins promotes breast cancer invasion and metastasis. *Proceedings of the National Academy of Sciences of the United States of America*, *103*(21), 8173–8178. <https://doi.org/10.1073/pnas.0510254103>
- Lemke, E. A., & Deniz, A. A. (2011). Förster Resonance Energy Transfer. In *Comprehensive Nanoscience and Technology* (Vols. 1–5, pp. 127–151). Elsevier Inc. <https://doi.org/10.1016/B978-0-12-374396-1.00080-5>
- London, M. J., Zaugg, M., Schaub, M. C., & Spahn, D. R. (2004). Perioperative  $\beta$ -Adrenergic Receptor Blockade: Physiologic Foundations and Clinical Controversies. In *Anesthesiology* (Vol. 100, Issue 1, pp. 170–175). *Anesthesiology*. <https://doi.org/10.1097/00000542-200401000-00027>
- Matúš, D., & Prömel, S. (2018). G Proteins and GPCRs in *C. elegans* Development: A Story of Mutual Infidelity. *Journal of Developmental Biology* *2018*, Vol. 6, Page 28, *6*(4), 28. <https://doi.org/10.3390/JDB6040028>
- Maurisse, R., de Semir, D., Emamekhoo, H., Bedayat, B., Abdolmohammadi, A., Parsi, H., & Gruenert, D. C. (2010). Comparative transfection of DNA into primary and transformed mammalian cells from different lineages. *BMC Biotechnology*, *10*(1), 1–9. <https://doi.org/10.1186/1472-6750-10-9>
- Mizuno, N., & Itoh, H. (2009). Fax +41 61 306 12 34 E-Mail [karger@karger.ch](mailto:karger@karger.ch)  
Functions and Regulatory Mechanisms of Gq-Signaling Pathways. *Neurosignals*, *17*, 42–54. <https://doi.org/10.1159/000186689>

- Monfort, B. M. (2018). *Interactions between the [FeFe]-hydrogenase maturation enzymes from Thermoanaerobacter italicus*.
- Monochromator vs Filter-Based Plate Reader: Which is Better? - Promega Connections*. (n.d.). Retrieved June 30, 2021, from <https://www.promegaconnections.com/monochromator-vs-filter-based-plate-reader-which-is-better/>
- Morris, A. J., & Malbon, C. C. (1999). Physiological regulation of G protein-linked signaling. In *Physiological Reviews* (Vol. 79, Issue 4, pp. 1373–1430). American Physiological Society.  
<https://doi.org/10.1152/physrev.1999.79.4.1373>
- Muratcioglu, S., Aydin, C., Odabasi, E., Ozdemir, E. S., Firat-Karalar, E. N., Jang, H., Tsai, C. J., Nussinov, R., Kavakli, I. H., Gursoy, A., & Keskin, O. (2020). Oncogenic K-Ras4B Dimerization Enhances Downstream Mitogen-activated Protein Kinase Signaling. *Journal of Molecular Biology*, 432(4), 1199–1215.  
<https://doi.org/10.1016/j.jmb.2020.01.002>
- Muratcioglu, S., Chavan, T. S., Freed, B. C., Jang, H., Khavrutskii, L., Natasha Freed, R., Dyba, M. A., Stefanisko, K., Tarasov, S. G., Gursoy, A., Keskin, O., Tarasova, N. I., Gaponenko, V., & Nussinov, R. (2015). GTP-Dependent K-Ras Dimerization. *Structure*, 23(7), 1325–1335.  
<https://doi.org/10.1016/j.str.2015.04.019>
- Nan, X., Tamgüney, T. M., Collisson, E. A., Lin, L. J., Pitt, C., Galeas, J., Lewis, S., Gray, J. W., McCormick, F., & Chu, S. (2015). Ras-GTP dimers activate the Mitogen-Activated Protein Kinase (MAPK) pathway. *Proceedings of the National Academy of Sciences of the United States of America*, 112(26), 7996–8001. <https://doi.org/10.1073/pnas.1509123112>
- Navarro, G., Cordoní, A., Brugarolas, M., Moreno, E., Aguinaga, D., Pérez-Benito, L., Ferre, S., Cortés, A., Casadó, V., Mallol, J., Canela, E. I., Lluís, C., Pardo, L., McCormick, P. J., & Franco, R. (2018). *Cross-communication*

*between G<sub>i</sub> and G<sub>s</sub> in a G-protein-coupled receptor heterotetramer guided by a receptor C-terminal domain.* <https://doi.org/10.1186/s12915-018-0491-x>

Navarro, G., Cordero, A., Zelman-Femiak, M., Brugarolas, M., Moreno, E., Aguinaga, D., Perez-Benito, L., Cortés, A., Casadó, V., Mallol, J., Canela, E. I., Lluís, C., Pardo, L., García-Sáez, A. J., McCormick, P. J., & Franco, R. (2016). Quaternary structure of a G-protein-coupled receptor heterotetramer in complex with G<sub>i</sub> and G<sub>s</sub>. *BMC Biology*, *14*(1).

<https://doi.org/10.1186/s12915-016-0247-4>

Nestler, E. J., & Duman, R. S. (1999). *Heterotrimeric G Proteins*.

<https://www.ncbi.nlm.nih.gov/books/NBK28116/>

Nussinov, R., Tsai, C. J., & Jang, H. (2019). Is Nanoclustering essential for all oncogenic KRas pathways? Can it explain why wild-type KRas can inhibit its oncogenic variant? In *Seminars in Cancer Biology* (Vol. 54, pp. 114–120). Academic Press.


<https://doi.org/10.1016/j.semcancer.2018.01.002>

Okamoto, K., & Sako, Y. (2017). Recent advances in FRET for the study of protein interactions and dynamics. In *Current Opinion in Structural Biology* (Vol. 46, pp. 16–23). Elsevier Ltd.

<https://doi.org/10.1016/j.sbi.2017.03.010>

Oldham, W. M., & Hamm, H. E. (2008). Heterotrimeric G protein activation by G-protein-coupled receptors. In *Nature Reviews Molecular Cell Biology* (Vol. 9, Issue 1, pp. 60–71). Nat Rev Mol Cell Biol.

<https://doi.org/10.1038/nrm2299>

(PDF)  *E Thesis Beata Monfort Dec 2018*. (n.d.). Retrieved July 27, 2021, from [https://www.researchgate.net/publication/331547561\\_E\\_Thesis\\_Beata\\_Monfort\\_Dec\\_2018](https://www.researchgate.net/publication/331547561_E_Thesis_Beata_Monfort_Dec_2018)

Peng, X., Wang, J., Peng, W., Wu, F. X., & Pan, Y. (2017). Protein-protein interactions: detection, reliability assessment and applications. In *Briefings in bioinformatics* (Vol. 18, Issue 5, pp. 798–819). Oxford Academic.

<https://doi.org/10.1093/bib/bbw066>



- Pincas, H., González-Maeso, J., Ruf-Zamojski, F., & Sealfon, S. C. (2018). *G Protein-Coupled Receptors* (pp. 85–120). Springer, Cham.  
[https://doi.org/10.1007/978-3-319-44675-2\\_6](https://doi.org/10.1007/978-3-319-44675-2_6)
- Repasky, G. A., Cox, A. D., Hanker, A. B., Mitin, N., & Der, C. J. (2010). Role of r-ras in cell growth. In *Handbook of Cell Signaling, 2/e* (Vol. 2, pp. 1753–1762). Elsevier Inc. <https://doi.org/10.1016/B978-0-12-374145-5.00214-X>
- Ro<sup>^</sup>mero<sup>^</sup>, J. É., Feige, R. N., Sage, D., Wahli, W., Desvergne, B. A., & Gelman, L. (n.d.). *PixFRET, an ImageJ Plug-in for FRET Calculation That Can Accommodate Variations in Spectral Bleed-throughs*.  
<https://doi.org/10.1002/jemt.20215>
- Sekar, R. B., & Periasamy, A. (2003). Fluorescence resonance energy transfer (FRET) microscopy imaging of live cell protein localizations. In *Journal of Cell Biology* (Vol. 160, Issue 5, pp. 629–633). The Rockefeller University Press. <https://doi.org/10.1083/jcb.200210140>
- Song, S., Cong, W., Zhou, S., Shi, Y., Dai, W., Zhang, H., Wang, X., He, B., & Zhang, Q. (2019). Small GTPases: Structure, biological function and its interaction with nanoparticles. In *Asian Journal of Pharmaceutical Sciences* (Vol. 14, Issue 1, pp. 30–39). Shenyang Pharmaceutical University.  
<https://doi.org/10.1016/j.ajps.2018.06.004>
- Spinning Disk vs. Laser-Scanning Confocal Microscopes | Features | Oct 2004 | Photonics Spectra*. (n.d.). Retrieved July 11, 2021, from [https://www.photonics.com/Articles/Spinning\\_Disk\\_vs\\_Laser-Scanning\\_Confocal/a20129](https://www.photonics.com/Articles/Spinning_Disk_vs_Laser-Scanning_Confocal/a20129)
- Sprang, S. R. (2016). Invited review: Activation of G proteins by GTP and the mechanism of G $\alpha$ -catalyzed GTP hydrolysis. In *Biopolymers* (Vol. 105, Issue 8, pp. 449–462). John Wiley and Sons Inc. <https://doi.org/10.1002/bip.22836>
- Structural similarities between Ras and Ga i1. (A) The Ga subunit of.. | Download Scientific Diagram*. (n.d.). Retrieved June 30, 2021, from

[https://www.researchgate.net/figure/Structural-similarities-between-Ras-and-Ga-i1-A-The-Ga-subunit-of-heterotrimeric\\_fig1\\_314139033](https://www.researchgate.net/figure/Structural-similarities-between-Ras-and-Ga-i1-A-The-Ga-subunit-of-heterotrimeric_fig1_314139033)

Syrovatkina, V., Alegre, K. O., Dey, R., & Huang, X. Y. (2016). Regulation, Signaling, and Physiological Functions of G-Proteins. In *Journal of Molecular Biology* (Vol. 428, Issue 19, pp. 3850–3868). Academic Press.  
<https://doi.org/10.1016/j.jmb.2016.08.002>

Tsvetanova, N. G., Irannejad, R., & von Zastrow, M. (2015). G protein-coupled receptor (GPCR) signaling via heterotrimeric G proteins from endosomes. In *Journal of Biological Chemistry* (Vol. 290, Issue 11, pp. 6689–6696). American Society for Biochemistry and Molecular Biology Inc.  
<https://doi.org/10.1074/jbc.R114.617951>

Vasan, N., Boyer, J. L., & Herbst, R. S. (2014). A RAS renaissance: Emerging targeted therapies for KRAS-mutated non-small cell lung cancer. In *Clinical Cancer Research* (Vol. 20, Issue 15, pp. 3921–3930). American Association for Cancer Research Inc. <https://doi.org/10.1158/1078-0432.CCR-13-1762>

Wallace, B., & Atzberger, P. J. (2017). Förster resonance energy transfer: Role of diffusion of fluorophore orientation and separation in observed shifts of FRET efficiency. *PLoS ONE*, *12*(5). <https://doi.org/10.1371/journal.pone.0177122>

Wettschureck, N., & Offermanns, S. (2005). Mammalian G proteins and their cell type specific functions. In *Physiological Reviews* (Vol. 85, Issue 4, pp. 1159–1204). *Physiol Rev*. <https://doi.org/10.1152/physrev.00003.2005>

Xing, S., Wallmeroth, N., Berendzen, K. W., & Grefen, C. (2016a). Techniques for the analysis of protein-protein interactions in vivo. *Plant Physiology*, *171*(2), 727–758. <https://doi.org/10.1104/pp.16.00470>

Xing, S., Wallmeroth, N., Berendzen, K. W., & Grefen, C. (2016b). Techniques for the analysis of protein-protein interactions in vivo. *Plant Physiology*, *171*(2), 727–758. <https://doi.org/10.1104/pp.16.00470>

Zachariou, V., Duman, R. S., & Nestler, E. J. (2012). G Proteins. In *Basic Neurochemistry* (pp. 411–422). Elsevier. <https://doi.org/10.1016/B978-0-12-374947-5.00021-3>

*ZEISS Microscopy Online Campus / Introduction to Spinning Disk Microscopy*. (n.d.). Retrieved June 30, 2021, from <http://zeiss-campus.magnet.fsu.edu/articles/spinningdisk/introduction.html>



## APPENDICES

### A. COMPOSITIONS OF SOLUTIONS

**Table A. 1:DMEM High Glucose Compomposition**

COMPONENT	CONCENTRATION (mg/L)
<b>Amino Acids</b>	
Glycine	30
L-Arginine hydrochloride	84
L-Cysteine 2HCl	63
L-Glutamine	580
L-Histidine hydrochloride-H <sub>2</sub> O	42
L-Isoleucine	105
L-Leucine	105
L-Lysine hydrochloride	146
L-Methionine	30
L-Phenylalanine	66
L-Serine	42
L-Threonine	95
L-Tryptophan	16
L-Tyrosine	72
L-Valine	94
<b>Vitamins</b>	
Choline chloride	4
D-Calcium pantothenate	4

Folic acid	4
Niacinamide	4
Pyridoxine hydrochloride	4
Riboflavin	0.4
Thiamine hydrochloride	4
i-Inositol	7.2
<b>Inorganic Salts</b>	
Calcium chloride	264
Ferric nitrate	0.1
Magnesium sulfate	200
Potassium chloride	400
Sodium bicarbonate	3700
Sodium chloride	6400
Sodium phosphate monobasic	141
<b>Other components</b>	
D-Glucose (Dextrose)	4500
Phenol Red	15
Sodium pyruvate	110

### **Luria Bertani (LB) Medium**

10 g/L Tryptone

5 g/L NaCl

5 g/L Yeast Extract

Ingredients were dissolved in distilled H<sub>2</sub>O. 20 g/L agar was added for LB Agar plate preparation. The pH of the prepared medium was adjusted to 7.0.

### **Phosphate Buffer Saline (PBS), 10X Stock Solution**

11.5g Na<sub>2</sub>

80g NaCl

2g KCl

Components were dissolved into 1L deionize sterilized water and pH adjusted 7.4 for 1X PBS.

### **1X Tris Base, Acetic acid, EDTA (TAE) Buffer**

40mM Tris

20mM Acetic Acid

1mM EDTA

All components were dissolved in dH<sub>2</sub>O.

**Table A. 2: Composition of TFB I Solution**

<b>TFB1</b>		
	<b>250mL</b>	
30 mM potassium acetate	0,74	g
10 mM CaCl <sub>2</sub>	1,25	mL of 2M
50 mM MnCl <sub>2</sub>	2,47	g
100 mM RbCl	3,023	g
15% glycerol	37,5	mL of 99%

Overall volume was completed to 100mL by using distilled H<sub>2</sub>O and pH was adjusted to 5.8. Solution autoclaved or filtered with 0.45mm filter.

**Table A. 3: Composition of TFB II Solution**

<b>TFB2</b>		
	<b>100mL</b>	
10 mM MOPS or PIPES	0,335	g
75 mM CaCl <sub>2</sub>	3,75	mL of 2M
10 mM RbCl	0,12	g
15% glycerol	15	mL of 99%

Overall volume was completed to 100mL by using distilled H<sub>2</sub>O and pH was adjusted to 5.8. Solution autoclaved or filtered with 0.45mm filter.

**Induction Buffer (1X)**

1X PBS with 100µM Ro 20-1724(4-(3-butoxy-4-methoxy-benzyl) imidazolidone) , Krebs Ringer Buffer and 500µM IBMX(3-isobutyl-1-methylxanthine).



## B. MAMMALIAN EXPRESSION MAPS

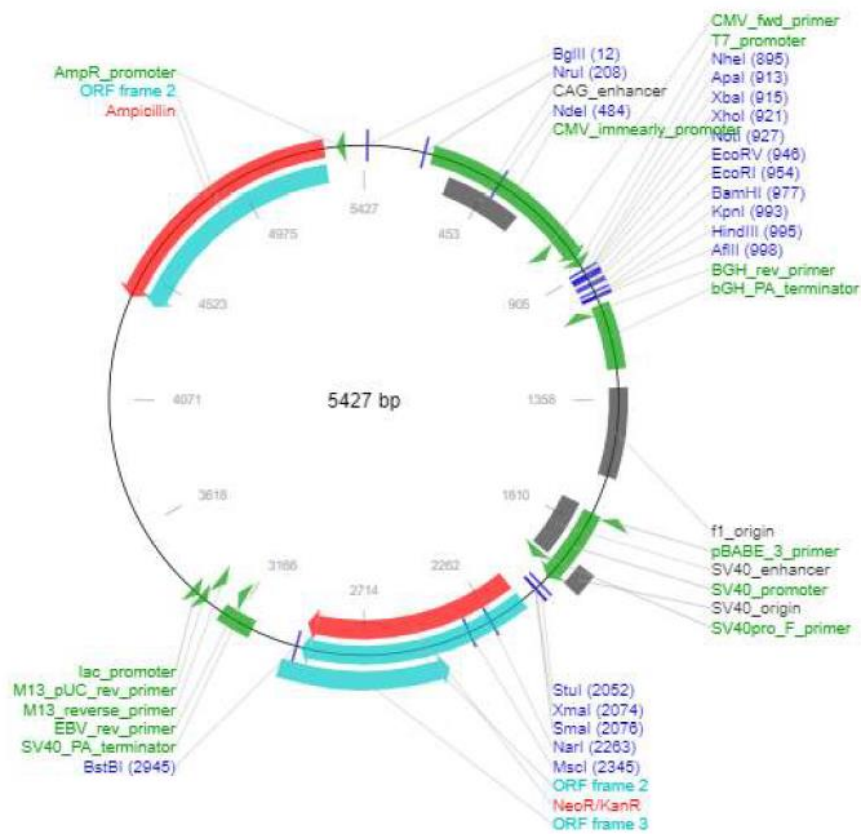


**Figure B. 1:** pcDNA3.1(-) expression vector map (taken from (*Addgene: Vector Database - PcDNA3.1(-)*, n.d.)

### C. DESIGNED PRIMERS

**Table C. 1: Minigene Cloning Primers**

<b>Gai Minigene Forward Primer</b>	5'GTTGTTGTTCTCGAGGCCGCCACCATGGGAAT AAAAATAATCTAAAAGA3'
<b>Gai Minigene Reverse Primer</b>	5'GTTGTTGTTAAGCTTTTATCCAAAGAGACCAC AA3'
<b>Gas Minigene Forward Primer</b>	5'GTTGTTGTTCTCGAGGCCGCCACCATGGGACA GCGCATGCACCTTCGTCAG3'
<b>Gas Minigene Reverse Primer</b>	5'AACAACAACAAGCTTTTATCCGAGCAGCTCG TACTGACGAAGG3'

## D. FUSION PROTEIN CODING SEQUENCES

### **G $\alpha$ i 121 EGFP Coding Sequence:**

ATGGGCTGCACGCTGAGCGCCGAGGACAAGGCGGCGGTGGAGCGGAGT  
AAGATGATCGACCGCAACCTCCGTGAGGACGGCGAGAAGGCGGCGCGC  
GAGGTCAAGCTGCTGCTGCTCGGTGCTGGTGAATCTGGTAAAAGTACA  
ATTGTGAAGCAGATGAAAATTATCCATGAAGCTGGTTATTCAGAAGAG  
GAGTGTAACAATACAAAGCAGTGGTCTACAGTAACACCATCCAGTCA  
ATTATTGCTATCATTAGGGCTATGGGGAGGTTGAAGATAGACTTTGGTG  
ACTCAGCCCGGGCGGATGATGCACGCCAACTCTTTGTGCTAGCTGGAGC  
TGCTGAAGAAGGCTTTATGACTGCA**TCTGGAGGAGGAGGATCTATGGT**  
**GAGCAAGGGCGAGGAGCTGTTACCGGGGTGGTGCCCATCCTGGTCTGA**  
**GCTGGACGGCGACGTAAACGGCCACAAGTTCAGCGTGTCCGGCGAGGG**  
**CGAGGGCGATGCCACCTACGGCAAGCTGACCCTGAAGTTCATCTGCAC**  
**CACCGGCAAGCTGCCCGTGCCCTGGCCACCCTCGTGACCACCCTGACC**  
**TACGGCGTGCAGTGCTTCAGCCGCTACCCCGACCACATGAAGCAGCAC**  
**GACTTCTTCAAGTCCGCCATGCCCGAAGGCTACGTCCAGGAGCGCACCA**  
**TCTTCTTCAAGGACGACGGCAACTACAAGACCCGCGCCGAGGTGAAGT**  
**TCGAGGGCGACACCCTGGTGAACCGCATCGAGCTGAAGGGCATCGACT**  
**TCAAGGAGGACGGCAACATCCTGGGGCACAAGCTGGAGTACA ACTACA**  
**ACAGCCACAACGTCTATATCATGGCCGACAAGCAGAAGAACGGCATCA**  
**AGGTGAACTTCAAGATCCGCCACAACATCGAGGACGGCAGCGTGCAGC**  
**TCGCCGACCACTACCAGCAGAACACCCCATCGGCGACGGCCCCGTGC**  
**TGCTGCCCCGACAACCACTACCTGAGCACCCAGTCCAAGCTTAGCAAAG**  
**ACCCCAACGAGAAGCGCGATCACATGGTCCTGCTGGAGTTCGTGACCG**  
**CCGCCGGGATCACTCTCGGCATGGACGAGCTGTACAAGTCTGGAGGAG**

GAGGATCTGAACTTGCTGGAGTTATAAAGAGATTGTGGAAAGATAGTG  
GTGTACAAGCCTGTTTCAACAGATCCCGAGAGTACCAGCTTAATGATTC  
TGCAGCATACTATTTGAATGACTTGGACAGAATAGCTCAACCAAATTAC  
ATCCCGACTCAACAAGATGTTCTCAGAACTAGAGTGAAAACACTACAGGA  
ATTGTTGAAACCCATTTTACTTTCAAAGATCTTCATTTTAAAATGTTTGA  
TGTGGGAGGTCAGAGATCTGAGCGGAAGAAGTGGATTTCATTGCTTCGA  
AGGAGTGGCGGCGATCATCTTCTGTGTAGCACTGAGTGACTACGACCTG  
GTTCTAGCTGAAGATGAAGAAATGAACCGAATGCATGAAAGCATGAAA  
TTGTTTGACAGCATATGTAACAACAAGTGGTTTACAGATACATCCATTA  
TACTTTTTCTAAACAAGAAGGATCTTTTTGAAGAAAAAATCAAAAAGA  
GCCCTCTCACTATATGCTATCAAGAATATGCAGGATCAAACACATATGA  
AGAGGCAGCTGCATATATTCAATGTCAGTTTGAAGACCTCAATAAAAG  
AAAGGACACAAAGGAAATATACACCCACTTCACATGTGCCACAGATAC  
TAAGAATGTGCAGTTTGTTTTTGATGCTGTAACAGATGTCATCATAAAA  
AATAATCTAAAAGATTGTGGTCTCTTTTAG

**Gai 121 mCherry Coding Sequence:**

ATGGGCTGCACGCTGAGCGCCGAGGACAAGGCGGCGGTGGAGCGGAGT  
AAGATGATCGACCGCAACCTCCGTGAGGACGGCGAGAAGGCGGCGCGC  
GAGGTCAAGCTGCTGCTGCTCGGTGCTGGTGAATCTGGTAAAAGTACA  
ATTGTGAAGCAGATGAAAATTATCCATGAAGCTGGTTATTCAGAAGAG  
GAGTGTAACAATACAAAGCAGTGGTCTACAGTAACACCATCCAGTCA  
ATTATTGCTATCATTAGGGCTATGGGGAGGTTGAAGATAGACTTTGGTG  
ACTCAGCCCGGGCGGATGATGCACGCCAACTCTTTGTGCTAGCTGGAGC  
TGCTGAAGAAGGCTTTATGACTGCATCTGGAGGAGGAGGATCTATGGT  
GAGCAAGGGCGAGGAGGATAACATGGCCATCATCAAGGAGTTCATGCG

CTTCAAGGTGCACATGGAGGGCTCCGTGAACGGCCACGAGTTCGAGAT  
CGAGGGCGAGGGCGAGGGCCGCCCTACGAGGGCACCCAGACCGCCA  
AGCTGAAGGTGACCAAGGGTGGCCCCCTGCCCTTCGCCTGGGACATCCT  
GTCCCCTCAGTTCATGTACGGCTCCAAGGCCTACGTGAAGCACCCCGCC  
GACATCCCCGACTACTTGAAGCTGTCCTTCCCCGAGGGCTTCAAGTGGG  
AGCGCGTGATGAACTTCGAGGACGGCGGGCGTGGTGACCGTGACCCAGG  
ACTCCTCCCTGCAGGACGGCGAGTTCATCTACAAGGTGAAGCTGCGCG  
GCACCAACTTCCCCTCCGACGGCCCCGTAATGCAGAAGAAGACCATGG  
GCTGGGAGGCTCCTCCGAGCGGATGTACCCCGAGGACGGCGCCCTGA  
AGGGCGAGATCAAGCAGAGGCTGAAGCTGAAGGACGGCGGGCCACTAC  
GACGCTGAGGTCAAGACCACCTACAAGGCCAAGAAGCCCGTGCAGCTG  
CCCGGGCGCCTACAACGTCAACATCAAGTTGGACATCACCTCCCACAACG  
AGGACTACACCATCGTGGAACAGTACGAACGCGCCGAGGGCCGCCACT  
CCACCGGCGGCATGGACGAGCTGTACAAGTCTGGAGGAGGAGGATCTG  
AACTTGCTGGAGTTATAAAGAGATTGTGGAAAGATAGTGGTGTACAAG  
CCTGTTTTCAACAGATCCCGAGAGTACCAGCTTAATGATTCTGCAGCATA  
CTATTTGAATGACTTGGACAGAATAGCTCAACCAAATTACATCCCGACT  
CAACAAGATGTTCTCAGAACTAGAGTGAAAACCTACAGGAATTGTTGAA  
ACCCATTTTACTTTCAAAGATCTTCATTTTAAAATGTTTGATGTGGGAGG  
TCAGAGATCTGAGCGGAAGAAGTGGATTCAATTGCTTCGAAGGAGTGGC  
GGCGATCATCTTCTGTGTAGCACTGAGTGACTACGACCTGGTTCTAGCT  
GAAGATGAAGAAATGAACCGAATGCATGAAAGCATGAAATTGTTTGAC  
AGCATATGTAACAACAAGTGGTTTACAGATACATCCATTATACTTTTTTC  
TAAACAAGAAGGATCTTTTTGAAGAAAAAATCAAAAAGAGCCCTCTCA  
CTATATGCTATCAAGAATATGCAGGATCAAACACATATGAAGAGGCAG  
CTGCATATATTCAATGTCAGTTTGAAGACCTCAATAAAAGAAAGGACA  
CAAAGGAAATATACACCCACTTCACATGTGCCACAGATACTAAGAATG  
TGCAGTTTGTTTTTGATGCTGTAACAGATGTCATCATAAAAAATAATCT  
AAAAGATTGTGGTCTCTTTTAG

**Gai 91 EGFP Coding Sequence:**

ATGGGCTGCACGCTGAGCGCCGAGGACAAGGCGGCGGTGGAGCGGAGT  
AAGATGATCGACCGCAACCTCCGTGAGGACGGCGAGAAGGCGGCGCGC  
GAGGTCAAGCTGCTGCTGCTCGGTGCTGGTGAATCTGGTAAAAGTACA  
ATTGTGAAGCAGATGAAAATTATCCATGAAGCTGGTTATTCAGAAGAG  
GAGTGTAACAATACAAAGCAGTGGTCTACAGTAACACCATCCAGTCA  
ATTATTGCTATCATTAGGGCTATGGGGAGGTTGTCTGGAGGAGGAGGAT  
CTATGGTGAGCAAGGGCGAGGAGCTGTTACCGGGGTGGTGCCCATCC  
TGGTCGAGCTGGACGGCGACGTAAACGGCCACAAGTTCAGCGTGTCCG  
GCGAGGGCGAGGGCGATGCCACCTACGGCAAGCTGACCCTGAAGTTCA  
TCTGCACCACCGGCAAGCTGCCCGTGCCCTGGCCCACCCTCGTGACCAC  
CCTGACCTACGGCGTGCAGTGCTTCAGCCGCTACCCCGACCACATGAAG  
CAGCACGACTTCTTCAAGTCCGCCATGCCCGAAGGCTACGTCCAGGAGC  
GCACCATCTTCTTCAAGGACGACGGCAACTACAAGACCCGCGCCGAGG  
TGAAGTTCGAGGGCGACACCCTGGTGAACCGCATCGAGCTGAAGGGCA  
TCGACTTCAAGGAGGACGGCAACATCCTGGGGCACAAGCTGGAGTACA  
ACTACAACAGCCACAACGTCTATATCATGGCCGACAAGCAGAAGAACG  
GCATCAAGGTGAACTTCAAGATCCGCCACAACATCGAGGACGGCAGCG  
TGCAGCTCGCCGACCACTACCAGCAGAACACCCCATCGGCGACGGCC  
CCGTGCTGCTGCCCGACAACCACTACCTGAGCACCCAGTCCAAGCTTAG  
CAAAGACCCCAACGAGAAGCGCGATCACATGGTCCTGCTGGAGTTCGT  
GACCGCCGCGGGATCACTCTCGGCATGGACGAGCTGTACAAGTCTGG  
AGGAGGAGGATCTAAGATAGACTTTGGTGACTCAGCCCGGGCGGATGA  
TGCACGCCAACTCTTTGTGCTAGCTGGAGCTGCTGAAGAAGGCTTTATG  
ACTGCAGAACTTGCTGGAGTTATAAAGAGATTGTGGAAAGATAGTGGT  
GTACAAGCCTGTTTCAACAGATCCCGAGAGTACCAGCTTAATGATTCTG  
CAGCATACTATTTGAATGACTTGGACAGAATAGCTCAACCAAATTACAT  
CCCGACTCAACAAGATGTTCTCAGAACTAGAGTGAAAACCTACAGGAAT  
TGTTGAAACCCATTTTACTTTCAAAGATCTTCATTTTAAAATGTTTGATG

TGGGAGGTCAGAGATCTGAGCGGAAGAAGTGGATTCATTGCTTCGAAG  
GAGTGGCGGGCGATCATCTTCTGTGTAGCACTGAGTGACTACGACCTGGT  
TCTAGCTGAAGATGAAGAAATGAACCGAATGCATGAAAGCATGAAATT  
GTTTGACAGCATATGTAACAACAAGTGGTTTACAGATACATCCATTATA  
CTTTTTCTAAACAAGAAGGATCTTTTTGAAGAAAAAATCAAAAAGAGC  
CCTCTCACTATATGCTATCAAGAATATGCAGGATCAAACACATATGAAG  
AGGCAGCTGCATATATTCAATGTCAGTTTGAAGACCTCAATAAAAGAA  
AGGACACAAAGGAAATATACACCCACTTCACATGTGCCACAGATACTA  
AGAATGTGCAGTTTGTTTTTGATGCTGTAACAGATGTCATCATAAAAAA  
TAATCTAAAAGATTGTGGTCTCTTTAG

**Gai 91 mCherry Coding Sequence:**

ATGGGCTGCACGCTGAGCGCCGAGGACAAGGCGGCGGTGGAGCGGAGT  
AAGATGATCGACCGCAACCTCCGTGAGGACGGCGAGAAGGCGGCGCGC  
GAGGTCAAGCTGCTGCTGCTCGGTGCTGGTGAATCTGGTAAAAGTACA  
ATTGTGAAGCAGATGAAAATTATCCATGAAGCTGGTTATTCAGAAGAG  
GAGTGTAACAATACAAAGCAGTGGTCTACAGTAACACCATCCAGTCA  
ATTATTGCTATCATTAGGGCTATGGGGAGGTTGTCTGGAGGAGGAGGAT  
CTATGGTGAGCAAGGGCGAGGAGGATAACATGGCCATCATCAAGGAGT  
TCATGCGCTTCAAGGTGCACATGGAGGGCTCCGTGAACGGCCACGAGT  
TCGAGATCGAGGGCGAGGGCGAGGGCCGCCCTACGAGGGCACCCAGA  
CCGCCAAGCTGAAGGTGACCAAGGGTGGCCCCCTGCCCTTCGCCTGGG  
ACATCCTGTCCCCTCAGTTCATGTACGGCTCCAAGGCCTACGTGAAGCA  
CCCCGCCGACATCCCCGACTACTTGAAGCTGTCCTTCCCCGAGGGCTTC  
AAGTGGGAGCGCGTGATGAACTTCGAGGACGGCGGGCGTGGTGACCGTG  
ACCCAGGACTCCTCCCTGCAGGACGGCGAGTTCATCTACAAGGTGAAG  
CTGCGCGGCACCAACTTCCCCTCCGACGGCCCCGTAATGCAGAAGAAG  
ACCATGGGCTGGGAGGCCTCCTCCGAGCGGATGTACCCCGAGGACGGC

GCCCTGAAGGGCGAGATCAAGCAGAGGCTGAAGCTGAAGGACGGCGG  
CCACTACGACGCTGAGGTCAAGACCACCTACAAGGCCAAGAAGCCCGT  
GCAGCTGCCCGGCGCCTACAACGTCAACATCAAGTTGGACATCACCTCC  
CACAACGAGGACTACACCATCGTGGAACAGTACGAACGCGCCGAGGGC  
CGCCACTCCACCGGCGGCATGGACGAGCTGTACAAGTCTGGAGGAGGA  
GGATCTAAGATAGACTTTGGTGACTCAGCCCGGGCGGATGATGCACGC  
CAACTCTTTGTGCTAGCTGGAGCTGCTGAAGAAGGCTTTATGACTGCAG  
AACTTGCTGGAGTTATAAAGAGATTGTGGAAAGATAGTGGTGTACAAG  
CCTGTTTCAACAGATCCCGAGAGTACCAGCTTAATGATTCTGCAGCATA  
CTATTTGAATGACTTGGACAGAATAGCTCAACCAAATTACATCCCGACT  
CAACAAGATGTTCTCAGAACTAGAGTGAAAACACTACAGGAATTGTTGAA  
ACCCATTTTACTTTCAAAGATCTTCATTTTAAAATGTTTGATGTGGGAGG  
TCAGAGATCTGAGCGGAAGAAGTGGATTCATTGCTTCGAAGGAGTGGC  
GGCGATCATCTTCTGTGTAGCACTGAGTGACTACGACCTGGTTCTAGCT  
GAAGATGAAGAAATGAACCGAATGCATGAAAGCATGAAATTGTTTGAC  
AGCATATGTAACAACAAGTGGTTTACAGATACATCCATTATACTTTTTTC  
TAAACAAGAAGGATCTTTTTGAAGAAAAAATCAAAAAGAGCCCTCTCA  
CTATATGCTATCAAGAATATGCAGGATCAAACACATATGAAGAGGCAG  
CTGCATATATTCAATGTCAGTTTGAAGACCTCAATAAAAGAAAGGACA  
CAAAGGAAATATACACCCACTTCACATGTGCCACAGATACTAAGAATG  
TGCAGTTTGTTTTTGATGCTGTAACAGATGTCATCATAAAAAATAATCT  
AAAAGATTGTGGTCTCTTTTAG

**Gas Δ 73-85 EGFP Coding Sequence:**

ATGGGCTGCCTCGGGAACAGTAAGACCGAGGACCAGCGCAACGAGGA  
GAAGGCGCAGCGTGAGGCCAACAAAAAGATCGAGAAGCAGCTGCAGA  
AGGACAAGCAGGTCTACCGGGCCACGCACCGCCTGCTGCTGCTGGGTG  
CTGGAGAATCTGGTAAAAGCACCATTGTGAAGCAGATGAGGATCCTGC



ATGTTAATGGGTTTAATGGAGAGGGCGGCGATGGTGAGAAGGCAACCA  
AAGTGCAGGACATCAAAAACAACCTGAAAGAGGCGATTGAAACCATTG  
TGGCCGCCATGAGCAACCTGGTGCCCCCGTGGAGCTGGCCAACCCCG  
AGAACCAGTTCAGAGTGGACTACATTCTGAGTGTGATGAACGTGCCTG  
ACTTTGACTTCCCTCCCGAATTCTATGAGCATGCCAAGGCTCTGTGGGA  
GGATGAAGGAGTGCCTGCTACGAACGCTCTGGAGGAGGAGGATC  
TATGGTGAGCAAGGGCGAGGAGCTGTTACCGGGGTGGTGCCCATCCT  
GGTCGAGCTGGACGGCGACGTAAACGGCCACAAGTTCAGCGTGTCCGG  
CGAGGGCGAGGGCGATGCCACCTACGGCAAGCTGACCCTGAAGTTCAT  
CTGCACCACCGGCAAGCTGCCCGTGCCCTGGCCACCCTCGTGACCACC  
CTGACCTACGGCGTGCAGTGCTTCAGCCGCTACCCCGACCACATGAAGC  
AGCACGACTTCTTCAAGTCCGCCATGCCCGAAGGCTACGTCCAGGAGC  
GCACCATCTTCTTCAAGGACGACGGCAACTACAAGACCCGCGCCGAGG  
TGAAGTTCGAGGGCGACACCCTGGTGAACCGCATCGAGCTGAAGGGCA  
TCGACTTCAAGGAGGACGGCAACATCCTGGGGCACAAGCTGGAGTACA  
ACTACAACAGCCACAACGTCTATATCATGGCCGACAAGCAGAAGAACG  
GCATCAAGGTGAACTTCAAGATCCGCCACAACATCGAGGACGGCAGCG  
TGCAGCTCGCCGACCACTACCAGCAGAACACCCCATCGGGCGACGGCC  
CCGTGCTGCTGCCCGACAACCACTACCTGAGCACCCAGTCCAAGCTTAG  
CAAAGACCCCAACGAGAAGCGCGATCACATGGTCCTGCTGGAGTTCGT  
GACCGCCGCCGGGATCACTCTCGGCATGGACGAGCTGTACAAGTCTGG  
AGGAGGAGGATCTTCCAACGAGTACCAGCTGATTGACTGTGCCAGTA  
CTTCCTGGACAAGATCGACGTGATCAAGCAGGCTGACTATGTGCCGAG  
CGATCAGGACCTGCTTCGCTGCCGTGTCCTGACTTCTGGAATCTTTGAG  
ACCAAGTTCCAGGTGGACAAAGTCAACTTCCACATGTTTGACGTGGGTG  
GCCAGCGCGATGAACGCCGCAAGTGGATCCAGTGCTTCAACGATGTGA  
CTGCCATCATCTTCGTGGTGGCCAGCAGCAGCTACAACATGGTCATCCG  
GGAGGACAACCAGACCAACCGCCTGCAGGAGGCTCTGAACCTCTTCAA  
GAGCATCTGGAACAACAGATGGCTGCGCACCATCTCTGTGATCCTGTTC  
CTCAACAAGCAAGATCTGCTCGCTGAGAAAGTCCTTGCTGGGAAATCG

AAGATTGAGGACTACTTTCCAGAATTTGCTCGCTACACTACTCCTGAGG  
ATGCTACTCCCGAGCCCGGAGAGGACCCACGCGTGACCCGGGCAAGT  
ACTTCATTCGAGATGAGTTTCTGAGGATCAGCACTGCCAGTGGAGATGG  
GCGTCACTACTGCTACCCTCATTTACCTGCGCTGTGGACACTGAGAAC  
ATCCGCCGTGTGTTCAACGACTGCCGTGACATCATTCAGCGCATGCACC  
TTCGTCAGTACGAGCTGCTCTAG

**Gas  $\Delta$  73-85 mCherry Coding Sequence:**

ATGGGCTGCCTCGGGAACAGTAAGACCGAGGACCAGCGCAACGAGGA  
GAAGGCGCAGCGTGAGGCCAACAAAAAGATCGAGAAGCAGCTGCAGA  
AGGACAAGCAGGTCTACCGGGCCACGCACCGCCTGCTGCTGCTGGGTG  
CTGGAGAATCTGGTAAAAGCACCATTGTGAAGCAGATGAGGATCCTGC  
ATGTTAATGGGTTTAATGGAGAGGGCGGCGATGGTGAGAAGGCAACCA  
AAGTGCAGGACATCAAAAACAACCTGAAAGAGGCGATTGAAACCATTG  
TGGCCGCCATGAGCAACCTGGTGCCCCCGTGGAGCTGGCCAACCCCG  
AGAACCAGTTCAGAGTGGACTACATTCTGAGTGTGATGAACGTGCCTG  
ACTTTGACTTCCCTCCCGAATTCTATGAGCATGCCAAGGCTCTGTGGGA  
GGATGAAGGAGTGCCTGCTACGAACGCTCTGGAGGAGGAGGATC  
TATGGTGAGCAAGGGCGAGGAGGATAACATGGCCATCATCAAGGAGTT  
CATGCGCTTCAAGGTGCACATGGAGGGCTCCGTGAACGGCCACGAGTT  
CGAGATCGAGGGCGAGGGCGAGGGCCGCCCTACGAGGGCACCCAGA  
CCGCCAAGCTGAAGGTGACCAAGGGTGGCCCCCTGCCCTTCGCCTGGG  
ACATCCTGTCCCCTCAGTTCATGTACGGCTCCAAGGCCTACGTGAAGCA  
CCCCGCCGACATCCCCGACTACTTGAAGCTGTCCTTCCCCGAGGGCTTC  
AAGTGGGAGCGCGTGATGAACTTCGAGGACGGCGGCGTGGTGACCGTG  
ACCCAGGACTCCTCCCTGCAGGACGGCGAGTTCATCTACAAGGTGAAG  
CTGCGCGGCACCAACTTCCCCTCCGACGGCCCCGTAATGCAGAAGAAG  
ACCATGGGCTGGGAGGCTCCTCCGAGCGGATGTACCCCGAGGACGGC

GCCCTGAAGGGCGAGATCAAGCAGAGGCTGAAGCTGAAGGACGGCGG  
CCACTACGACGCTGAGGTCAAGACCACCTACAAGGCCAAGAAGCCCGT  
GCAGCTGCCCCGGCGCCTACAACGTCAACATCAAGTTGGACATCACCTCC  
CACAACGAGGACTACACCATCGTGGAACAGTACGAACGCGCCGAGGGC  
CGCCACTCCACCGGGCGGCATGGACGAGCTGTACAAGTCTGGAGGAGGA  
GGATCTTCCAACGAGTACCAGCTGATTGACTGTGCCAGTACTTCCTGG  
ACAAGATCGACGTGATCAAGCAGGCTGACTATGTGCCGAGCGATCAGG  
ACCTGCTTCGCTGCCGTGTCCTGACTTCTGGAATCTTTGAGACCAAGTTC  
CAGGTGGACAAAGTCAACTTCCACATGTTTGACGTGGGTGGCCAGCGC  
GATGAACGCCGCAAGTGGATCCAGTGCTTCAACGATGTGACTGCCATC  
ATCTTCGTGGTGGCCAGCAGCAGCTACAACATGGTCATCCGGGAGGAC  
AACCAGACCAACCGCCTGCAGGAGGCTCTGAACCTCTTCAAGAGCATC  
TGGAACAACAGATGGCTGCGCACCATCTCTGTGATCCTGTTCTCAACA  
AGCAAGATCTGCTCGCTGAGAAAGTCCTTGCTGGGAAATCGAAGATTG  
AGGACTACTTTCCAGAATTTGCTCGCTACACTACTCCTGAGGATGCTAC  
TCCCGAGCCCGGAGAGGACCCACGCGTGACCCGGGCCAAGTACTTCAT  
TCGAGATGAGTTTCTGAGGATCAGCACTGCCAGTGGAGATGGGCGTCA  
CTACTGCTACCCTCATTTACCTGCGCTGTGGACACTGAGAACATCCGC  
CGTGTGTTCAACGACTGCCGTGACATCATTCAGCGCATGCACCTTCGTC  
AGTACGAGCTGCTCTAG

**GAP43 EGFP Coding Sequence:**

ATGCTGTGCTGTATGAGAAGAACCAAACAGGTTGAAAAGAATGATGAG  
GACCAAAGATTGAACAAGATGGTGTCAAGCCGGAAGATAAGGCTCAT  
AAGGCTGCGACCAAATTCAGGCTAGCTTCCGTGGACACATAACAAGG  
AAAAAGCTCAAAGGCGAGAAGAAGGGTGATGGTGAGCAAGGGCGAGG  
AGCTGTTACCGGGGTGGTGCCATCCTGGTCGAGCTGGACGGCGACGT  
AAACGGCCACAAGTTCAGCGTGTCCGGCGAGGGCGAGGGCGATGCCAC

CTACGGCAAGCTGACCCTGAAGTTCATCTGCACCACCGGCAAGCTGCCC  
GTGCCCTGGCCACCCTCGTGACCACCCTGACCTACGGCGTGACGTGCT  
TCAGCCGCTACCCCGACCACATGAAGCAGCACGACTTCTTCAAGTCCGC  
CATGCCCCGAAGGCTACGTCCAGGAGCGCACCATCTTCTTCAAGGACGA  
CGGCAACTACAAGACCCGCGCCGAGGTGAAGTTCGAGGGGCGACACCCT  
GGTGAACCGCATCGAGCTGAAGGGCATCGACTTCAAGGAGGACGGCAA  
CATCCTGGGGCACAAGCTGGAGTACAACACTACAACAGCCACAACGTCTA  
TATCATGGCCGACAAGCAGAAGAACGGCATCAAGGTGAACTTCAAGAT  
CCGCCACAACATCGAGGACGGCAGCGTGCAGCTCGCCGACCACTACCA  
GCAGAACACCCCCATCGGGCAGCGGCCCCGTGCTGCTGCCCCGACAACCA  
CTACCTGAGCACCCAGTCCAAGCTTAGCAAAGACCCCAACGAGAAGCG  
CGATCACATGGTCCTGCTGGAGTTCGTGACCGCCGCCGGGATCACTCTC  
GGCATGGACGAGCTGTACAAGTAG

**GAP43 mCherry Coding Sequence:**

ATGCTGTGCTGTATGAGAAGAACCAAACAGGTTGAAAAGAATGATGAG  
GACCAAAGATTGAACAAGATGGTGTCAAGCCGGAAGATAAGGCTCAT  
AAGGCTGCGACCAAATTCAGGCTAGCTTCCGTGGACACATAACAAGG  
AAAAAGCTCAAAGGCGAGAAGAAGGGTGATGGTGAGCAAGGGCGAGG  
AGGATAACATGGCCATCATCAAGGAGTTCATGCGCTTCAAGGTGCACA  
TGGAGGGCTCCGTGAACGGCCACGAGTTCGAGATCGAGGGCGAGGGCG  
AGGGCCGCCCTACGAGGGCACCCAGACCGCCAAGCTGAAGGTGACCA  
AGGGTGGCCCCCTGCCCTTCGCCTGGGACATCCTGTCCCCTCAGTTCAT  
GTACGGCTCCAAGGCCTACGTGAAGCACCCCGCCGACATCCCCGACTA  
CTTGAAGCTGTCTTCCCCGAGGGCTTCAAGTGGGAGCGCGTGATGAAC  
TTCGAGGACGGCGGCGTGGTGACCGTGACCCAGGACTCCTCCCTGCAG  
GACGGCGAGTTCATCTACAAGGTGAAGCTGCGCGGCACCAACTTCCCCT  
CCGACGGCCCCGTAATGCAGAAGAAGACCATGGGCTGGGAGGCCTCCT

CCGAGCGGATGTACCCCGAGGACGGCGCCCTGAAGGGCGAGATCAAGC  
AGAGGCTGAAGCTGAAGGACGGCGGCCACTACGACGCTGAGGTCAAGA  
CCACCTACAAGGCCAAGAAGCCCGTGCAGCTGCCCGGCGCCTACAACG  
TCAACATCAAGTTGGACATCACCTCCCACAACGAGGACTACACCATCGT  
GGAACAGTACGAACGCGCCGAGGGCCGCGCCACTCCACCGGCGGCATGGA  
CGAGCTGTACAAGTAG

**GAP43 mCherry-RGSLVPR-EGFP (Positive FRET Control) Coding**

**Sequence:**

ATGCTGTGCTGTATGAGAAGAACCAAACAGGTTGAAAAGAATGATGAG  
GACCAAAGATTGAACAAGATGGTGTCAAGCCGGAAGATAAGGCTCAT  
AAGGCTGCGACCAAATTCAGGCTAGCTTCCGTGGACACATAACAAGG  
AAAAAGCTCAAAGGCGAGAAGAAGGGTGATGGTGAGCAAGGGCGAGG  
AGGATAACATGGCCATCATCAAGGAGTTCATGCGCTTCAAGGTGCACA  
TGGAGGGCTCCGTGAACGGCCACGAGTTCGAGATCGAGGGCGAGGGCG  
AGGGCCGCCCCTACGAGGGCACCCAGACCGCCAAGCTGAAGGTGACCA  
AGGGTGGCCCCCTGCCCTTCGCTGGGACATCCTGTCCCCTCAGTTCAT  
GTACGGCTCCAAGGCCTACGTGAAGCACCCCGCCGACATCCCCGACTA  
CTTGAAGCTGTCCTTCCCCGAGGGCTTCAAGTGGGAGCGCGTGATGAAC  
TTCGAGGACGGCGGCGTGGTGACCGTGACCCAGGACTCCTCCCTGCAG  
GACGGCGAGTTCATCTACAAGGTGAAGCTGCGCGGCACCAACTTCCCCT  
CCGACGGCCCCGTAATGCAGAAGAAGACCATGGGCTGGGAGGCCTCCT  
CCGAGCGGATGTACCCCGAGGACGGCGCCCTGAAGGGCGAGATCAAGC  
AGAGGCTGAAGCTGAAGGACGGCGGCCACTACGACGCTGAGGTCAAGA  
CCACCTACAAGGCCAAGAAGCCCGTGCAGCTGCCCGGCGCCTACAACG  
TCAACATCAAGTTGGACATCACCTCCCACAACGAGGACTACACCATCGT  
GGAACAGTACGAACGCGCCGAGGGCCGCGCCACTCCACCGGCGGCATGGA  
CGAGCTGTACAAGCGGGGCAGCCTGGTCCCTGGAATGGTGAGCAAGGG  
CGAGGAGCTGTTACCGGGGTGGTGCCCATCCTGGTTCGAGCTGGACGG

CGACGTAAACGGCCACAAGTTCAGCGTGTCCGGCGAGGGCGAGGGCGA  
TGCCACCTACGGCAAGCTGACCCTGAAGTTCATCTGCACCACCGCAAG  
CTGCCCGTGCCCTGGCCACCCTCGTGACCACCCTGACCTACGGCGTGC  
AGTGCTTCAGCCGCTACCCCGACCACATGAAGCAGCACGACTTCTTCAA  
GTCCGCCATGCCCCGAAGGCTACGTCCAGGAGCGCACCATCTTCTTCAAG  
GACGACGGCAACTACAAGACCCGCGCCGAGGTGAAGTTCGAGGGCGAC  
ACCCTGGTGAACCGCATCGAGCTGAAGGGCATCGACTTCAAGGAGGAC  
GGCAACATCCTGGGGCACAAGCTGGAGTACAACACTACAACAGCCACAAC  
GTCTATATCATGGCCGACAAGCAGAAGAACGGCATCAAGGTGAACTTC  
AAGATCCGCCACAACATCGAGGACGGCAGCGTGCAGCTCGCCGACCAC  
TACCAGCAGAACACCCCATCGGCGACGGCCCCGTGCTGCTGCCCGAC  
AACCCTACCTGAGCACCCAGTCCAAGCTTAGCAAAGACCCCAACGAG  
AAGCGCGATCACATGGTCCTGCTGGAGTTCGTGACCGCCGCCGGGATC  
ACTCTCGGCATGGACGAGCTGTACAAGTAG

**Gai Minigene Cassette Sequence:**

GCCGCCACCATGGGAATAAAAAATAATCTAAAGATTGTGGTCTCTTT

**Gai Minigene Cassette Sequence:**

GCCGCCACCATGGGACAGCGCATGCACCTTCGTGACGAGCTGCTC

## E. cAMP GLO ASSAY STATISTICAL ANALYSIS

A Unpaired t test		B Unpaired t test			
1	Table Analyzed	Data 2	1 Table Analyzed	Data 2	
2			2		
3	Column D	Wild Type Goi Quinpirole	3	Column F	Goi 91 mCherry Quinpirole
4	vs.	vs.	4	vs.	vs.
5	Column C	Wild Type Goi	5	Column E	Goi 91 mCherry
6			6		
7	Unpaired t test		7	Unpaired t test	
8	P value	0.0003	8	P value	0.0347
9	P value summary	***	9	P value summary	*
10	Significantly different (P < 0.05)?	Yes	10	Significantly different (P < 0.05)?	Yes
11	One- or two-tailed P value?	Two-tailed	11	One- or two-tailed P value?	Two-tailed
12	t, df	t=57.76, df=2	12	t, df	t=3.683, df=3
13			13		
14	How big is the difference?		14	How big is the difference?	
15	Mean of column C	93.34	15	Mean of column E	61.87
16	Mean of column D	140.1	16	Mean of column F	96.97
17	Difference between means (D - C) ± SE	46.76 ± 0.8095	17	Difference between means (F - E) ± SE	35.10 ± 9.530
18	95% confidence interval	43.27 to 50.24	18	95% confidence interval	4.771 to 65.43
19	R squared (eta squared)	0.9994	19	R squared (eta squared)	0.8189
20			20		

C Unpaired t test		D Unpaired t test			
1	Table Analyzed	Data 2	1 Table Analyzed	Data 2	
2			2		
3	Column H	Goi 121 mCherry Quinpirole	3	Column B	Goi 91 EGFP Quinpirole
4	vs.	vs.	4	vs.	vs.
5	Column G	Goi 121 mCherry	5	Column A	Goi 91 EGFP
6			6		
7	Unpaired t test		7	Unpaired t test	
8	P value	0.4627	8	P value	0.0323
9	P value summary	ns	9	P value summary	*
10	Significantly different (P < 0.05)?	No	10	Significantly different (P < 0.05)?	Yes
11	One- or two-tailed P value?	Two-tailed	11	One- or two-tailed P value?	Two-tailed
12	t, df	t=0.7949, df=5	12	t, df	t=2.772, df=6
13			13		
14	How big is the difference?		14	How big is the difference?	
15	Mean of column G	165.4	15	Mean of column A	54.35
16	Mean of column H	187.3	16	Mean of column B	117.7
17	Difference between means (H - G) ± SE	21.96 ± 27.62	17	Difference between means (B - A) ± SE	63.31 ± 22.84
18	95% confidence interval	-49.05 to 92.96	18	95% confidence interval	7.430 to 119.2
19	R squared (eta squared)	0.1122	19	R squared (eta squared)	0.5616
20			20		

**Figure E. 1:** Statistical analysis of Goi fusion protein functional assay results. A) Wild type group signal comparison with and without CGS+Quinpirole treatment, B) Goi 91 mCherry fusion protein signal comparison with and without CGS+Quinpirole treatment, C) Goi 121 mCherry fusion protein signal comparison with and without CGS+Quinpirole treatment, D) Goi 91 EGFP fusion protein signal comparison with and without CGS+Quinpirole treatment.

## F. STATISTICAL ANALYSIS OF THE CONFOCAL MICROSCOPY RESULTS Of *Gai-Gas* FRET PAIRS

ANOVA results		Multiple comparisons				
Ordinary one-way ANOVA		Multiple comparisons				
1	Number of families	1				
2	Number of comparisons per family	6				
3	Alpha	0.05				
4						
5	<b>Tukey's multiple comparisons test</b>	<b>Mean Diff.</b>	<b>95.00% CI of diff.</b>	<b>Significant?</b>	<b>Summary</b>	<b>Adjusted P Value</b>
6	<i>Gai</i> 121- <i>Gas</i> 73-85 vs. <i>Gai</i> 91- <i>Gas</i> 73-85	0.0007713	-0.004557 to 0.006099	No	ns	0.9819
7	<i>Gai</i> 121- <i>Gas</i> 73-85 vs. Gap43 EGFP +Gap43 mCherry	-0.007123	-0.01245 to -0.001795	Yes	**	0.0036
8	<i>Gai</i> 121- <i>Gas</i> 73-85 vs. Gap43 mCherry-L-EGFP	-0.001780	-0.007108 to 0.003548	No	ns	0.8223
9	<i>Gai</i> 91- <i>Gas</i> 73-85 vs. Gap43 EGFP +Gap43 mCherry	-0.007894	-0.01322 to -0.002566	Yes	***	0.0010
10	<i>Gai</i> 91- <i>Gas</i> 73-85 vs. Gap43 mCherry-L-EGFP	-0.002551	-0.007879 to 0.002777	No	ns	0.6014
11	Gap43 EGFP +Gap43 mCherry vs. Gap43 mCherry-L-EGFP	0.005343	1.468e-005 to 0.01067	Yes	*	0.0491
12						

**Figure F. 1:** Ordinary One way ANOVA analysis of *Gai*(121) EGFP-*Gas*(73-85)mCherry , *Gai*(91) EGFP-*Gas*(73-85)mCherry and Gap43 EGFP+ Gap43 mCherry negative control group confocal microscope results calculated with Pix FRET.



## G. MONOCHROMATOR PLATE READER RESULT STATISTICAL ANALYSYS OF $G_{\alpha i}$ - $G_{\alpha s}$ FRET PAIRS

ANOVA results		Multiple comparisons							
Ordinary one-way ANOVA									
Multiple comparisons									
1	Number of families	1							
2	Number of comparisons per family	6							
3	Alpha	0.05							
4									
5	<b>Tukey's multiple comparisons test</b>	<b>Mean Diff.</b>	<b>95.00% CI of diff.</b>	<b>Significant?</b>	<b>Summary</b>	<b>Adjusted P Value</b>			
6	Goi 121 EGFP-Gus 73-85 mCherry vs. Goi 91 EGFP-Gus 73-85 mCherry	-0.001334	-0.003049 to 0.0003799	No	ns	0.1634	A-B		
7	Goi 121 EGFP-Gus 73-85 mCherry vs. Gap43 EGFP-L-mCherry	0.0001492	-0.001585 to 0.001884	No	ns	0.9947	A-C		
8	Goi 121 EGFP-Gus 73-85 mCherry vs. Gap43 EGFP + Gap43 mCherry	0.005923	0.004209 to 0.007637	Yes	****	<0.0001	A-D		
9	Goi 91 EGFP-Gus 73-85 mCherry vs. Gap43 EGFP-L-mCherry	0.001484	-0.0002307 to 0.003198	No	ns	0.1049	B-C		
10	Goi 91 EGFP-Gus 73-85 mCherry vs. Gap43 EGFP + Gap43 mCherry	0.007257	0.005543 to 0.008972	Yes	****	<0.0001	B-D		
11	Gap43 EGFP-L-mCherry vs. Gap43 EGFP + Gap43 mCherry	0.005774	0.004059 to 0.007488	Yes	****	<0.0001	C-D		
12									
13	<b>Test details</b>	<b>Mean 1</b>	<b>Mean 2</b>	<b>Mean Diff.</b>	<b>SE of diff.</b>	<b>n1</b>	<b>n2</b>	<b>q</b>	<b>DF</b>
14	Goi 121 EGFP-Gus 73-85 mCherry vs. Goi 91 EGFP-Gus 73-85 mCherry	0.01119	0.01252	-0.001334	0.0006125	6	6	3.081	20
15	Goi 121 EGFP-Gus 73-85 mCherry vs. Gap43 EGFP-L-mCherry	0.01119	0.01104	0.0001492	0.0006125	6	6	0.3446	20
16	Goi 121 EGFP-Gus 73-85 mCherry vs. Gap43 EGFP + Gap43 mCherry	0.01119	0.005295	0.005923	0.0006125	6	6	13.68	20
17	Goi 91 EGFP-Gus 73-85 mCherry vs. Gap43 EGFP-L-mCherry	0.01252	0.01104	0.001484	0.0006125	6	6	3.426	20
18	Goi 91 EGFP-Gus 73-85 mCherry vs. Gap43 EGFP + Gap43 mCherry	0.01252	0.005295	0.007257	0.0006125	6	6	16.76	20
19	Gap43 EGFP-L-mCherry vs. Gap43 EGFP + Gap43 mCherry	0.01104	0.005295	0.005774	0.0006125	6	6	13.33	20
20									
21									
22									

**Figure G. 1:**  $G_{\alpha i}(121)$  EGFP- $G_{\alpha s}(73-85)$ mCherry ,  $G_{\alpha i}(91)$  EGFP- $G_{\alpha s}(73-85)$ mCherry and Gap43 FRET control groups mCherry spectral peak region result analysis with Ordinary One way ANOVA .

ANOVA results		Multiple comparisons							
Ordinary one-way ANOVA									
Multiple comparisons									
1	Number of families	1							
2	Number of comparisons per family	6							
3	Alpha	0.05							
4									
5	<b>Tukey's multiple comparisons test</b>	<b>Mean Diff.</b>	<b>95.00% CI of diff.</b>	<b>Significant?</b>	<b>Summary</b>	<b>Adjusted P Value</b>			
6	Goi 121 EGFP-Gus 73-85 mCherry vs. Goi 91 EGFP-Gus 73-85 mCherry	-0.04260	-0.09539 to 0.01020	No	ns	0.1485	A-B		
7	Goi 121 EGFP-Gus 73-85 mCherry vs. Gap43 EGFP-L-mCherry	0.04106	0.01128 to 0.07084	Yes	**	0.0039	A-C		
8	Goi 121 EGFP-Gus 73-85 mCherry vs. gap43 EGFP + gap43mCherry	0.2507	0.2209 to 0.2804	Yes	****	<0.0001	A-D		
9	Goi 91 EGFP-Gus 73-85 mCherry vs. Gap43 EGFP-L-mCherry	0.08366	0.03208 to 0.1352	Yes	***	0.0007	B-C		
10	Goi 91 EGFP-Gus 73-85 mCherry vs. gap43 EGFP + gap43mCherry	0.2933	0.2417 to 0.3448	Yes	****	<0.0001	B-D		
11	Gap43 EGFP-L-mCherry vs. gap43 EGFP + gap43mCherry	0.2096	0.1820 to 0.2372	Yes	****	<0.0001	C-D		
12									
13	<b>Test details</b>	<b>Mean 1</b>	<b>Mean 2</b>	<b>Mean Diff.</b>	<b>SE of diff.</b>	<b>n1</b>	<b>n2</b>	<b>q</b>	<b>DF</b>
14	Goi 121 EGFP-Gus 73-85 mCherry vs. Goi 91 EGFP-Gus 73-85 mCherry	0.4099	0.4525	-0.04260	0.01945	9	2	3.097	31
15	Goi 121 EGFP-Gus 73-85 mCherry vs. Gap43 EGFP-L-mCherry	0.4099	0.3688	0.04106	0.01097	9	12	5.293	31
16	Goi 121 EGFP-Gus 73-85 mCherry vs. gap43 EGFP + gap43mCherry	0.4099	0.1592	0.2507	0.01097	9	12	32.31	31
17	Goi 91 EGFP-Gus 73-85 mCherry vs. Gap43 EGFP-L-mCherry	0.4525	0.3688	0.08366	0.01900	2	12	6.226	31
18	Goi 91 EGFP-Gus 73-85 mCherry vs. gap43 EGFP + gap43mCherry	0.4525	0.1592	0.2933	0.01900	2	12	21.82	31
19	Gap43 EGFP-L-mCherry vs. gap43 EGFP + gap43mCherry	0.3688	0.1592	0.2096	0.01016	12	12	29.18	31

**Figure G. 2:**  $G_{\alpha i}(121)$  EGFP- $G_{\alpha s}(73-85)$ mCherry ,  $G_{\alpha i}(91)$  EGFP- $G_{\alpha s}(73-85)$ mCherry and Gap43 FRET control groups Acceptor/Donor peak area result analysis with Ordinary One way ANOVA .

## H. STATISTICAL ANALYSIS OF THE CONFOCAL MICROSCOPY RESULTS Of *Gai*-*Gas* FRET PAIRS WITH *Gai* and *Gas* PROTEIN SPECIFIC MINIGENES

Ordinary one-way ANOVA								
Multiple comparisons								
1	Number of families	1						
2	Number of comparisons per family	3						
3	Alpha	0.05						
4								
5	<b>Tukey's multiple comparisons test</b>	<b>Mean Diff.</b>	<b>95.00% CI of diff.</b>	<b>Significant?</b>	<b>Summary</b>	<b>Adjusted P Value</b>		
6	<i>Gai</i> 91- <i>Gas</i> 73-85 vs. Column B	0.004886	0.004120 to 0.005652	Yes	****	<0.0001	A-B	
7	<i>Gai</i> 91- <i>Gas</i> 73-85 vs. <i>Gai</i> 121- <i>Gas</i> 73-85	0.006141	0.005376 to 0.006907	Yes	****	<0.0001	A-C	
8	Column B vs. <i>Gai</i> 121- <i>Gas</i> 73-85	0.001256	0.0004897 to 0.002021	Yes	***	0.0005	B-C	
9								
10	<b>Test details</b>	<b>Mean 1</b>	<b>Mean 2</b>	<b>Mean Diff.</b>	<b>SE of diff.</b>	<b>n1</b>	<b>n2</b>	<b>q</b>
11	<i>Gai</i> 91- <i>Gas</i> 73-85 vs. Column B	0.008664	0.003778	0.004886	0.0003233	48	48	21.37
12	<i>Gai</i> 91- <i>Gas</i> 73-85 vs. <i>Gai</i> 121- <i>Gas</i> 73-85	0.008664	0.002523	0.006141	0.0003233	48	48	26.86
13	Column B vs. <i>Gai</i> 121- <i>Gas</i> 73-85	0.003778	0.002523	0.001256	0.0003233	48	48	5.492
14								
15								
16								

**Figure H. 1:** LSM Confocal microscope result from *Gai*(121) EGFP-*Gas*(73-85)mCherry , *Gai*(91) EGFP-*Gas*(73-85)mCherry and *Gai*(121) EGFP-*Gas*(73-85)mCherry with minigene FRET groups analyzed with Ordinary One Way Anova analysis.

# I. MONOCHROMATOR PLATE READER RESULT STATISTICAL ANALYSYS OF *Gai*-*Gas* FRET PAIRS WITH *Gai* and *Gas* PROTEIN SPECIFIC MINIGENES

ANOVA results		Multiple comparisons	
Ordinary one-way ANOVA			
Multiple comparisons			
1	Number of families	1	
2	Number of comparisons per family	6	
3	Alpha	0.05	
4			
5	<b>Tukey's multiple comparisons test</b>	<b>Mean Diff.</b>	<b>95.00% CI of diff.</b>
6	Gap43 EGFP-L-mCherry vs. Gap43 EGFP + Gap43 mCherry	0.005774	0.004339 to 0.007208
7	Gap43 EGFP-L-mCherry vs. Gai 121 EGFP-Gas 73-85 mCherry	-0.0001492	-0.001584 to 0.001285
8	Gap43 EGFP-L-mCherry vs. Column D	-0.0006126	-0.002047 to 0.0008221
9	Gap43 EGFP + Gap43 mCherry vs. Gai 121 EGFP-Gas 73-85 mCherry	-0.005923	-0.007358 to -0.004488
10	Gap43 EGFP + Gap43 mCherry vs. Column D	-0.005386	-0.007821 to -0.004952
11	Gai 121 EGFP-Gas 73-85 mCherry vs. Column D	-0.004634	-0.001998 to 0.0009713
12			
13	<b>Test details</b>	<b>Mean 1</b>	<b>Mean 2</b>
14	Gap43 EGFP-L-mCherry vs. Gap43 EGFP + Gap43 mCherry	0.01104	0.005265
15	Gap43 EGFP-L-mCherry vs. Gai 121 EGFP-Gas 73-85 mCherry	0.01104	0.01119
16	Gap43 EGFP-L-mCherry vs. Column D	0.01104	0.01165
17	Gap43 EGFP + Gap43 mCherry vs. Gai 121 EGFP-Gas 73-85 mCherry	0.005265	0.01119
18	Gap43 EGFP + Gap43 mCherry vs. Column D	0.005265	0.01165
19	Gai 121 EGFP-Gas 73-85 mCherry vs. Column D	0.01119	0.01165
20			
21			
22			
23			
24			
25			
26			

**Figure I. 1:** Monochromator plate reader results of *Gai*(121) EGFP-*Gas*(73-85)mCherry , *Gai*(91) EGFP-*Gas*(73-85)mCherry and *Gai*(121) EGFP-*Gas*(73-85)mCherry with minigene FRET groups Ordinary One Way Anova analysis

ANOVA results		Multiple comparisons	
Ordinary one-way ANOVA			
Multiple comparisons			
1	Number of families	1	
2	Number of comparisons per family	6	
3	Alpha	0.05	
4			
5	<b>Tukey's multiple comparisons test</b>	<b>Mean Diff.</b>	<b>95.00% CI of diff.</b>
6	Gai 121 EGFP-Gas 73-85 mCherry vs. Column B	-0.02257	-0.04319 to -0.001957
7	Gai 121 EGFP-Gas 73-85 mCherry vs. Gap43 EGFP-L-mCherry	0.01344	-0.01064 to 0.03751
8	Gai 121 EGFP-Gas 73-85 mCherry vs. Gap43 EGFP + Gap43mCherry	0.1793	0.1552 to 0.2034
9	Column B vs. Gap43 EGFP-L-mCherry	0.03601	0.01115 to 0.06087
10	Column B vs. Gap43 EGFP + Gap43mCherry	0.2019	0.1770 to 0.2267
11	Gap43 EGFP-L-mCherry vs. Gap43 EGFP + Gap43mCherry	0.1659	0.1381 to 0.1937
12			
13	<b>Test details</b>	<b>Mean 1</b>	<b>Mean 2</b>
14	Gai 121 EGFP-Gas 73-85 mCherry vs. Column B	0.3022	0.3248
15	Gai 121 EGFP-Gas 73-85 mCherry vs. Gap43 EGFP-L-mCherry	0.3022	0.2888
16	Gai 121 EGFP-Gas 73-85 mCherry vs. Gap43 EGFP + Gap43mCherry	0.3022	0.1229
17	Column B vs. Gap43 EGFP-L-mCherry	0.3248	0.2888
18	Column B vs. Gap43 EGFP + Gap43mCherry	0.3248	0.1229
19	Gap43 EGFP-L-mCherry vs. Gap43 EGFP + Gap43mCherry	0.2888	0.1229
20			

**Figure I. 2:** Acceptor/Donor spectral peak area results of *Gai*(121) EGFP-*Gas*(73-85)mCherry , *Gai*(91) EGFP-*Gas*(73-85)mCherry and *Gai*(121) EGFP-*Gas*(73-85)mCherry with minigene FRET groups Ordinary One Way Anova analysis

## J. WITH/WITHOUT CGS+QUINPIROLE TREATMENT RESULT ANALYSIS OF Gai-Gas FRET GROUP WITH/WITHOUT MINIGENE

Ordinary one-way ANOVA Multiple comparisons							
1	Number of families	1					
2	Number of comparisons per family	15					
3	Alpha	0.05					
4							
5	<b>Tukey's multiple comparisons test</b>	<b>Mean Diff.</b>	<b>95.00% CI of diff.</b>	<b>Significant?</b>	<b>Summary</b>	<b>Adjusted P Value</b>	
6	Gai 121 EGFP-Gas 73-85 mCherry vs. Column B	-0.0002228	-0.002092 to 0.001646	No	ns	0.9991	A-B
7	Gai 121 EGFP-Gas 73-85 mCherry vs. Gap43 mCherry-L-EGFP	0.0001492	-0.001720 to 0.002018	No	ns	0.9999	A-C
8	Gai 121 EGFP-Gas 73-85 mCherry vs. Gap43 EGFP + Gap43mCherry	0.0005923	0.004054 to 0.007792	Yes	****	<0.0001	A-D
9	Gai 121 EGFP-Gas 73-85 mCherry vs. Column E	-0.0007222	-0.002591 to 0.001147	No	ns	0.8449	A-E
10	Gai 121 EGFP-Gas 73-85 mCherry vs. Column F	0.0005139	-0.001355 to 0.002383	No	ns	0.9582	A-F
11	Column B vs. Gap43 mCherry-L-EGFP	0.0003721	-0.001497 to 0.002241	No	ns	0.9898	B-C
12	Column B vs. Gap43 EGFP + Gap43mCherry	0.006146	0.004277 to 0.008015	Yes	****	<0.0001	B-D
13	Column B vs. Column E	-0.0004994	-0.002368 to 0.001370	No	ns	0.9629	B-E
14	Column B vs. Column F	0.0007367	-0.001132 to 0.002606	No	ns	0.8338	B-F
15	Gap43 mCherry-L-EGFP vs. Gap43 EGFP + Gap43mCherry	0.005774	0.003905 to 0.007642	Yes	****	<0.0001	C-D
16	Gap43 mCherry-L-EGFP vs. Column E	-0.0008714	-0.002740 to 0.0009975	No	ns	0.7160	C-E
17	Gap43 mCherry-L-EGFP vs. Column F	0.0003646	-0.001504 to 0.002234	No	ns	0.9907	C-F
18	Gap43 EGFP + Gap43mCherry vs. Column E	-0.006645	-0.008514 to -0.004776	Yes	****	<0.0001	D-E
19	Gap43 EGFP + Gap43mCherry vs. Column F	-0.005409	-0.007278 to -0.003540	Yes	****	<0.0001	D-F
20	Column E vs. Column F	0.001236	-0.0006328 to 0.003105	No	ns	0.3597	E-F

**Figure J. 1:** Ordinary One Way ANOVA analysis of mCherry spectrum peak normalized area comparison of Gai-Gas FRET pairs with/without Gα protein specific minigenes and with/without CGS+Quinpirole treatment.

ANOVA results							
Ordinary one-way ANOVA Multiple comparisons							
1	Number of families	1					
2	Number of comparisons per family	15					
3	Alpha	0.05					
4							
5	<b>Tukey's multiple comparisons test</b>	<b>Mean Diff.</b>	<b>95.00% CI of diff.</b>	<b>Significant?</b>	<b>Summary</b>	<b>Adjusted P Value</b>	
6	Gai 121 EGFP-Gas 73-85 mCherry vs. Column B	-0.02535	-0.04706 to -0.003635	Yes	*	0.0179	A-B
7	Gai 121 EGFP-Gas 73-85 mCherry vs. Column C	-0.05088	-0.07259 to -0.02917	Yes	****	<0.0001	A-C
8	Gai 121 EGFP-Gas 73-85 mCherry vs. Column D	-0.02802	-0.05147 to -0.004566	Yes	*	0.0151	A-D
9	Gai 121 EGFP-Gas 73-85 mCherry vs. Gap43 EGFP-L-mCherry	-0.007202	-0.01625 to 0.03066	No	ns	0.9116	A-E
10	Gai 121 EGFP-Gas 73-85 mCherry vs. Gap43 EGFP + Gap43mCherry	0.1731	0.1496 to 0.1965	Yes	****	<0.0001	A-F
11	Column B vs. Column C	-0.02553	-0.04725 to -0.003818	Yes	*	0.0170	B-C
12	Column B vs. Column D	-0.002670	-0.02612 to 0.02078	No	ns	0.9989	B-D
13	Column B vs. Gap43 EGFP-L-mCherry	0.03255	0.009097 to 0.05600	Yes	**	0.0046	B-E
14	Column B vs. Gap43 EGFP + Gap43mCherry	0.1984	0.1750 to 0.2219	Yes	****	<0.0001	B-F
15	Column C vs. Column D	0.02286	-0.0005920 to 0.04631	No	ns	0.0581	C-D
16	Column C vs. Gap43 EGFP-L-mCherry	0.05808	0.03463 to 0.08154	Yes	****	<0.0001	C-E
17	Column C vs. Gap43 EGFP + Gap43mCherry	0.2239	0.2005 to 0.2474	Yes	****	<0.0001	C-F
18	Column D vs. Gap43 EGFP-L-mCherry	0.03522	0.01015 to 0.06029	Yes	**	0.0041	D-E
19	Column D vs. Gap43 EGFP + Gap43mCherry	0.2011	0.1760 to 0.2261	Yes	****	<0.0001	D-F
20	Gap43 EGFP-L-mCherry vs. Gap43 EGFP + Gap43mCherry	0.1659	0.1408 to 0.1909	Yes	****	<0.0001	E-F

**Figure J. 2:** One way ANOVA analysis of Acceptor/Donor spectral area normalized peak results of Gai-Gas FRET pairs with/without Gα protein specific minigenes and with/without CGS+Quinpirole treatment.

## K. CURVE FITTING STATISTICAL ANALYSIS

ANOVA results						
2way ANOVA						
Multiple comparisons						
Within each row, compare columns (simple effects within rows)						
1						
2						
3	Number of families	3				
4	Number of comparisons per family	6				
5	Alpha	0.05				
6						
7	<b>Tukey's multiple comparisons test</b>	<b>Mean Diff.</b>	<b>95.00% CI of diff.</b>	<b>Significant?</b>	<b>Summary</b>	<b>Adjusted P Value</b>
8						
9	negative					
10	Goi 91 EGFP-Gos 73-85 mCherry vs. Goi 121 EGFP-Gos 73-85 mCherry	-197.4	-463.5 to 68.77	No	ns	0.2228
11	Goi 91 EGFP-Gos 73-85 mCherry vs. Gap43 EGFP-L-mCherry	60.37	-205.8 to 326.5	No	ns	0.9359
12	Goi 91 EGFP-Gos 73-85 mCherry vs. Gap43 EGFP + Gap43mCherry	-1116	-1386 to -846.8	Yes	****	<0.0001
13	Goi 121 EGFP-Gos 73-85 mCherry vs. Gap43 EGFP-L-mCherry	257.7	-8.396 to 523.9	No	ns	0.0616
14	Goi 121 EGFP-Gos 73-85 mCherry vs. Gap43 EGFP + Gap43mCherry	-919.0	-1189 to -649.4	Yes	****	<0.0001
15	Gap43 EGFP-L-mCherry vs. Gap43 EGFP + Gap43mCherry	-1177	-1446 to -907.2	Yes	****	<0.0001
16						
17	membrane					
18	Goi 91 EGFP-Gos 73-85 mCherry vs. Goi 121 EGFP-Gos 73-85 mCherry	-154.5	-420.6 to 111.6	No	ns	0.4377
19	Goi 91 EGFP-Gos 73-85 mCherry vs. Gap43 EGFP-L-mCherry	-489.6	-755.7 to -223.5	Yes	****	<0.0001
20	Goi 91 EGFP-Gos 73-85 mCherry vs. Gap43 EGFP + Gap43mCherry	137.9	-131.7 to 407.5	No	ns	0.5485
21	Goi 121 EGFP-Gos 73-85 mCherry vs. Gap43 EGFP-L-mCherry	-335.1	-601.2 to -68.98	Yes	**	0.0070
22	Goi 121 EGFP-Gos 73-85 mCherry vs. Gap43 EGFP + Gap43mCherry	292.4	22.80 to 562.0	Yes	*	0.0277
23	Gap43 EGFP-L-mCherry vs. Gap43 EGFP + Gap43mCherry	627.5	357.9 to 897.1	Yes	****	<0.0001
24						
25	organelle					
26	Goi 91 EGFP-Gos 73-85 mCherry vs. Goi 121 EGFP-Gos 73-85 mCherry	92.92	-173.2 to 359.0	No	ns	0.8029
27	Goi 91 EGFP-Gos 73-85 mCherry vs. Gap43 EGFP-L-mCherry	71.46	-194.7 to 337.6	No	ns	0.8989
28	Goi 91 EGFP-Gos 73-85 mCherry vs. Gap43 EGFP + Gap43mCherry	221.8	-47.76 to 491.4	No	ns	0.1468
29	Goi 121 EGFP-Gos 73-85 mCherry vs. Gap43 EGFP-L-mCherry	-21.46	-287.6 to 244.7	No	ns	0.9968
30	Goi 121 EGFP-Gos 73-85 mCherry vs. Gap43 EGFP + Gap43mCherry	128.9	-140.7 to 398.5	No	ns	0.6036
31	Gap43 EGFP-L-mCherry vs. Gap43 EGFP + Gap43mCherry	150.4	-119.2 to 420.0	No	ns	0.4735

Figure K. 1: Signal localization curve fit Two way ANOVA analysis results of FRET pairs.

Ordinary one-way ANOVA								
Multiple comparisons								
1	Number of families	1						
2	Number of comparisons per family	6						
3	Alpha	0.05						
4								
5	<b>Tukey's multiple comparisons test</b>	<b>Mean Diff.</b>	<b>95.00% CI of diff.</b>	<b>Significant?</b>	<b>Summary</b>	<b>Adjusted P Value</b>		
6	1 vs. 2	-154.5	-362.5 to 53.51	No	ns	0.2159	A-B	
7	1 vs. 3	-489.6	-697.6 to -281.6	Yes	****	<0.0001	A-C	
8	1 vs. 4	138.7	-69.28 to 346.7	No	ns	0.3046	A-D	
9	2 vs. 3	-335.1	-543.1 to -127.1	Yes	***	0.0004	B-C	
10	2 vs. 4	293.2	85.20 to 501.2	Yes	**	0.0022	B-D	
11	3 vs. 4	628.3	420.3 to 836.3	Yes	****	<0.0001	C-D	
12								
13	<b>Test details</b>	<b>Mean 1</b>	<b>Mean 2</b>	<b>Mean Diff.</b>	<b>SE of diff.</b>	<b>n1</b>	<b>n2</b>	<b>q</b>
14	1 vs. 2	156.3	310.7	-154.5	79.18	20	20	2.759
15	1 vs. 3	156.3	645.8	-489.6	79.18	20	20	8.744
16	1 vs. 4	156.3	17.55	138.7	79.18	20	20	2.478
17	2 vs. 3	310.7	645.8	-335.1	79.18	20	20	5.985
18	2 vs. 4	310.7	17.55	293.2	79.18	20	20	5.237
19	3 vs. 4	645.8	17.55	628.3	79.18	20	20	11.22

Figure K. 2: Membrane curve fit result One Way ANOVA analysis of FRET pairs